

University of Windsor

## Scholarship at UWindor

---

Electronic Theses and Dissertations

Theses, Dissertations, and Major Papers

---

9-16-2019

## Spectrum Occupancy Estimation and Analysis

Danilo Roberto Corral-De-Witt

*University of Windsor*

Follow this and additional works at: <https://scholar.uwindsor.ca/etd>

---

### Recommended Citation

Corral-De-Witt, Danilo Roberto, "Spectrum Occupancy Estimation and Analysis" (2019). *Electronic Theses and Dissertations*. 7803.

<https://scholar.uwindsor.ca/etd/7803>

This online database contains the full-text of PhD dissertations and Masters' theses of University of Windsor students from 1954 forward. These documents are made available for personal study and research purposes only, in accordance with the Canadian Copyright Act and the Creative Commons license—CC BY-NC-ND (Attribution, Non-Commercial, No Derivative Works). Under this license, works must always be attributed to the copyright holder (original author), cannot be used for any commercial purposes, and may not be altered. Any other use would require the permission of the copyright holder. Students may inquire about withdrawing their dissertation and/or thesis from this database. For additional inquiries, please contact the repository administrator via email ([scholarship@uwindsor.ca](mailto:scholarship@uwindsor.ca)) or by telephone at 519-253-3000ext. 3208.

# **Spectrum Occupancy Estimation and Analysis**

by

**Danilo Roberto CORRAL DE WITT**

A Dissertation

Submitted to the **Faculty of Graduate Studies** through  
the Department of **Electrical and Computer Engineering**  
in Partial Fulfillment of the Requirements for  
the Degree of **Doctor of Philosophy**  
at the University of Windsor

Windsor, Ontario, Canada

2019

© 2019 Danilo Corral De Witt

# Spectrum Occupancy Estimation and Analysis

by

Danilo Roberto CORRAL DE WITT

APPROVED BY:

---

I. Mora-Jiménez, External Examiner  
Universidad Rey Juan Carlos

---

Z. Kobti  
School of Computer Science

---

E. Abdel-Raheem  
Department of Electrical and Computer Engineering

---

B. Balasingam  
Department of Electrical and Computer Engineering

---

K. Tepe, Advisor  
Department of Electrical and Computer Engineering

September 16, 2019

# Declaration of Co-authorship / Previous Publications

## I. Co-authorship

I hereby declare that this thesis incorporates material that is a result of joint research. This thesis contains the outcome of research undertaken by me under the supervision of Dr. K. E. Tepe with the collaborative help from my colleagues in WiCIP lab in the form of advice, critiques, observations, and mentoring. This thesis also reflects the outcomes of joint work realized with Aaron Younan, Arooj Fatima, Jose Matamoros-Vargas, Dr. Farooq Awin, Dr. Esam Abdel-Raheem, Dewan M. Ariful, Lining Zhang, Dr. Sabbir Ahmed, and Dr. Jose Luis Rojo-Álvarez. The mathematical analysis, probabilistic model, data collected, results obtained and presented among the thesis were the outcome of this joint research and collaboration. In all cases, the key ideas, primary contributions, experimental designs, data collection, analysis and interpretation, were performed by the author of this thesis, and the contribution of co-authors was primarily through the provision of valuable suggestions and help in the comprehensive analysis of the experimental results submitted for the published articles.

I am aware of the University of Windsor Senate Policy on Authorship and I certify that I have properly acknowledged the contribution of other researchers to my thesis, and have obtained written permission from each of the co-author(s) to include the above material(s) in my thesis.

I certify that, with the above qualification, this thesis, and the research to which it refers, is the product of my own work.

## II. Previous Publications

This thesis includes parts from four original papers that have been previously published and submitted for publication in peer-reviewed conferences and journals, as follows:

Thesis Chapter	Publication title/full citation	Publication status
Part of Chapter 1, 2, and 3	<b>Corral-De-Witt, D.</b> , Younan, A., Fatima, A., Matoros, J., Awin, F. A., Tepe, K., & Abdel-Raheem, E. (2017, April). Sensing TV Spectrum Using Software Defined Radio Hardware. In 2017 IEEE 30th Canadian Conference on Electrical and Computer Engineering (CCECE) (pp. 1-4). IEEE.	Published
Part of Chapter 3, 4, and 5	<b>Corral-De-Witt, D.</b> , Younan, A., Ariful, D., Zhang, L., & Tepe, K. (2018, August). Multiplatform Spectrum Sensing Prototype. In 2018 IEEE 61st International Midwest Symposium on Circuits and Systems (MWSCAS) (pp. 198-201). IEEE.	Published
Part of Chapter 2	Hassan, D. M. A., <b>Corral-De-Witt, D.</b> , Ahmed, S., & Tepe, K. (2018, December). Narrowband Data Transmission in TV White Space: An Experimental Performance Analysis. In 2018 IEEE International Symposium on Signal Processing and Information Technology (ISSPIT) (pp. 252-257). IEEE.	Published
Part of Chapter 4, 5, and 6	<b>Corral-De-Witt, D.</b> , Ahmed, S., Awin, F., Rojo-Álvarez, J. L., & Tepe, K. (2019). An Accurate Probabilistic Model for TVWS Identification. MDPI Applied Sciences.	Submitted

I certify that I have obtained a written permission from the copyright owner(s) to include the above published material(s) in my thesis, as observed in Appendix A. I certify that the above material describes work completed during my registration as a graduate student at the University of Windsor.

### III. General

I declare that, to the best of my knowledge, my thesis does not infringe upon anyone's copyright nor violate any proprietary rights and that any ideas, techniques, quotations, or any other material from the work of other people included in my thesis, published or otherwise, are fully acknowledged in accordance with the standard referencing practices. Furthermore, to the extent that I have included copyrighted material that surpasses the bounds of fair dealing within the meaning of the Canada Copyright Act, I certify that I have obtained

a written permission from the copyright owner(s) to include such material(s) in my thesis.

I declare that this is a true copy of my thesis, including any final revisions, as approved by my thesis committee and the Graduate Studies office, and that this thesis has not been submitted for a higher degree to any other University or Institution.

# Abstract

The goal of Cognitive Radio (CR) is to facilitate efficient utilization of the electromagnetic spectrum. CR applies spectrum sensing techniques to detect unused channels and then allows opportunistic usage of such channels by secondary users, i.e., un-licensed users, without interfering with primary users, i.e., licensed users. In order to implement a complete TV White Spaces (TVWS) based CR system, at first a model is needed that can be used for identifying TVWS, which can then be exploited for dynamic spectrum access. This work is focused on proposing a sensing method and building a probabilistic model for identifying the occupancy of the electromagnetic spectrum within the UHF TV bands. It also develops a hardware prototype for demonstrating the performance of the proposed technique. It proposes simultaneous sensing both noise and noise-contaminated user's signal (composite signal) for detecting spectrum occupancy minimizing errors. The proposed sensing technique combines energy detection, pilot detection, and information obtained from an external source in order to reduce missed-detection probability. In addition to pre-defined threshold levels, the proposed probabilistic model considers parameters like probability of false alarm and probability of detection for measuring detection accuracy. Finally, a mobile sensing station is designed and implemented using off-the-shelf components to verify the developed technique for TVWS spectrum sensing. Using this mobile station, the UHF TV channels within the spectrum band of 500MHz-698MHz (Channel#19 to Channel#51) are scanned. Covering the total bandwidth of 198MHz, over 8 million data samples are collected through repeated scanning, ensuring possible spatio-temporal variations are taken into account. Results show that the availability of TVWS changes quite significantly with spatial variations. But, even in the most crowded spectrum locations, 28% of UHF channels were identified as TVWS. The model demonstrates about 10% improvement in detecting accuracy compared to other existing models.

# Dedication

To all those wonderful persons who walked this hard road next to me, Claudia my lovely wife, Sebastian, Sofía, and Daniella my kids, the memory of my parents, my family, friends and all the persons who in one or another manner, are part of this achievement, thanks to you all.



# Acknowledgements

I sincerely want to thank all the persons and institutions who were involved in the development of this research project:

To Dr. Kemal Tepe, who encouraged me to develop this research, and all the time was aware of my progress and results.

To Dr. Esam Abdel-Raheem, Dr. Balakumar Balansingam, and Dr. Ziad Kobti, the Ph.D. Committee Members, for all the advisory, recommendations and feedback received during these years.

To Dr. Inmaculada Mora Jiménez, External Committee Member for agreed to be part of this project.

To my professors, lecturers, authorities, technical team, and all the administrative personnel of the University of Windsor, especially to Ms. Andria Ballo, for supporting me during the development of this research.

To SENESCYT and Universidad de las Fuerzas Armadas ESPE of Ecuador, for its support and the facilities provided in the development of my Ph.D. program.

A special mention to the WiCIP lab of the University of Windsor, Dr. Sabbir Ahmed and all the members for sharing their knowledge and experience with me during my time as a Ph.D. student.

# Contents

<b>Declaration of Co-authorship / Previous Publications</b>	<b>iii</b>
<b>Abstract</b>	<b>vi</b>
<b>Dedication</b>	<b>vii</b>
<b>Acknowledgements</b>	<b>viii</b>
<b>List of Figures</b>	<b>xv</b>
<b>List of Tables</b>	<b>xvi</b>
<b>List of Abbreviations</b>	<b>xvii</b>
<b>1 Introduction</b>	<b>1</b>
1.1 Research Objectives . . . . .	1
1.2 Radio Electrical Spectrum Basics . . . . .	2
1.3 Motivation . . . . .	3
1.4 Contributions . . . . .	3
1.5 Thesis Organization . . . . .	4
<b>2 Background</b>	<b>5</b>
2.1 TVWS at a Glance . . . . .	5
2.2 Cognitive Radio Fundamentals . . . . .	6
2.3 Cognitive Radio at a Glance . . . . .	9
2.4 Applications for TVWS . . . . .	10
2.5 Use of TVWS for Disaster Relief Communications . . . . .	11
2.6 Use of TVWS for Rescue and E-calls . . . . .	12
<b>3 Sensing the Spectrum</b>	<b>13</b>
3.1 Spectrum Sensing Techniques . . . . .	13
3.1.1 Energy Detection . . . . .	13
3.1.2 Noise Considerations . . . . .	14
3.1.3 Additional Considered Parameters . . . . .	15

	Pilot Detection (PD) . . . . .	15
	Information from an External Source . . . . .	16
	TV Decoded Signal Visualization Device . . . . .	17
3.2	Designing a Spectrum Sensing Station . . . . .	17
	Hardware . . . . .	18
	Software . . . . .	18
3.2.1	Spectrum Analyzer Tektronix MDO4054-3 . . . . .	19
	SA Technical characteristics . . . . .	19
3.2.2	RF Explorer Sub1G . . . . .	19
	RFE Technical characteristics . . . . .	19
	Technical characteristics . . . . .	20
3.3	Designing a Mobile Spectrum Sensing Station . . . . .	21
3.4	Data Collection Procedure . . . . .	22
3.4.1	Fixed Data Collection . . . . .	23
	Sensing Procedure . . . . .	23
	Comparing the DAI Performance . . . . .	24
3.4.2	Mobile Data Collection . . . . .	25
<b>4</b>	<b>Stochastic Analysis of TVWS</b>	<b>27</b>
4.1	Sensing the TV Signal . . . . .	27
4.2	Identifying the Noise Level . . . . .	28
4.3	Threshold Considerations . . . . .	30
4.4	Probabilistic Considerations . . . . .	32
4.4.1	Working with Normal Distributions . . . . .	32
4.4.2	Obtaining pdfs . . . . .	36
	RFE Device . . . . .	36
	SA Device . . . . .	37
4.4.3	Performance Metrics . . . . .	37
	Probability of False Alarm: $P_{fa}$ . . . . .	37
	Probability of Detection: $P_d$ . . . . .	38
	Probability of Missed-Detection: $P_m$ . . . . .	38
4.4.4	Calculation of Threshold $T$ . . . . .	38
	Threshold Minimum and Maximum . . . . .	40
4.4.5	Adaptive Threshold . . . . .	42
<b>5</b>	<b>Proposed Model</b>	<b>45</b>
5.1	Hardware Configuration . . . . .	45
5.1.1	Spectrum Sensing Station (SSS) . . . . .	45
	Energy considerations . . . . .	46

Attenuation Consideration . . . . .	47
Devices Connection and Communication . . . . .	48
5.1.2 Mobile Spectrum Sensing Station (M-SSS) . . . . .	49
Energy considerations . . . . .	50
Spatial Separation of the Data Readings . . . . .	50
Amount of Data Collected . . . . .	50
5.2 Data Processing . . . . .	51
5.2.1 Data Processing - SSS . . . . .	51
5.2.2 Data Processing - M-SSS . . . . .	52
5.3 Stochastic Considerations . . . . .	53
5.3.1 Decision Procedure . . . . .	54
5.3.2 Output Representation . . . . .	55
<b>6 Results and Discussion</b>	<b>56</b>
6.1 Data Characteristics . . . . .	56
Considerations . . . . .	57
6.2 Samples Analysis . . . . .	57
6.3 Results Presentation . . . . .	63
Channels Occupancy . . . . .	63
Spectrum Sensing Station SSS . . . . .	64
Mobile Spectrum Sensing Station M-SSS . . . . .	64
6.4 Variability of the sensed Signals . . . . .	65
<b>7 Conclusion and Future Work</b>	<b>67</b>
7.1 Conclusions . . . . .	67
7.2 Future Work . . . . .	68
<b>Bibliography</b>	<b>70</b>
<b>Appendix A</b>	<b>75</b>
<b>Appendix B</b>	<b>79</b>
<b>Appendix C</b>	<b>80</b>
<b>Vita Auctoris</b>	<b>82</b>

# List of Figures

2.1	CR cycle, the spectrum is sensed, analyzed, and a decision is taken based on the presence or absence of PUs. . . . .	8
2.2	Use of TVWS to provide communications to the First Response Institutions (FRI) and the Public Safety Answering Point (PSAP) during an earthquake. . . . .	11
2.3	Diagram of the E-call procedure, the accident vehicle send a message through the idle channels of TV spectrum to reach the nearest PSAP. . . . .	12
3.1	Graphical representation of Energy Detection when peaks of the signal contain a power (yellow area) higher than the Threshold (green line). . . . .	14
3.2	Overlapped plots for the composed signal in red and noise in blue, (a) for RFE and (b) for SA. . . . .	15
3.3	Pilot tone detected in channel 20 ( $506.31\text{MHz} \pm 100\text{KHz}$ ). . . . .	16
3.4	Proposed SSS to sense spectrum in indoor and outdoor fixed locations. . . . .	18
3.5	A portable version of the SSS used to sense indoor spectrum. . . . .	20
3.6	Initial diagram for the M-SSS, designed to be mounted in a vehicle and sense the TV spectrum in wide geographical areas. . . . .	21
3.7	M-SSS (a) design diagram, (b) station mounted, (c) supporting structure built in CPVC, (d) supporting installed in the vehicle, (e) Winegard and GPS antennas, and (f) M-SSS in operation. . . . .	22
3.8	TV Signal sensed an RFE (blue line) and a SA (red line) are compared. The general shape that contains the energy is easily identified in the plot obtained with both devices. . . . .	24
3.9	Trajectories and locations to represent the TV spectrum sensed in the city of Windsor. . . . .	25
3.10	Visualization of the TV signal sensed using an RFE device, the readings were taken every 0.340s, the axis represents frequency, time and power in dBm, respectively. . . . .	26

4.1 TV Signal sensed with (a) RFE and (b) SA are compared. The general shape that contains the energy under the red line is easily identified in both devices. . . . . 28

4.2 Proposed M-SSS to sense in parallel the Noise  $W(f)$  and the composite signal  $X(f)$ . . . . . 29

4.3 TV Signal sensed with (a) RFE and (b) SA are compared. The  $W(f)$  and  $X(f)$  are observed and permit infer their possible relationship. . . . . 29

4.4 TV Signal sensed with (a) RFE and (b) SA are compared. The  $\bar{W}(f)$  and  $X(f)$  are observed and it is considered the noise level for that specific data collected. . . . . 30

4.5 Comparison of the signal sensed with (a) RFE and (b) SA. In both sub-figures are plotted  $X(f)$ ,  $\bar{W}(f)$ , and the different values for  $M$  or  $T$ . . . . . 31

4.6 Noise signal sensed  $W(p)$ . (a) Histogram of the collected data. (b) Normal probability plot of the same data read. (c) CDF of the Kolmogorov-Smirnov Test (KST) applied. . . . . 32

4.7 Composite signal plus noise sensed  $Xo(p)$ . (a) Histogram of the collected data. (b) Normal probability plot of the distribution for the same reading (c) CDF of the Kolmogorov-Smirnov Test (KST) applied. . . . . 33

4.8 The curve  $Xo(p)$  of the multi-modal distribution of (a) can be assumed as the normal distribution curve  $X(p)$  of (b), this assumption summarized in (c) allow us to reduce the calculation complexity of the proposed model. . . . . 33

4.9 Readings taken in three different points, the pdf for the noise  $W(p)$  is plotted in blue, multi-modal composite signal  $Xo(p)$  in magenta, and composite signal  $X(p)$  in red. In (a) are shown the pdf of the noise for each location. In (b), the intersection point "A" of  $W(p) \cap Xo(p)$  and its projection to the power axis "A'". In (c), the intersection point "B" of  $W(p) \cap X(p)$ , and its projection to the power axis "B'", we also observe that the difference between A' and B' is minimum concerning the power level of the signal in dBm. . . . . 34

4.10 Normal distribution pdfs for  $W(p)$  in blue and assumed  $X(p)$  in red, both used to calculate the  $P_{fa}$  and the  $P_d$  according to the model proposed in this dissertation. . . . . 35

4.11	Neyman Pearson model, the null hypothesis and the alternative hypothesis are observed. . . . .	36
4.12	Pdf of $W(p)$ in blue and $X(p)$ in red, taken from the data collected with (a) RFE and (b) SA. . . . .	37
4.13	Graphical representation of the $P_m$ , $P_{fa}$ , and $P_d$ , generated by the $T$ and the pdf curves for $W(p)$ and $X(p)$ . . . . .	38
4.14	Minimum and maximum possible values for $M$ . . . . .	39
4.15	pdf of the $W(p)$ and $X(p)$ taken from the data read with (a) RFE and (b) SA, the $M_{min}$ and $M_{max}$ are identified. . . . .	40
4.16	Comparison of the signal sensed with (a) RFE and (b) SA. In both panels the adaptive $T$ is plotted, comparing with the $T$ proposed by other related works. . . . .	42
4.17	Composite signal and noise sensed in point P11, (a) Frequency vs power, (b) pdf of the sensed signals. . . . .	42
4.18	Visual representation of a $T$ that observes a $P_{fa}=3\%$ . . . . .	43
4.19	ROC: (a) for the proposed model with the area of interest coloured; (b) for Neyman Pearson model. . . . .	43
4.20	Detailed ROC curve for samples taken. . . . .	44
5.1	Proposed SSS for fixed outdoor and portable indoor sensing purposes. . . . .	46
5.2	Portable SSS to sense the spectrum in indoor environments. . . . .	47
5.3	Attenuation introduced by the splitter, the theoretical value is 7 dB, (a) for RFE and (b) for SA. . . . .	47
5.4	Applications used to collect data, (a) for RFE, (b) for SA, and (c) for RTL-SDR. . . . .	48
5.5	M-SSS to sense spectrum over a mobile platform to sense wide geographical areas, (a) original diagram, (b) proposed configuration. . . . .	49
5.6	Data collection, 1 reading is composed by 112 samples for the composite signal, 112 samples for noise, separation between two samples is 1.76 MHz, all 112 samples covers 198 MHz which is the UHF TV bandwidth. . . . .	51
5.7	Proposed SSS for fixed and portable sensing purposes in outdoor and indoor environments. . . . .	52
5.8	Proposed M-SSS to sense spectrum over a mobile platform to sense wide geographical areas. . . . .	53
5.9	Proposed M-SSS to sense spectrum over a mobile platform to sense wide geographical areas. . . . .	54

5.10 Proposed graphical representations of results. . . . . 55

6.1 Four trajectories were defined to sense the UHF TV spectrum in the city of Windsor, T1 red, T2 purple, T3 blue, and T4 orange. . . 57

6.2 P11 (a) Spectrum diagram, (b) pdf of the noise and composite signal, and (c) Receiver Operation Characteristics curve with the  $P_{fa}$  vs  $P_d$ . . . . . 58

6.3 Sub-figures (a) to (j) spectrum vs power sensed in Points 1 - 10, there are variations on the energy detected due to the different location in which the samples were taken. . . . . 59

6.4 Sub-figures (a) to (j) pdf of the  $W(p)$  and  $X(p)$  sensed in Points 1 - 10. . . . . 60

6.5 Sub-figures (a) to (j) ROC curves of the signal sensed in Points 1 to 10. . . . . 61

6.6 ROC curves obtained from P1 - P10, in (a) are present all the curves, and in (b) are shown the same plot but zooming in to observe the curves with a  $P_{fa}$  closer to the one defined by the adaptive  $T$  of 3%. . . . . 62

6.7 Dotted lines are the  $P_{famax}$ ,  $P_{fa}$  calculated with the adaptive  $T$ , and  $T$  obtained by using a  $M$  of 5, 7, and 10dB respectively. It is observed that the adaptive  $T$  proposed increases at least 9.63% of  $P_d$  than the values used by other authors. . . . . 63

6.8 Location of the represented points . . . . . 64

6.9 Spectrum detected and analyzed with the proposed model. (a) central south part of the city, (b) southeast, (c) middle east, and (d) eastern limit of the city of Windsor. Note that as far of the center the sample is taken, less PU are detected. . . . . 65

6.10 Plot of the Confidence Interval (CI) of average values for  $W(p)$  and  $X(p)$ , the variations are represented in dB. . . . . 66



# List of Tables

2.1	Bands assigned to the TV broadcasting service, frequencies, channel numbers, partial Bandwidth (BW), and ITU regions. . . . .	5
2.2	UHF TV channels with their characteristics frequencies in MHz. . . . .	7
3.1	Active TV channels received in Windsor area. . . . .	17
3.2	DAI's features and performance comparison . . . . .	25
3.3	Trajectories defined to sense the TV spectrum in the city of Windsor	26
4.1	Estimated values for $P_{fa}$ , $F(z)$ , and $z$ . . . . .	41
5.1	Communication from the three DAI to the PC to save data collected in the DB. . . . .	48
5.2	Communication from the three DAI to the PC to save data collected in the DB. . . . .	49
5.3	Distance between data readings and speed. . . . .	50
5.4	Decision Procedure, true table. . . . .	55
6.1	Number of readings and samples collected with each RFE. . . . .	56

# List of Abbreviations

<b>AWGN</b>	Additive White Gaussian Noise
<b>BS</b>	Base Station
<b>CAD</b>	Canadian Dollar
<b>CBD</b>	Co-variance Based Detection
<b>CDF</b>	Cumulative Density Function
<b>CEI</b>	Centre for Engineering and Innovation
<b>CI</b>	Confidence Interval
<b>CPVC</b>	Chlorinated Polyvinyl Chloride
<b>CR</b>	Cognitive Radio
<b>CSD</b>	Cyclo-Stationary Detection
<b>CSV</b>	Comma Separated Values
<b>DAI</b>	Data Acquisition Instrument
<b>DB</b>	Database
<b>dB</b>	Decibel
<b>dBm</b>	Decibel with reference to one milliwatt
<b>DSA</b>	Dynamic Spectrum Access
<b>ED</b>	Energy Detection
<b>EDRC</b>	Emergencies and Disaster Relief Communications
<b>FCC</b>	Federal Communications Commission
<b>FRI</b>	First Response Institutions
<b>GHz</b>	Gigahertz
<b>GPS</b>	Global Positioning System
<b>HD</b>	High Definition
<b>IEEE</b>	Institute of Electrical and Electronic Engineers
<b>ISM</b>	Industrial, Scientific and Medical
<b>IoT</b>	Internet of Things
<b>ITU</b>	International Telecommunications Union
<b>KHz</b>	Kilohertz
<b>KST</b>	Kolmogorov-Smirnov Test
<b>M</b>	Margin
<b>Mmin</b>	Minimum Margin
<b>Mmax</b>	Maximum Margin

<b>MFD</b>	Matched Filtering Detection
<b>MHz</b>	Megahertz
<b>ML</b>	Machine Learning
<b>M-SSS</b>	Mobile Spectrum Sensing Station
<b>OS</b>	Operating System
<b>PD</b>	Pilot Detection
<b>Pd</b>	Probability of Detection
<b>pdf</b>	Probability Density Function
<b>Pfa</b>	Probability of False Alarm
<b>PHY</b>	Physical Layer
<b>Pm</b>	Probability of Missed-detection
<b>PSAP</b>	Public Safety Answering Point
<b>PU</b>	Primary User
<b>RBW</b>	Resolution Bandwidth
<b>RF</b>	Radio Frequency
<b>RFE</b>	Radio Frequency Explorer
<b>ROC</b>	Receiver Operating Characteristic
<b>RTL-SDR</b>	Register-Transfer Level Software Defined Radio
<b>SA</b>	Spectrum Analyzer
<b>SD</b>	Standard Definition
<b>SDR</b>	Software Defined Radio
<b>SSS</b>	Spectrum Sensing Station
<b>SU</b>	Secondary User
<b>T</b>	Threshold
<b>TDR</b>	Telecommunications for Disaster Relief
<b>Tmax</b>	Threshold maximum
<b>Tmin</b>	Threshold minimum
<b>TVBS</b>	Television Black Spaces
<b>TVGS</b>	Television Gray Spaces
<b>TVWS</b>	Television White Spaces
<b>UHF</b>	Ultra High Frequency
<b>U-NII</b>	Unlicensed National Information Infrastructure
<b>USB</b>	Universal Serial Bus
<b>WiCIP</b>	Wireless Communications and Information Processing Lab
<b>WLAN</b>	Wireless Local Area Network
<b>WRAN</b>	Wireless Regional Area Network
<b>WS</b>	White Spaces
<b>WSN</b>	Wireless Sensor Network

# Chapter 1

## Introduction

In the last 10 years, the world has experienced impressive growth in wireless communication technologies leading to the emergence of new devices and services at an unprecedented pace. This, in turn, has created a great and ever-increasing demand for electromagnetic spectrum for data transfer. Usage of the electromagnetic spectrum, as it stands today, shows a peculiar characteristic. While some parts of the spectrum are extremely crowded, some other parts are underutilized. Thus there is scarcity as well as wastage [1], [2].

Cognitive Radio or CR that proposes smart sharing of the unused frequencies can be a promising solution to increasing spectrum usage efficiency. CR uses different spectrum sensing techniques to detect unused channels and then allows opportunistic usage of such channels by Secondary Users (SU), i.e., unlicensed users, without interfering with Primary Users (PU), i.e., licensed users. The unused electromagnetic spectrum bands are known as White Spaces (WS), and the technique of opportunistically using the WS is called Dynamic Spectrum Access (DSA). Again, WS that fall in the electromagnetic spectrum bands used by Television broadcasting services is known as TV White Spaces (TVWS) [3]. Irrespective of which spectrum is being used, CR requires that harmful interference to PU must be avoided at all time.

TV spectrum bands often show underutilization by PU and hence use of TVWS in CR is a promising solution to spectrum scarcity. In context to this, the Institute of Electrical and Electronics Engineers (IEEE) approved the 802.22 standard in 2011 [4]. But finding a model that allows accurate identification of TVWS, minimizing false alarms and errors is a challenging issue.

### 1.1 Research Objectives

This work is oriented to develop an accurate probabilistic model to identify the occupancy of the spectrum in UHF TV bands, based on the Probability of False

Alarm ( $P_{fa}$ ) and the Probability of Detection ( $P_d$ ) of the sensed signals. Thus the research objectives are:

- To develop a probabilistic and accurate model to identify TVWS.
- To design and implement a Spectrum Sensing Station (SSS) and a Mobile Spectrum Sensing Station (M-SSS).
- To find the best low-cost detector for TVWS.
- To collect, analyze, and find the characteristics of the data related to UHF TV Spectrum in the city of Windsor - ON, Canada.

## 1.2 Radio Electrical Spectrum Basics

Radio spectrum is a part of the electromagnetic spectrum that corresponds to the frequencies used by wireless based communications, i.e., radio, TV, cell-phone companies, satellite services, and more. The frequency used for each service has a direct relationship between distance and data rate that the signal can transmit [5].

There are two types of frequency bands, licensed and unlicensed. The first group requires a payment of a licensing fee to use it, which implies the exclusivity and the certainty of no interference from other wireless users [6]. The local regulation authority is the entity that manages the radio-electrical spectrum and obtains funds from the auction of those licensed bands. The second group are the unlicensed bands, which do not require any permissions or payment for use the spectrum, but for that reason, they are vulnerable to interference due to the reduced number of unlicensed bands and the increasing number of users that are competing for accessing to those free bands.

According to [5], *"A common misconception is that the escalating number of consumers and their rapidly growing usage of futuristic devices is causing a shortage of radio spectrum. A major reason for spectrum scarcity is conventional static spectrum management, which utilizes the spectral resources inefficiently"*. In other words, the actual spectrum distribution was made by the regulators in the last century, when radio or TV broadcast were the latest technologies, a scenario which is entirely different to current situation where new technologies and applications are demanding more spectrum for their data transmission needs. This is the cause of the spectrum scarcity, as indicated in [5].

To solve this scarcity, the use of CR has been proposed [7]. The International Telecommunications Union (ITU) defines CR as “*A radio system employing technology that allows the system to obtain knowledge of its operational and geographical environment established policies and its internal state; to dynamically and autonomously adjust its operational parameters and protocols according to its obtained knowledge in order to achieve predefined objectives, and to learn from the results obtained*” [8].

### 1.3 Motivation

The motivation of this research endeavour is to use CR techniques to discover TVWS for other spectrum demanding wireless services and applications. For example, Wireless Regional Area Networks (WRAN), internet access for rural areas, Wireless Sensor Networks (WSN), Emergency Communications (EC), and Telecommunications for Disaster Relief (TDR). Particularly, the last two applications, i.e., EC and TDR, attracted all my attention because they are both related to rescuing lives. With a long experience in public safety issues, i.e., as a former member of the armed forces and as part of the 911 emergency services implementation team, I feel that using CR based wireless communications as the communications platform, should be given a priority for providing emergency services. For this, the first step is to identify which frequencies can be used to provide those services. Again for identifying available frequencies, a probabilistic model is needed, complemented with a novel low-cost sensing technique.

### 1.4 Contributions

The contributions in this thesis can be divided into four parts, e.g. technique and configuration of the sensing hardware used, sensing techniques applied, probabilistic model applied, and results of the sensed spectrum in the city of Windsor.

- Propose a technique that senses the spectrum in a different manner that considers the simultaneous use of hardware to measure the noise and the composite signal and noise, to improve detection accuracy.
- Propose a technique by combining Energy Detection (ED), Pilot Detection (PD), and information obtained from an external source to reduce the missed detection probability.

- The develop a probabilistic model consisting of false alarm probability and detection probability to ensure better results than other methods applied to identify TVWS.
- A prototype was designed and implemented to demonstrate the developed technique for TVWS spectrum sensing. This prototype was used to sense the spectrum across the city of Windsor in Canada.

## 1.5 Thesis Organization

This dissertation is composed of 6 chapters.

Chapter 1 provides an introduction, contributions of the research, and explains the general organization of the document.

Chapter 2 presents the background and motivation for the study. Major concepts used, a brief discussion of the applications of TVWS in telecommunications, and a special mention in telecommunications for disaster relief.

Chapter 3 provides TVWS concepts, spectrum bands used, sensing techniques, and additional parameters needed to understand and exploit the smart spectrum sharing.

Chapter 4 presents the mathematical and statistical considerations oriented to identify the parameters that take part in this dissertation, characteristics of the sensed signals, probabilities, and more related information.

Chapter 5 presents the proposed model, the hardware configuration to sense the spectrum results obtained in the survey conducted along the city of Windsor, and the contributions.

Chapter 6 describes the results obtained in the survey and information collected in the city of Windsor.

In Chapter 7, conclusions from the thesis will be provided. The strengths of the proposed model and its applicability in different types of wireless telecommunications services. Scope and constraints of this research will be explained along with some directions for future research.

## Chapter 2

# Background

In this chapter, the basic concepts of spectrum, TVWS, CR fundamentals, Literature review, applications and specific cases of the use of TVWS will be reviewed.

### 2.1 TVWS at a Glance

In general, the unused and underutilized frequency spectrum spaces are referred to as WS. Efficient utilization of these white spaces has the potential to reduce the spectrum scarcity faced nowadays with the fast growth of wireless technologies. According to [5], the characteristics of the WS are:

- (i) A white space is an unused radio frequency.
- (ii) Its existence depends on time, frequency, and geographical location.
- (iii) Its utilization should not cause any harm to the PU.

If this concept is transferred to the spectrum dedicated to TV broadcasting services, it is known as TVWS.

TABLE 2.1: Bands assigned to the TV broadcasting service, frequencies, channel numbers, partial Bandwidth (BW), and ITU regions.

Name	Frequencies	Channels	Partial BW	ITU Regions
Band I	54 - 72	2 to 4	18MHz	R1, R2, R3
Band I (Cont.)	76 - 88	5 to 6	12MHz	R2
Band III	174 - 216	7 to 13	42MHz	R1, R2, R3
Band IV	500 - 644	19 to 42	144MHz	R1, R2, R3
Band V	644 - 698	43 to 51	54MHz	R1, R2, R3

In this research, we are interested in the frequency bands assigned to the TV service, Table 2.1 illustrates the frequency ranges, channel numbers, bandwidth for each band, and the respective ITU regions [9] where the bands are allocated.



And from them, the sensing procedure took place in band IV and V, it means from 500 MHz to 698 MHz [10]. Frequency ranges for each channel, upper and lower limits, pilot tone, audio and video carriers of channels 19 to 51, are shown in Table 2.2. Note that channel 37 is used for radio astronomy and is excluded from TV broadcast services.

The reasons to choose the spectrum from bands IV and V (500 and 698 MHz) are explained next. First, there are standards as IEEE 802.22 that considers the TV band to access as a Secondary User (SU), it is due to the propagation characteristics of frequencies under 1 GHz. This standard is being applied and accepted by regulators in different countries [4]. This fact provides practical information, technically verified, and supported by an important organization like IEEE. Second, the selected range of frequencies offers 198 MHz (32 channels) of a continuous spectrum, excepting for channel 37 (608 to 614 MHz) the rest of bands IV and V are located continuously with more possibilities to find and use idle channels without significant modifications in the transmission parameters of the antennas. Third, more than one study has been demonstrated that exists underused TV spectrum in urban areas which present a significant increment in the rural areas [5].

## 2.2 Cognitive Radio Fundamentals

CR techniques provide the capability to share the spectrum in an opportunistic manner. DSA techniques allow cognitive radio to operate in the best available channel. The functionalities of CR are [11]:

- **Spectrum Sensing:** refers to identify the available spectrum channels and detect the presence of PU operating in a licensed band.
- **Spectrum Management:** is the possibility to select the best available channel from all the idle channels detected.
- **Spectrum Sharing:** refers to coordinate the smart access to a channel assigned to a PU when it is unused.
- **Spectrum Mobility:** is the option to vacate the channel when a PU is detected.

According to the Federal Communications Commission (FCC), a formal definition of CR is *"A Cognitive Radio is a radio that can change its transmitter parameters based on interaction with the environment in which it operates"* [12]. From the

TABLE 2.2: UHF TV channels with their characteristics frequencies in MHz.

Channel	Lower F.	Upper F.	Pilot	Video C.	Audio C.
19	500	506	500.31	501.25	505.75
20	506	512	506.31	507.25	511.75
21	512	518	312.31	513.25	507.75
22	518	524	518.31	519.25	523.75
23	524	530	524.31	525.25	529.75
24	530	536	530.31	531.25	535.75
25	536	542	536.31	537.25	541.75
26	542	548	542.31	543.25	547.75
27	548	554	548.31	549.25	553.75
28	554	560	554.31	555.25	559.75
29	560	566	560.31	561.25	565.75
30	566	572	560.31	567.25	571.75
31	572	578	572.31	573.25	577.75
32	578	584	578.31	579.25	583.75
33	584	590	584.31	585.25	589.75
34	590	596	590.31	591.25	595.75
35	596	602	596.31	597.25	601.75
36	602	608	602.31	603.25	607.75
37	608	614	Radio Astronomy		
38	614	620	614.31	615.25	619.75
39	620	626	620.31	621.25	625.75
40	626	632	626.31	627.25	631.75
41	632	638	632.31	633.25	637.75
42	638	644	638.31	639.25	643.75
43	644	650	644.31	645.25	649.75
44	650	656	650.31	651.25	655.75
45	656	662	656.31	657.25	661.75
46	662	668	662.31	663.25	667.75
47	668	674	668.31	669.25	673.75
48	674	680	674.31	675.25	679.75
49	680	686	680.31	681.25	685.75
50	686	692	686.31	687.25	691.75
51	692	698	692.31	693.25	697.75

above-cited definition, CR has two characteristics, i. e., *cognitivity* and *reconfigurability*. *Cognitivity* is the possibility of the device to sense the spectrum. This is not the simple monitoring of the power in a determined frequency band, it requires more elements to identify the temporal and spatial variations in the radio environment, all the time avoiding harmful interference to PU or to another SU. With this, it is possible to identify the unused channels or WS at a specific time or geographical location, giving the possibility to select the best operational parameters [13]. *Reconfigurability* is the capability that permits a dynamic reconfiguration of the operational parameters according to the radio environment. In other words, CR devices can transmit and receive on a variety of frequencies with different access technologies, thanks to its dynamic hardware features [14].

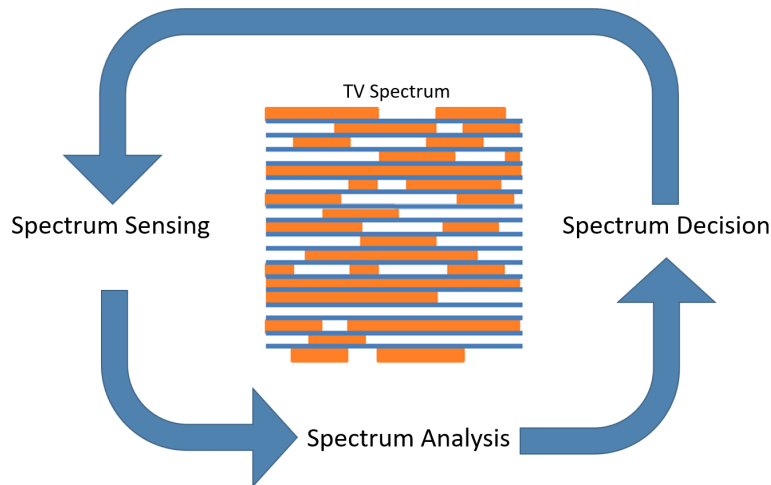


FIGURE 2.1: CR cycle, the spectrum is sensed, analyzed, and a decision is taken based on the presence or absence of PUs.

The cycle of the CR can be observed in Figure 2.1, a portion of the spectrum in a period of time  $t_i$  is represented, in orange are the signals of the PUs, in white are the TVWS, the first step consists in sensing the spectrum, this information is analyzed, and based on the result obtained, the device decides which TVWS is the best option to transmit its information.

This research is focused on the spectrum sensing and spectrum analysis stages of the CR cycle, specifically in the composite signal that contains the PU information.

## 2.3 Cognitive Radio at a Glance

Joseph Mitola coined Cognitive Radio as a term on his article published in 1999. There, the author describes how a CR could enhance the flexibility of personal wireless services through a new language called the radio knowledge representation language [7]. CR has a great potential to access the spectrum allowing the DSA, it can be described as “disruptive, but unobtrusive technology” [13], disruptive because it enables the SU to access to the PU licensed bands, and is unobtrusive because by controlling different parameters as access or transmission power, harmful interference to the PU are avoided.

The massive use of wireless services and devices to apply in mobile communications for public or private purposes is becoming very popular and is a clear example of how the actual society depends on the wireless services and of course on the radio spectrum [15]. It is very important to understand that the core of the wireless services that customers use are the unlicensed bands, i.e., Industrial, Scientific, and Medicine (ISM) band at 2.4 GHz and the Unlicensed National Information Infrastructure (U-NII) band at 5.2 GHz. These bands are accessed by users without the payment of any fee or the need to obtain a specific license. These bands have similar counterparts around the world, with international regulatory bodies working to align bands and regulations [16]. *“The popular use of unlicensed bands and the development of new devices and technologies led regulatory bodies like the FCC to consider opening further bands for unlicensed use. Whereas, spectrum occupancy measurements show that licensed bands, such as the TV bands, are significantly underutilized”* [15]. As an alternative to this particular fact, CR is considered the solution to the low usage of the radio spectrum [13]. This technology will permit the efficient and reliable spectrum usage by adapting the operation parameters of the radio according to the conditions of the environment, providing the capability to identify and exploit a large amount of unused or underused spectrum bands, allowing a smart sharing of this valuable limited resource.

In May 2004, the Federal Communications Commission (FCC) of the United States, proposed the creation of the 802.22 work-group for WRAN, the objective was to allow unlicensed users (SU) to operate in the TV broadcast bands, avoiding harmful interferences to the PU [17], the specific tasks were to develop the Physical (PHY) and Media Access Control (MAC) air interfaces.

Different authors started to write and propose spectrum sensing simulation models and techniques [4], [18]. The idea of a smart sharing of the spectrum is winning more adepts and the DSA considered as viable.

In 2011 the IEEE approves the IEEE 802.22 WRAN standard [17]. This is the first worldwide effort to define a standardized air interface based on CR techniques for the opportunistic use of TV bands on a non-interfering basis [15], [19].

Several articles consider different methods to identify idle channel over the spectrum, not only TV frequencies, in the case of [20], a detailed list of considerations and articles are described to know the different parameters considered to identify the occupation or not of a channel. In analyzed models are statistics with power detections, occupation and duty cycle; probability density function or cumulative density function with power detection, occupation and duty cycle; Markov chains; Linear regression; and spectrum prediction.

In [21], the authors propose a spectrum scanning method, considering the Bayesian inference, to estimate the channel occupancy rate, when taking into consideration the probabilities of false alarm and detection of the spectrum sensor, the author has an advantage over other methods that only consider the energy detection as unique element to define the presence or absence of a PU.

After analyzing the articles mentioned above, the author realized that there is the need to consider several parameters to evaluate a TV channel, the real instantaneous signal of the noise separately of the composite signal, the combining of sensing techniques, i.e. energy detection, pilot detection, and the information of an external source. These elements ensure the accuracy of the detected channels and can be used to apply or adapt the IEEE 802.22 standard.

## 2.4 Applications for TVWS

With the clear idea that TVWS are oriented to alleviate the spectrum scarcity, the potential applications have a wide range of possibilities. Among others are:

- Internet of Things (IoT).
- Wireless Local Area Networks (WLAN).
- Wireless Regional Area Networks (WRAN).
- Wireless Sensor Networks (WSN).
- Emergencies and Disaster Relief Communications (EDRC).

In the particular case of the author, EDRC are of special interest and the last objective of the present research, as is explained in [22].

## 2.5 Use of TVWS for Disaster Relief Communications

In any catastrophic event, the first few hours are the most critical time for locating and rescuing people alive. Usually, in a high impact disaster like an earthquake, a hurricane or a tsunami, most of the basic services and telecommunications networks collapse. But it is essential to provide communications to the First Response Institutions (FRIs) like Police, Health Services, Fire Brigades, National Guard, and other units deployed over the affected area [23].

A critical case was registered in 2005 when Hurricane Katrina hit the south of the United States and caused more than 1,900 casualties, about three million of landline phones were disconnected and more than 2,000 cell sites were out of service. In addition, 50% of radio stations and 44% of TV stations were put out of service [24]. Now, in such situations, it becomes essential to deploy alternative communication systems.

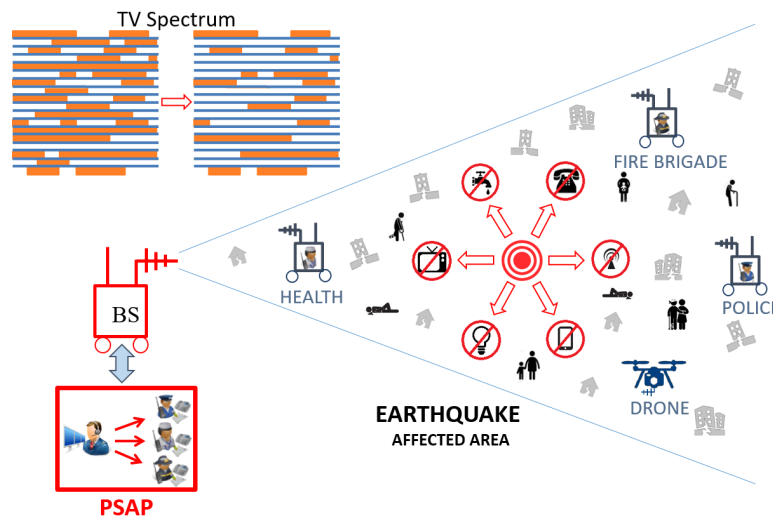


FIGURE 2.2: Use of TVWS to provide communications to the First Response Institutions (FRI) and the Public Safety Answering Point (PSAP) during an earthquake.

For example, the use of SDR and CR techniques can provide an alternative communications system to connect FRI and the Public Safety Answering Point (PSAP) in the specific case of an earthquake that affects a populated area, as is illustrated in Figure 2.2, another additional element to regard is the increasing of TVWS in the affected area, considering that after the earthquake most of the basic services including cellphone networks, radio and TV broadcast companies result affected and its service is not available.

In the same scenario, the use of Unmanned Aerial Vehicles (UAVs) would solve the problem of the telecommunications infrastructure to be deployed in the affected area, if they are equipped with a portable TVWS radio. After identifying the area impressed by a disaster, i.e. an earthquake, the nearest PSAP dispatches the respective FRIs to the affected area. The units bring with them all the operative equipment, including the UAVs for telecommunications.

When the units arrive, each FRI deploys its UAV equipped with an SDR on board. The device will search the radio-electrical spectrum, looking for other similar radios or Base Stations (BS) in the area. Once the radio connects with other active radio(s), the repeater mode will start to operate. The UAV can be used as a mobile BS that allows the operative communications between the rescue teams deployed over the mentioned affected area.

All of these initiatives have been motivated by the regulation of FCC for CR deployment [25], and it has produced an increasing interest in the TVWS spectrum bands.

## 2.6 Use of TVWS for Rescue and E-calls

The advanced automatic collision notifications or E-call is a system automatically activated when the in-vehicle sensors receive signals of a serious accident or crash [26]. At that moment, a telecommunications transceiver sends the accident alert information to the nearest PSAP, and this information can include the time of the accident, the location of the crashed vehicle, reference points, or the last-known travel direction. An additional way to activate this alarm is by manually pushing the emergency button when an accident is witnessed. The option to use TVWS to transmit E-calls service in rural roads is very interesting, in Figure 2.3 is represented how a crashed vehicle is sending a basic E-call packet of information over the TV spectrum, taking advantage of the TVWS and reaches the nearest PSAP.

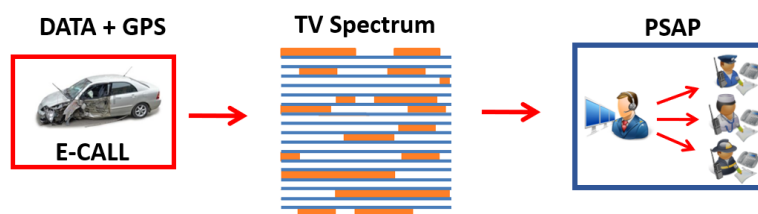


FIGURE 2.3: Diagram of the E-call procedure, the accident vehicle send a message through the idle channels of TV spectrum to reach the nearest PSAP.

## Chapter 3

# Sensing the Spectrum

As depicted in Figure 2.1, CR works in a cycle of operations that include spectrum sensing, spectrum analysis, and spectrum decision. In this chapter, we review the applied spectrum sensing techniques and present the design of a Spectrum Sensing Station (SSS) and a Mobile Spectrum Sensing Station (M-SSS) which are used to collect data. Also, we report the on-field UHF TV spectrum detection survey conducted in the city of Windsor. The survey data and analyzed results show characteristics of the channels mentioned above.

### 3.1 Spectrum Sensing Techniques

Spectrum sensing is the first and the most important functionalities of CR. The objective of spectrum sensing is to detect the presence of a PU. Considering that PU has the licence to use the spectrum band, its opportune detection is a critical part of the smart spectrum sharing. With this in mind, spectrum sensing techniques are able to detect those unused portions of the spectrum. The most frequently used spectrum sensing techniques are Energy Detection (ED), Matched Filter Detection (MFD), Cyclo-Stationary feature Detection (CSD), and Co-variance Based Detection (CBD) [27] [28] [29] [30] [31]. In this research, ED has been used for its simplicity but combined with other elements to ensure its accuracy and effectiveness.

#### 3.1.1 Energy Detection

Energy Detection (ED) technique is the simplest and most commonly used approach in CR. To apply ED, it is not necessary to have a deep knowledge of the PU signal, it only needs to have a valid reference of the noise power [32]. To apply this technique, the average of the signal sensed in a channel is compared with a predetermined Threshold ( $T$ ), which depends on the noise power [31], [33].



Figure 3.1 illustrates a portion of the UHF TV spectrum, it is easy to observe a yellow peak of the signal which has a higher power in relation to the selected  $T$  represented in this case with a green line.

The energy of the signal  $E_c$  along channel  $C$  is obtained by dividing the sum of the magnitude squared of the measured signal,  $|x_i(\Delta f)|^2$ , by the number of collected samples,  $n$ , as is shown in Eq. (3.1).

$$E_c = \frac{1}{n} \sum_{i=1}^n |x_i(\Delta f)|^2 \quad (3.1)$$

where  $\Delta f$  is the bandwidth of the channel sensed [10], [34]. Here, we observe again, the need to define the noise reference level to calculate the  $T$ .

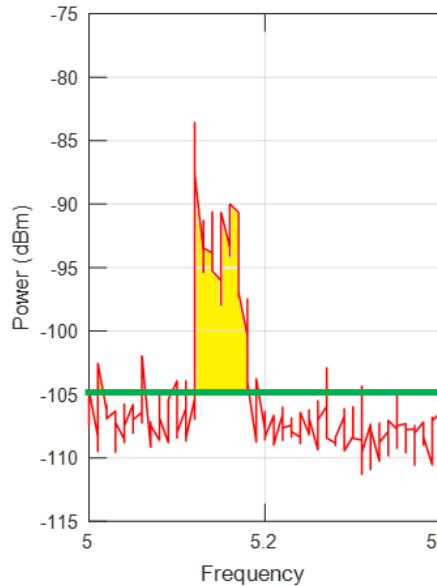


FIGURE 3.1: Graphical representation of Energy Detection when peaks of the signal contain a power (yellow area) higher than the Threshold (green line).

### 3.1.2 Noise Considerations

It is evident that a valid reference of the noise level  $W(f)$  is needed to determine the value of  $T$ . Here, there are two possibilities, one is to sense the TV spectrum and compare with a statistical parameter of the noise  $W(f)$  obtained in previous measurements and observations. Second is to have an instantaneous sample of the pure noise  $W(f)$  taken simultaneously to the TV signal for each geographical point and  $(t_i)$  time instant.

The level of  $W(f)$  can be obtained by replacing the Winegard antenna with a  $50\Omega$  load and taking measurements for this load, to register the noise of the system at that precise instant of time [20]. The  $50\Omega$  load corresponds to the input impedance of the RF-Explorer (RFE) used to sense the noise signal [35].

For this research, we decided to use this second option, adding an extra RFE device with a  $50\Omega$  load attached to the main RFE that senses the TV signal.

In Figure 3.2 are illustrated both signals sensed and plotted together, the noise and the composed signal plus noise, collected with a RFE and Spectrum Analyzer (SA) respectively.

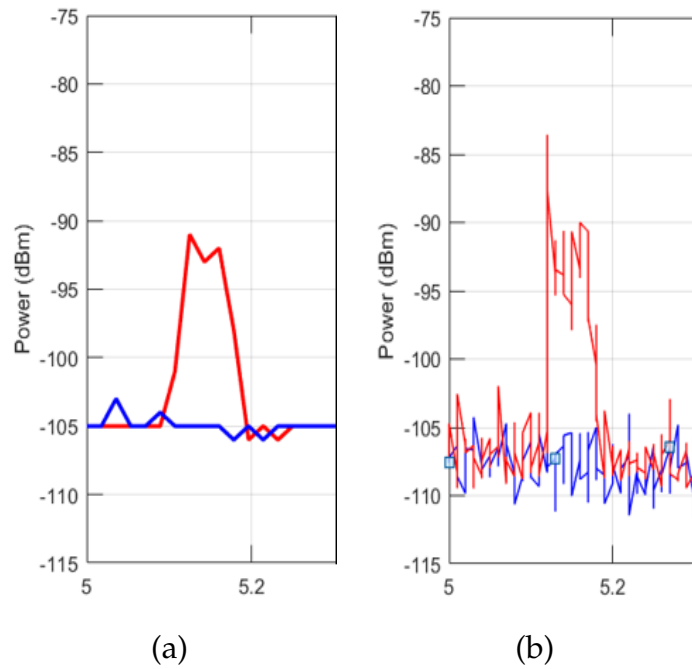


FIGURE 3.2: Overlapped plots for the composed signal in red and noise in blue, (a) for RFE and (b) for SA.

### 3.1.3 Additional Considered Parameters

With the purpose of ensuring the PU detection, additional parameters had been considered. First is the pilot tone which can be found in specific frequencies of the channel. Second is the information obtained from an external source. And third, a TV device attached to the SSS.

#### Pilot Detection (PD)

The pilot tone of a TV channel usually is located at a frequency of  $310\text{KHz} \pm 5\%$  above the lower edge of the channel [36]. By configuring the RTL-SDR device to sense the pilot tone frequency with a bandwidth  $\pm 100\text{KHz}$ , for each

channel, it is possible to collect the samples, the device then jumps to the next channel by increasing 6MHz to the sampled frequency, when it reaches channel 51 (592.310MHz), it returns to channel 19 (500.310MHz) and repeats the cycle. If a pilot tone was detected, that channel was considered as a potentially used.

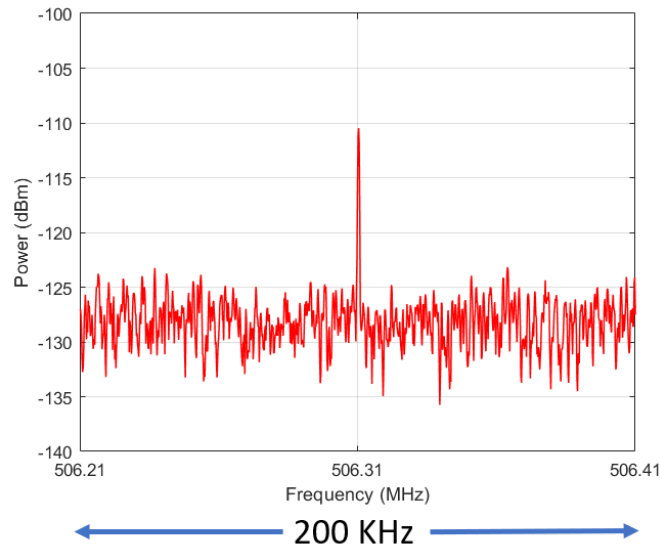


FIGURE 3.3: Pilot tone detected in channel 20 ( $506.31\text{MHz} \pm 100\text{KHz}$ ).

### Information from an External Source

In this case, it is a database (DB) of the channels, frequencies, and signal strength available in the city of Windsor, according to an authorized provider. Additionally, we use the information of those channels received and decoded by a conventional TV receptor attached to the SSS. The channels with enough nominal reception power, are considered as TV Black Spaces (TVBS), and its use is banned. Results of the  $E(f)$  are displayed in Table 3.1.

Here is observed that six channels have high power and presence detected by our TV set, they are divided into 19 sub-channels; six of them are High Definition (HD), 12 are Standard Definition (SD), and one is used for audio only (used to re-transmit the 910KHz AM radio signal).

TABLE 3.1: Active TV channels received in Windsor area.

Channel	Sub-channel	Type	Station/Network
20	1	HD	WYMD-HD
	2	SD	WMYD-AT
	3	SD	WMYD-ES
26	1	HD	CHWI
31	1	HD	ION
	2	SD	QUBO
	3	SD	IONLIFE
	4	SD	SHOP
	5	SD	QVC
	6	SD	HSN
32	1	HD	TVO
38	1	HD	WADL-HD
	2	SD	GRIT
	3	SD	GET TV
	4	SD	COZI TV
	5	SD	THE WORD
	6	SD	JUSTICE
	7	Audio	910 AM
50	1	HD	WKBD-HD

### TV Decoded Signal Visualization Device

It consists of a TV set connected to the receptor antenna of the SSS. Its purpose is to visualize the decoded signal of the received channels. In other words, it is used to verify the real reception of the TV stations that are mentioned as active in the DB of the previous point, as a redundant resource to ascertain the presence of PU.

## 3.2 Designing a Spectrum Sensing Station

Once the spectrum to be analyzed was selected, the next step is to identify the software and hardware that allow us to collect information of the UHF TV spectrum from the Wireless Communications and Information Processing Research (WiCIP) Laboratory.

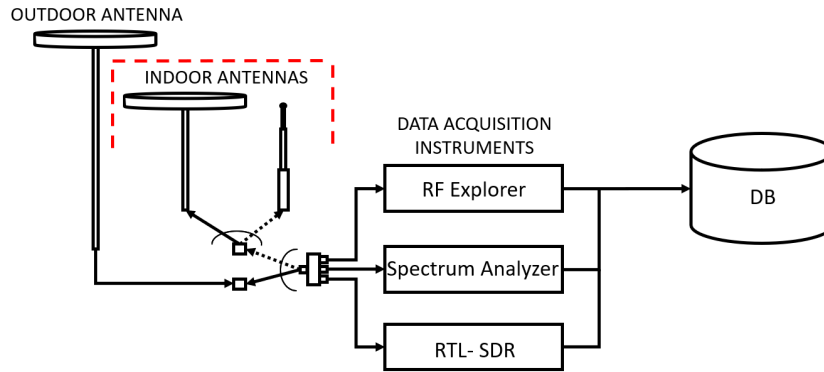


FIGURE 3.4: Proposed SSS to sense spectrum in indoor and outdoor fixed locations.

Figure 3.4 shows a diagram for the SSS, it has three versions: A fixed SSS, for outdoor spectrum sensing, a portable SSS for indoor spectrum sensing, and a M-SSS, Figure 3.5 shows the portable version for indoor use. For implement the SSS the components described below were used.

### Hardware

- Antenna Winegard, model MS-3005 VHF/UHF, 14.9".
- 3-way satellite TV splitter, 5MHz to 2050MHz, F - female connectors, 75 $\Omega$  nom. impedance.
- Spectrum Analyzer Tektronix MDO4054-3.
- RF Explorer Sub1G.
- RTL SDR 2832U.
- DELL laptop, Intel i-5-5200U CPU @ 2.20GHz, RAM 6GB, 64-bits OS.

### Software

- RF Explorer for Windows, Version v1.23.1711 - for use with firmware v1.23.
- AIRSPY Windows SDR Software Package.
- Matlab Student version 2017.
- CubicSDR v0.2.2- OS X.
- Gqrx Mac OS X 10.11.
- Tektronix Openchoice Desktop Application TDSPCS1 - v2.6

### 3.2.1 Spectrum Analyzer Tektronix MDO4054-3

It is an oscilloscope with a built-in spectrum analyzer, made by Tektronix [37], it permits to capture time-correlated analog, digital, and RF signals.

#### SA Technical characteristics

- Frequency Range 50KHz to 3GHz.
- Bandwidth 500MHz.
- Span 1KHz to 3GHz.
- Frequency Resolution 20Hz to 10MHz.
- Average Noise Level -115dBm.
- Amplitude Resolution 0.5dBm.
- Automatic RBW 2.6KHz to 600KHz.
- Price: \$7,950.00CAD.

### 3.2.2 RF Explorer Sub1G

RF Explorer is a portable spectrum analyzer designed for the specific needs of digital radio frequency communication. It is able to display full frequency spectrum in the band, existed spread spectrum activity, bandwidth to monitor collisions, and frequency deviation from the expected tone, etc. The workflows are supported by RF Explorer, which include detection of expected transmission and power, automatically resolving Resolution Bandwidth (RBW) and sweep time and spectrum data calculations. Moreover, real-time or adjusted signals, 3D spectrogram waterfall, Comma-Separated Values (CSV) export, high-quality graphics, and a large feature set can be performed through cooperated work between RFE and Windows on PC [35].

#### RFE Technical characteristics

- Frequency Range 240MHz to 960MHz.
- Span 0.112MHz to 300MHz.
- Frequency Resolution 1KHz.
- Average Noise Level -115dBm.

- Amplitude Resolution 0.5dBm.
- Automatic RBW 2.6KHz to 600KHz.
- Price: \$198.13CAD.

NooElec RTL-SDR is an inexpensive software define radio hardware which supports wide variance of the cross-platform Operative System (OS), for example, OS10, Windows 32 & 64 bit, MacOS, Linux etc. It uses USB Interface IC RTL2832U and Tuner IC R820T2. We have used a sampling rate of 2.56MHz, which is 80% of the resources of the SDR. Due to its modulation techniques, it is easy and quick to identify the type of signal is broadcasting. Moreover, it shows how the waveform changes. It is a simple handy to find the signal and decode the information and does not use the whole bunches of resources [38], [39].

#### Technical characteristics

- Sample rate from 250KHz up to 3.2MHz.
- Modulation techniques: FM, FMS, NBFM, AM, LSB, USB, DSB & I/Q.
- Audio sample rate 44.1KHz to 96KHz.
- Frequency range is 25MHz to 1750MHz.
- Price: \$ 40.95CAD.



FIGURE 3.5: A portable version of the SSS used to sense indoor spectrum.

### 3.3 Designing a Mobile Spectrum Sensing Station

With the SSS implemented and its functionality tested using the fixed and portable antennas, it is necessary to design a mobile version to obtain information of the spectrum in the city, by mounting it in a vehicle to cover broad areas.

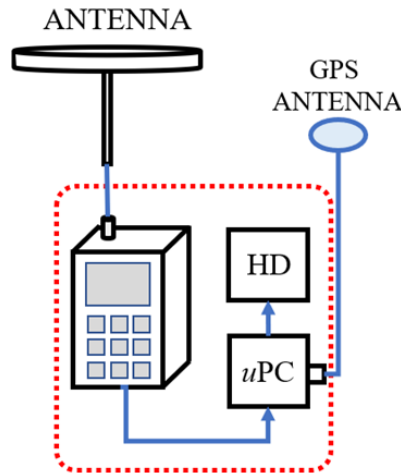


FIGURE 3.6: Initial diagram for the M-SSS, designed to be mounted in a vehicle and sense the TV spectrum in wide geographical areas.

As observed in Figure 3.2, both devices, the SA and RFE detect energy in the UHF TV band, the only difference is the number of samples taken by each device, but in general, they are able to detect the presence or absence of a PU.

With this in mind, the M-SSS originally was designed as is shown in Figure 3.6, using a Winegard antenna, only one RFE device, a portable computer and a storage device to save the collected data. For this mobile configuration, it is mandatory to attach a Global Positioning System (GPS) antenna to collect the geographical location for each reading.

The M-SSS works mounted in a moving vehicle, to reach this, a support was assembled using Chlorinated Polyvinyl Chloride (CPVC) pipes, it was designed to fit in a Dodge Grand Caravan vehicle, as is shown in Figure 3.7, where (a) is the design draft, (b) the M-SSS mounted, (c) the supporting structure built with CPVC, (d) the support mounted in the vehicle, (e) Winegard and GPS antennas, and (e) the M-SSS collecting data.

The antenna and the designed structure, support a speed up to 120Km/h, verified, and theoretically, a speed up to 144Km/h, according to data provided by the maker.



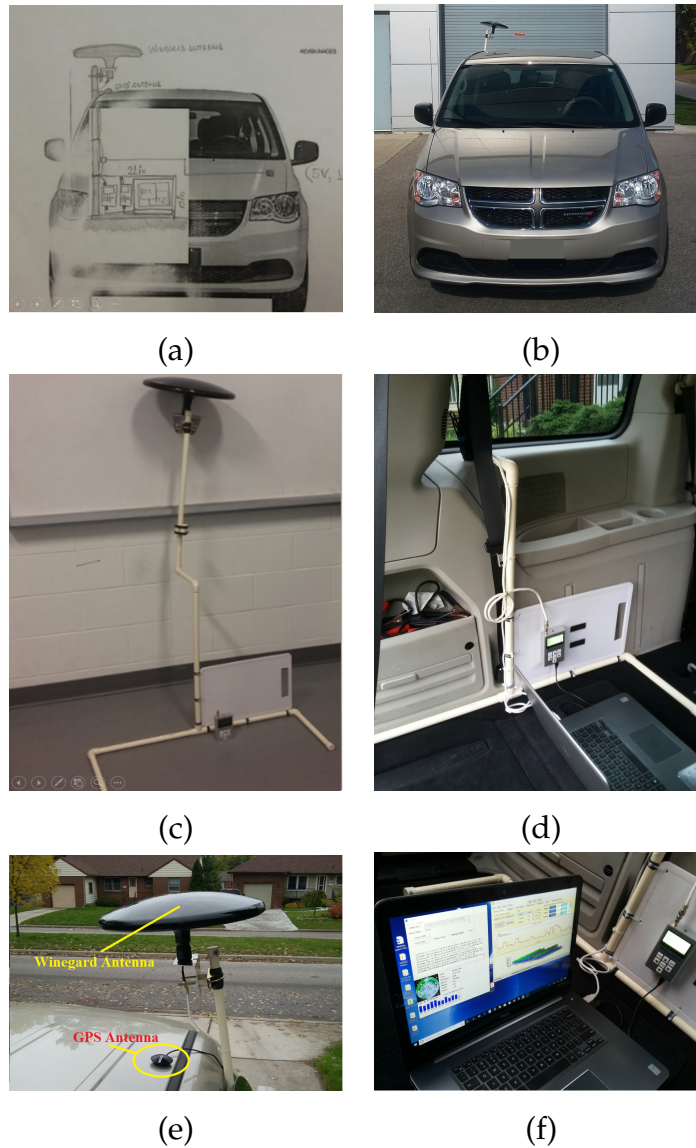


FIGURE 3.7: M-SSS (a) design diagram, (b) station mounted, (c) supporting structure built in CPVC, (d) supporting installed in the vehicle, (e) Winegard and GPS antennas, and (f) M-SSS in operation.

### 3.4 Data Collection Procedure

In this section, there are two well-differentiated stages, the fixed data collection and the mobile data collection.

### 3.4.1 Fixed Data Collection

Samples were collected in the Centre for Innovation and Engineering (CEI) building, located in the city of Windsor, coordinates (Latitude 42.3044 N, Longitude -83.061263 W). The Winegard antenna, model MS-3005 was installed on the roof of the building it means about 12 meters height over the city, which has an altitude of 190 meters above sea level. Measurements were taken several times at different hours of the day and in different periods of time. The radio-electric signals received by the omnidirectional antenna were carried by the coaxial cable to the 3-way splitter input, in the outputs, the RF signal theoretically has the same attenuation level, it was feed into the different Data Acquisition Instrument (DAI) to ensure similar electromagnetic characteristics of the sampled signal. With this parallel feed, the lecture of the different DAI can be compared, due to the similarity of the analyzed signals.

#### Sensing Procedure

Using the RFE, a single reading of the UHF TV spectrum obtains 112 samples, the RFE can take a reading every 0.340s, the plot of a single reading is represented in Figure 3.8 using a blue line. When the reading is made with the SA, this device obtains 1005 samples. The collected information of 198MHz bandwidth is represented in Figure 3.8 using a red line.

Comparing the overlapped plots, the general shape of the spectrum energy is observed without major variations. This interesting fact, give us the possibility to use the RFE device to replace the voluminous, heavy, and costly SA.

When an RTL-SDR device is used, not all the 198MHz band or a single 6MHz channel is read at a time. This device can collect the information from a 3MHz maximum bandwidth. It has a high performance reading narrow bands to detect pilot tones. From the mentioned features of the DAI, we decided to combine their attributes to achieve the best results in the spectrum sensing campaign. The sensing techniques select for this work are ED and PD.

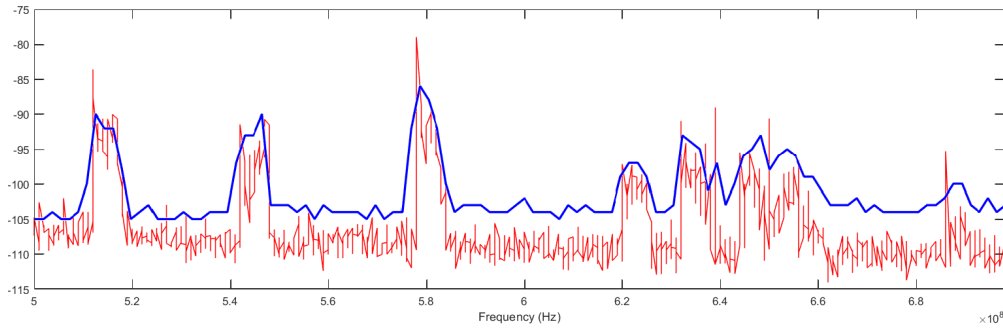


FIGURE 3.8: TV Signal sensed an RFE (blue line) and a SA (red line) are compared. The general shape that contains the energy is easily identified in the plot obtained with both devices.

### Comparing the DAI Performance

Three different DAI are combined in the designed SSS, to know the characteristics of each device, a performance comparison is needed. In Table 3.2 are detailed the DAI, the sensing technique, the whole 198MHz bandwidth, the number of channels sensed, and the performance observed when each device was used.

The SA, an expensive and accurate device has a high performance to sense the whole bandwidth of 32 TV channels or a single 6MHz channel, with this DAI is possible to apply the ED and the PD techniques simultaneously.

Using the RFE, when it senses all the 198MHz band, it only can detect the energy of the TV channels but is not able to detect the pilot tones of the 32 channels sensed at time, on the other hand, if it senses only one 6MHz channel, its performance increases and can detect both, the energy and pilot presence in a single TV channel.

In the case of the RTL-SDR, this DAI can sense a part of a single TV channel, it is not applicable to sense the 198MHz or a single 6MHz bandwidth. When it senses a small portion of the channel it has a high performance, for that reason this DAI is used to detect the pilot tones in a 200KHz bandwidth only. The results of this comparison are detailed in Table 3.2.

TABLE 3.2: DAI's features and performance comparison

DAI	ED	PD	Bandwidth	# Channels	Performance
SA	✓	✓	198 MHz	32	High
SA	✓	✓	6 MHz	1	High
RFE	✓	N/A	198 MHz	32	Medium
RFE	✓	✓	6 MHz	1	High
RTL	N/A	N/A	198 MHz	32	N/A
RTL	N/A	✓	3 MHz	0.5	High

### 3.4.2 Mobile Data Collection

To sense the TV spectrum data in the city of Windsor using the M-SSS, four trajectories were defined, as is illustrated in Figure 3.9. In total more than 36,176 readings or 4,051,712 samples for noise and 4,051,712 samples for the composite signal plus noise were taken. From these readings, 53 points distributed across the city were selected to plot the information obtained. The trajectories are detailed in Table 3.3.

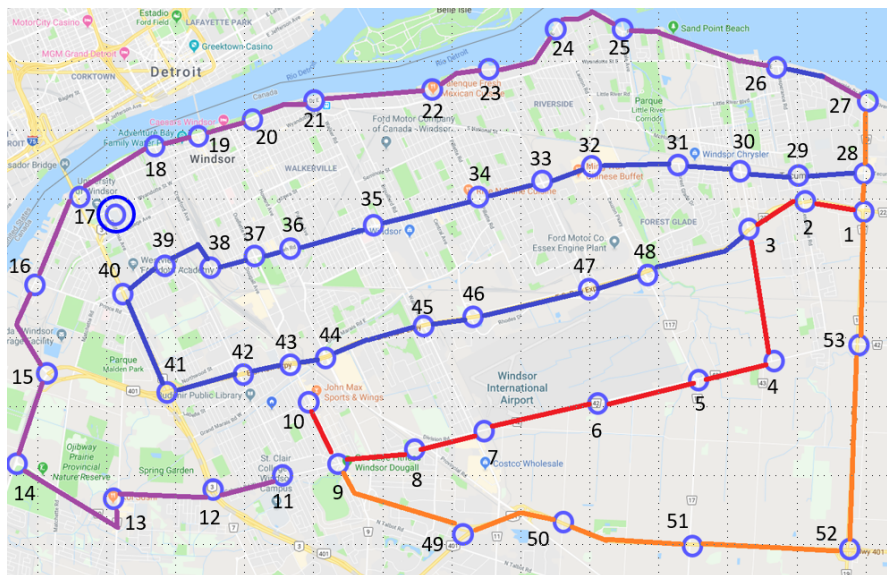


FIGURE 3.9: Trajectories and locations to represent the TV spectrum sensed in the city of Windsor.

In each selected point, there are 112 samples for noise and 112 samples for the composite signal saved in the DB, with its respective Latitude and Longitude coordinates.

TABLE 3.3: Trajectories defined to sense the TV spectrum in the city of Windsor

Trajectory	Color	Initial Point	Final Point	Observations
1	Red	1	10	10 Points
2	Purple	11	27	17 Points
3	Blue	28	48	21 Points
4	Orange	49	53	5 Points
			<b>Total</b>	<b>53 Points</b>

As is mentioned above, in Figure 3.9, the coloured line represents the trajectories followed by the M-SSS and blue circles represent the points in which the data are plotted and analyzed. It is necessary to note that all the time during the movement of the M-SSS along the trajectories the information is saved in the DB, Figure 3.10 illustrates how the TV signal contained in the 198MHz band is saved, and in this case, visualized by using the RFE software [35].

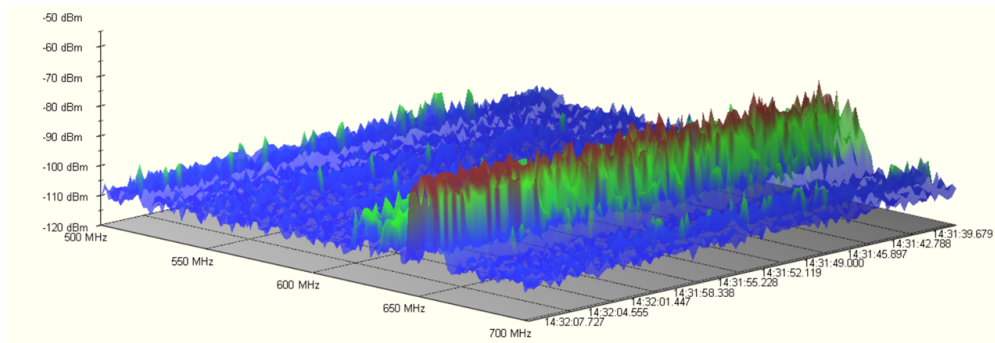


FIGURE 3.10: Visualization of the TV signal sensed using an RFE device, the readings were taken every 0.340s, the axis represents frequency, time and power in dBm, respectively.

## Chapter 4

# Stochastic Analysis of TVWS

As mentioned in the objectives of the research, a model based on the probabilistic characteristics of the sensed signal needs to be developed for identifying TVWS. This model and the mechanism of finding TVWS are described in this chapter. Additionally a table with a mathematical notation and units of measurement has been included in Appendix B.

### 4.1 Sensing the TV Signal

The existence of the PU can be verified by using the following hypotheses:

$$H_0 : X(f) = W(f) \quad (4.1)$$

$$H_1 : X(f) = S(f) + W(f) \quad (4.2)$$

where  $W(f)$  denotes Additive White Gaussian Noise (AWGN),  $S(f)$  is the received signal of the PU,  $X(f)$  is the sensed signal, and  $H_0$  represents the absence of PU over the channel, whereas  $H_1$  represents the presence of the PU over the channel.

By using the SSS, the information from the UHF TV spectrum was collected at each instant of time  $t_i$  and plotted as is shown in Figure 4.1. In both cases, (a) for RFE and (b) for SA, the signal presents a similar shape in general terms, with specific frequencies in which the energy rise to its maximum values and other frequencies in which minimum values are reached. The observed variations in the mentioned Figure are due to the internal characteristics of each device.

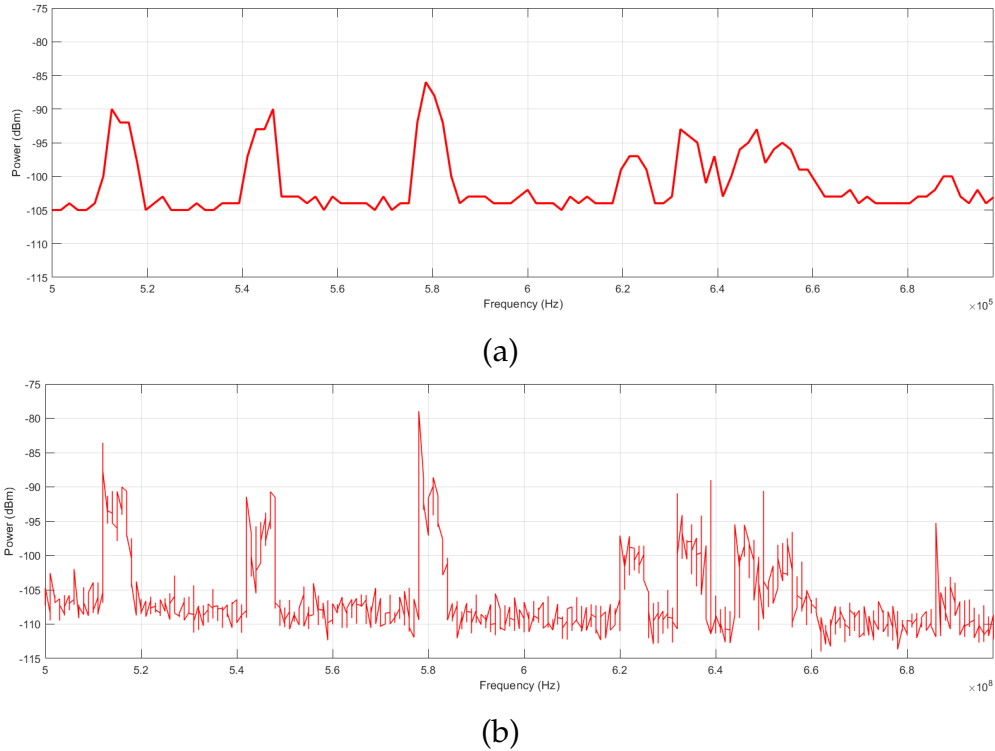


FIGURE 4.1: TV Signal sensed with (a) RFE and (b) SA are compared. The general shape that contains the energy under the red line is easily identified in both devices.

With only the information of  $X(f)$  is not enough to identify TVWS, it is evident that more data is needed to find them. So it is mandatory to find more parameters that permit to detect the presence of PU.

## 4.2 Identifying the Noise Level

A crucial element to be considered is how the noise is measured, and the mean of the noise  $\bar{W}(f)$  is calculated. In some cases, the noise is sensed at the beginning of the measurement campaign and that value is used to be compared with all the readings. In other cases, a theoretical value is considered. Again a third approach is to consider a fixed  $T$ , we can recall  $T$  is the threshold. In practice, it is very difficult to obtain accurate information about the noise power [40].

According to the IEEE 802.22 standard [4], [17], the channel in operation must be sensed several times, namely, during the transmission, inter-framing and in-framing. Here, it is important to obtain trustful and accurate channel noise and signal samples.

In order to obtain accurate information regarding the noise, simultaneous sensing of the noise and the signal is proposed. As can be seen in Figure 4.2,

the signal  $X(f)$  is received through the antenna and sensed with one DAI, and at the same time, another DAI of similar characteristics with a  $50\Omega$  matched impedance is used to sense the noise of the system. As a result, both the signals, i.e.,  $X(f)$  and  $W(f)$  are used in our proposed channel sensing mechanism.

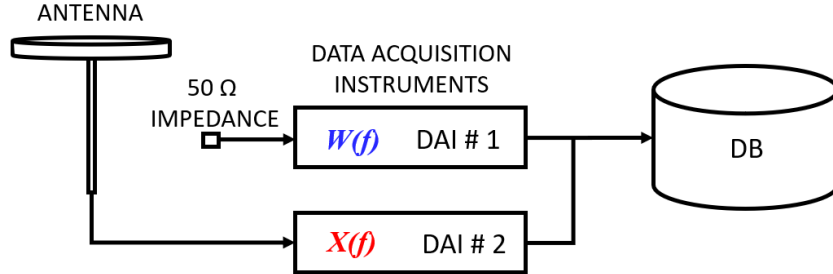
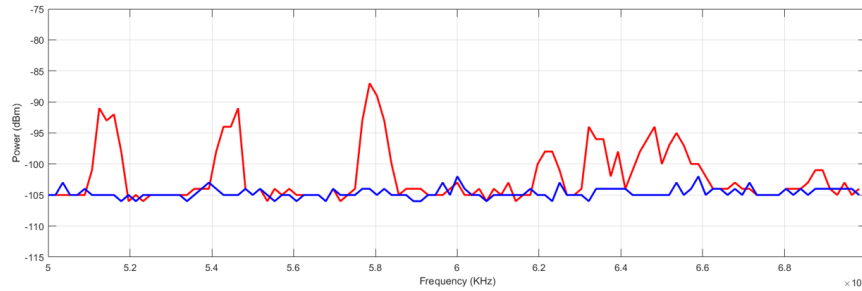
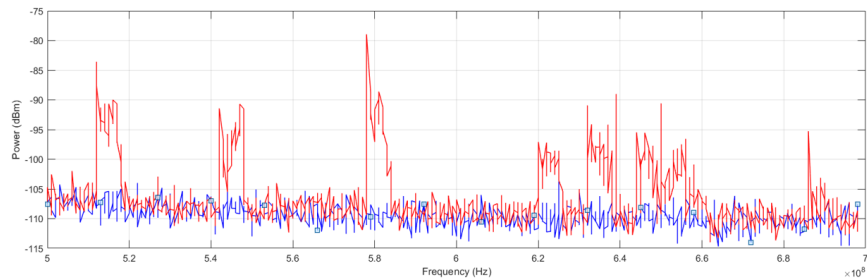


FIGURE 4.2: Proposed M-SSS to sense in parallel the Noise  $W(f)$  and the composite signal  $X(f)$ .

With the above-mentioned configuration, the UHF TV spectrum was sensed, and the obtained results are shown in Figure 4.3.



(a)



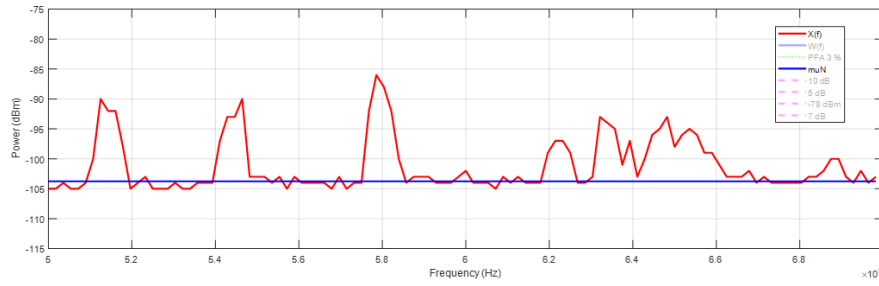
(b)

FIGURE 4.3: TV Signal sensed with (a) RFE and (b) SA are compared. The  $W(f)$  and  $X(f)$  are observed and permit infer their possible relationship.

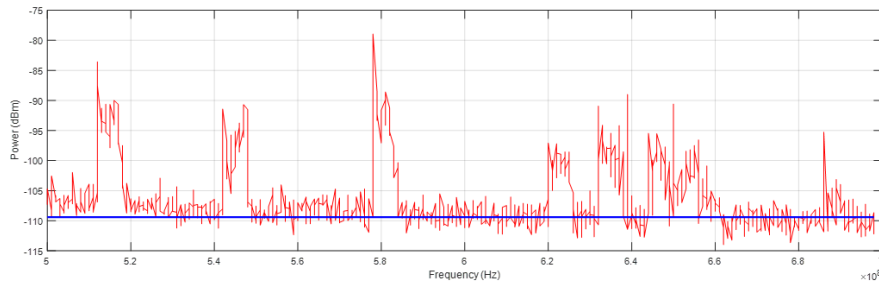
From the collected information, specifically for  $W(f)$ , the next logical step is to calculate the statistical mean of the noise, i.e.,  $\overline{W}(f)$ . Figure 4.4 shows this



$\bar{W}(f)$  and that indicates the real noise level at an instant  $t_j$ . This is the reference level for calculating  $T$ .



(a)



(b)

FIGURE 4.4: TV Signal sensed with (a) RFE and (b) SA are compared. The  $\bar{W}(f)$  and  $X(f)$  are observed and it is considered the noise level for that specific data collected.

### 4.3 Threshold Considerations

As found in the literature of TVWS sensing, the sensed signal  $X(f)$  is compared with  $T$ , which is obtained from

$$T = \bar{W}(f) + M \quad (4.3)$$

where  $\bar{W}(f)$  is the mean of the noise. Here  $M$  is a margin that can be calculated from different manners and is a crucial element to consider a channel as a TVWS [20].

Literature shows different values of  $M$  have been used in the past. For example, [41] considered an  $M$  of 5dB, [42] used a value of 7dB. Again as far ITU recommendation the value of  $M$  should be 10dB [43]. Finally, in [44], a fixed  $T = -78$  dBm was used.

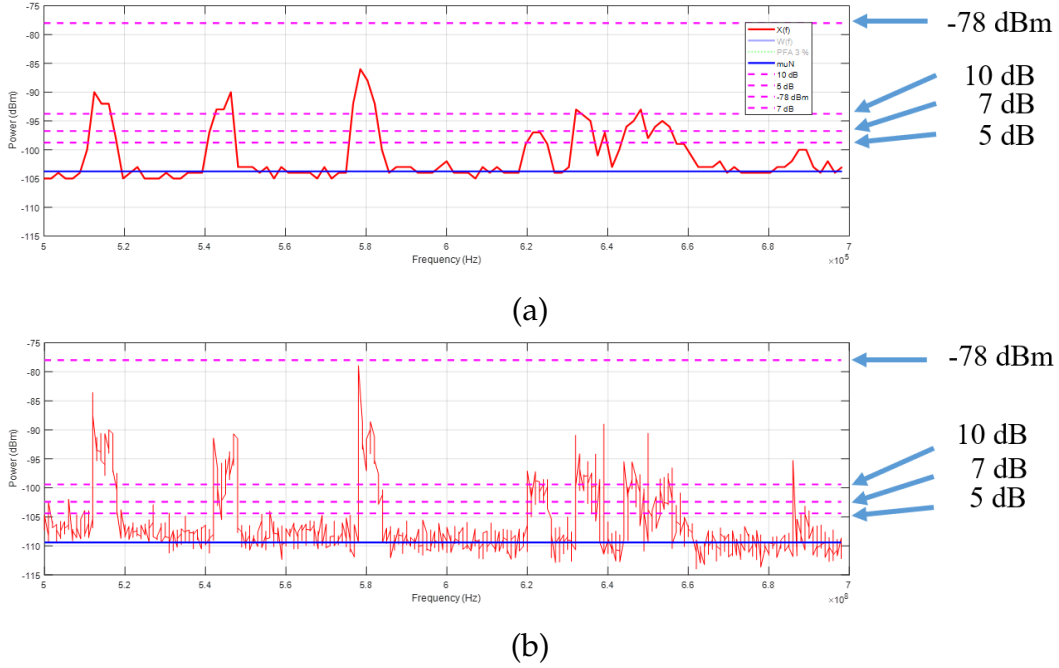


FIGURE 4.5: Comparison of the signal sensed with (a) RFE and (b) SA. In both sub-figures are plotted  $X(f)$ ,  $\bar{W}(f)$ , and the different values for  $M$  or  $T$ .

In Figure 4.5 we can observe  $X(f)$ , sampled with RFE in (a) and with SA in (b). Both the sub-figures show the previously discussed  $M$  and  $T$ . It is obvious from these figures that the higher is the chosen value of  $M$ , the higher is the occurrence of signal missed-detection.

In the specific case of  $T = -78\text{dBm}$ , all the 32 channels appears to be idle; which is not necessarily true because at least 8 signal peaks can be observed.

The purpose of sensing and plotting two signals, i.e.,  $W(f)$  and  $X(f)$  is to identify the characteristics of each signal and compare with the other. This will permit to obtain enough parameters to develop the proposed probabilistic model.

The above discussion reveals that in order to sense the UHF TV spectrum for accurate identification of idle channels, it is imperative to define an adaptive  $T$ . The value of  $T$  should satisfy the following conditions.

- (i) It should be close enough from  $\bar{W}(f)$  to avoid missed-detection.
- (ii) It should be far enough from  $\bar{W}(f)$  to avoid false alarms.
- (iii) It should be adaptive to the possible changes experienced by  $W(f)$  and  $X(f)$ , specially when the M-SSS is used.

## 4.4 Probabilistic Considerations

### 4.4.1 Working with Normal Distributions

As mentioned earlier, two signals, i.e., the noise  $W(f)$  and the composite signal plus noise  $X(f)$  are collected simultaneously by the RFE devices connected in parallel. It is imperative to verify that the sensed noise  $W(f)$  is a normally distributed signal. There are two ways to do this, i.e., graphical and mathematical methods [45], [46]. The first one considers graphical methods where the samples of the noise signal are plotted to observe the distribution. Following this method, Figure 4.6(a) shows the histogram of noise samples taken in a particular location and Figure 4.6(b) shows the normal probability distribution plot of the same samples. It is visually evident that the plotted samples correspond to a normal distribution.

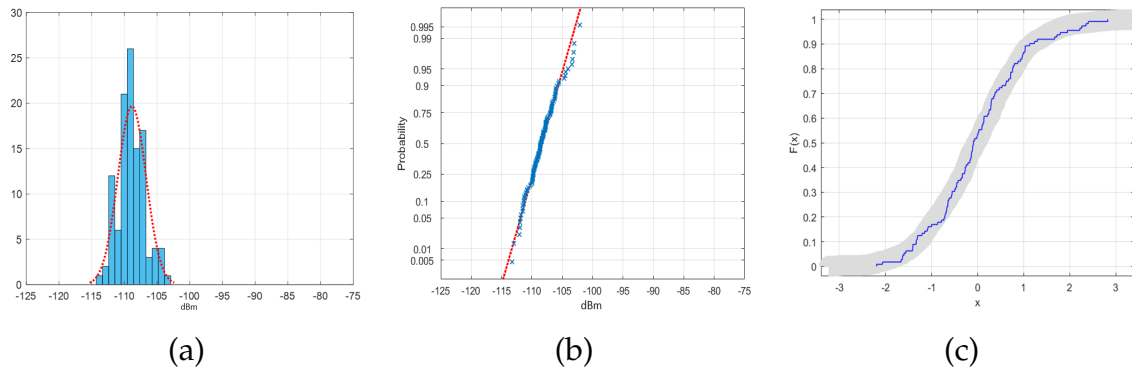


FIGURE 4.6: Noise signal sensed  $W(p)$ . (a) Histogram of the collected data. (b) Normal probability plot of the same data read. (c) CDF of the Kolmogorov-Smirnov Test (KST) applied.

The second method is a mathematical test; in this case, the Kolmogorov-Smirnov Test (KST) [46]. This test with a significance level of 5% has been applied to the collected noise samples, and the corresponding results of the Cumulative Density Function (CDF) are shown in Figure 4.6(c). The plots suggest that the tested samples are normally distributed.

On the other hand, as shown by Figures 4.7(a) and (b), the composite signal  $Xo(p)$  presents a multi-modal distribution. Let us named as  $Xo(p)$  to the multi-modal curve that corresponds to the histogram of the composite signal. Here it is easy to identify the component of noise represented by higher peak and the signal of PU represented by the multi-modes on the right tail. When the Kolmogorov-Smirnov Test (KST) [46] with a significance level of 5% is applied to the composite signal samples, results suggests that it does not correspond to a normally distributed signal, as is observed in Figure 4.7(c).

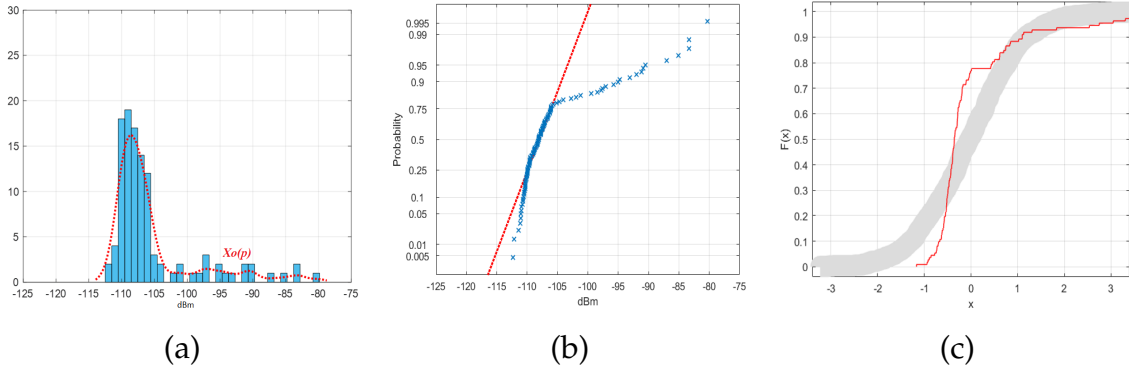


FIGURE 4.7: Composite signal plus noise sensed  $Xo(p)$ . (a) Histogram of the collected data. (b) Normal probability plot of the distribution for the same reading (c) CDF of the Kolmogorov-Smirnov Test (KST) applied.

To apply the proposed model, it is necessary to assume that the composed signal  $X(p)$  is a normally distributed signal, as illustrates Figure 4.8. This assumption is needed in order to reduce the computational complexity in terms of probabilistic analysis while accuracy is preserved in the TVWS identification procedure.

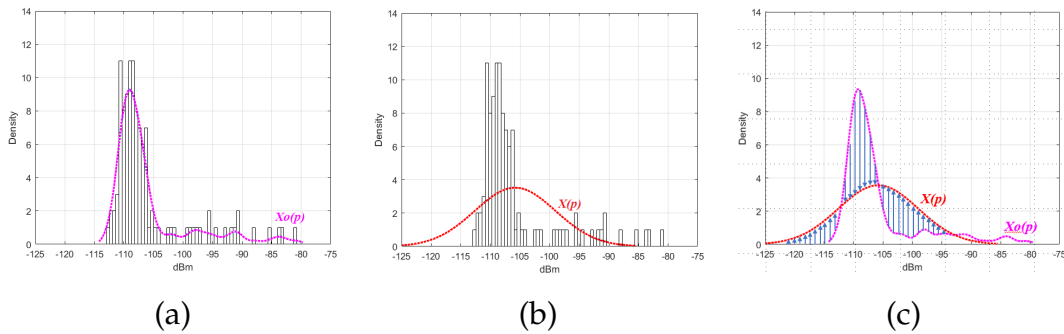


FIGURE 4.8: The curve  $Xo(p)$  of the multi-modal distribution of (a) can be assumed as the normal distribution curve  $X(p)$  of (b), this assumption summarized in (c) allow us to reduce the calculation complexity of the proposed model.

In Figure 4.9 are plotted the pdfs of  $W(p)$  in blue,  $Xo(p)$  in magenta, which is the multi-modal curve of the composite signal, and  $X(p)$  in red. In these figures, it is easy to observe that the intersections of  $W(p) \cap X(p)$  and  $W(p) \cap Xo(p)$  are very close in terms of the X-axis (power in dBm) for three different locations, the absolute value of this difference is minimal in relation to the absolute value of the signal power, and can be disregarded. This fact supports that the composite signal  $X(p)$  can be assumed as a normally distributed signal to reduce the mathematical calculations complexity without affecting the accuracy of the obtained results of the proposed model.

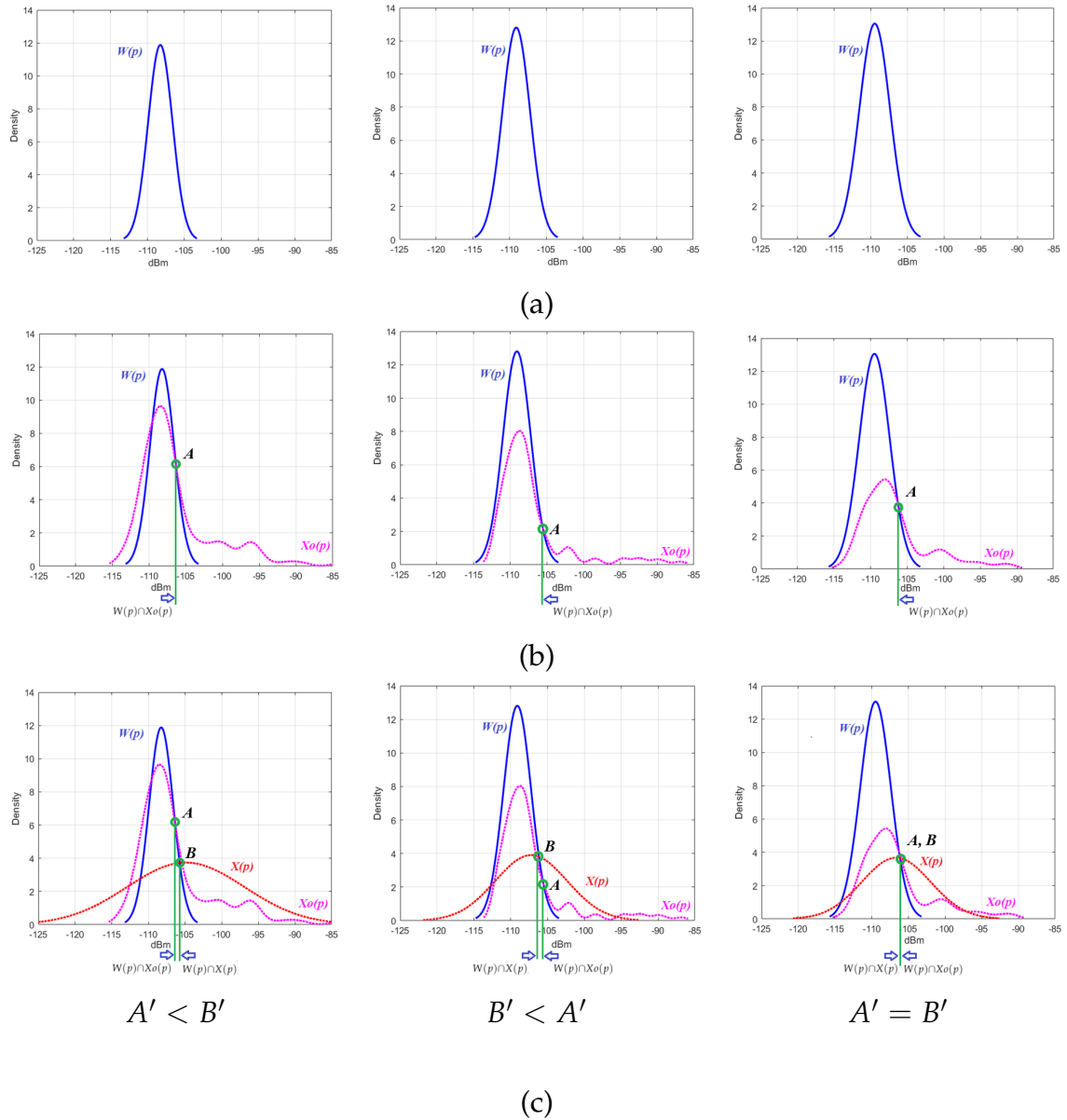


FIGURE 4.9: Readings taken in three different points, the pdf for the noise  $W(p)$  is plotted in blue, multi-modal composite signal  $Xo(p)$  in magenta, and composite signal  $X(p)$  in red. In (a) are shown the pdf of the noise for each location. In (b), the intersection point "A" of  $W(p) \cap Xo(p)$  and its projection to the power axis "A'". In (c), the intersection point "B" of  $W(p) \cap X(p)$ , and its projection to the power axis "B'", we also observe that the difference between  $A'$  and  $B'$  is minimum concerning the power level of the signal in dBm.

Now, this assumption is supported by the fact that the calculation of the Probability of False Alarm ( $P_{fa}$ ) will be done on the noise signal, i.e.,  $W(p)$ , which corresponds to a normal distribution.

In addition, the following two points should also be noted, as is observed in Figure 4.10.

- (i) For calculation of  $P_{fa}$ , the left intersection point "C" of the pdf of  $W(p)$  and  $X(p)$  will not be considered, because it is located below the mean value of the noise signal  $\bar{W}(p)$ .
- (ii) For calculation of the Probability of Detection ( $P_d$ ), the right intersection point "B" of the pdf of  $W(p)$  and  $X(p)$  will be considered.

Once this assumption has been accepted, then the pdf that represent the noise  $W(p)$  and the composite signal  $X(p)$  are those illustrated in Figure 4.10.

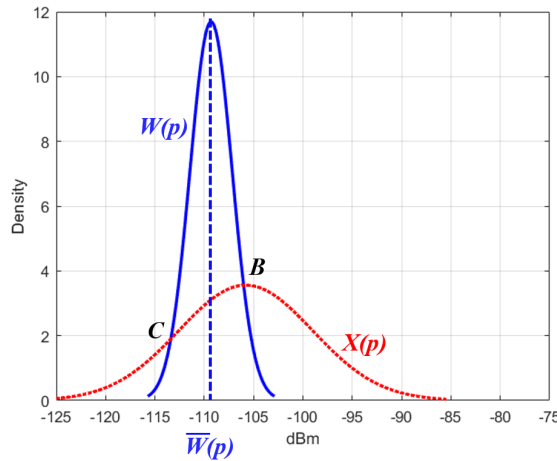


FIGURE 4.10: Normal distribution pdfs for  $W(p)$  in blue and assumed  $X(p)$  in red, both used to calculate the  $P_{fa}$  and the  $P_d$  according to the model proposed in this dissertation.

In this point, it is precise to refer to the Neyman-Pearson article, named *On the Problem of the Most Efficient Tests of Statistical Hypotheses* [47]. The authors used Fisher's null hypothesis significance testing [48] and the p-value as part of a formal decision process. Thus, they raised a real choice between two rival hypotheses. The hypothesis contrast became a method to distinguish between the null hypothesis and the alternative hypothesis, as observed in Figure 4.11.

In the proposed model, the pdf of the composite signal contains the pdf of noise, while in the Neyman Pearson model, both pdf are partially overlapped. On the other hand, the  $P_{fa}$  and  $P_d$  are similarly defined and related.

The frequently used statistical parameters regarding the sensed signals are  $P_{fa}$ ,  $P_d$ , and the probability of missed-detection ( $P_m$ ). With the collected information of  $W(p)$  and  $X(p)$ , and considering that both signals correspond to normal distributions, other statistical parameter can be calculated, i.e., mean values of the signals ( $\bar{W}(p)$ ,  $\bar{X}(p)$ ) or the standard deviations ( $\sigma_W$ ,  $\sigma_X$ ). An interesting manner to relate the obtained parameters is by using the pdf of the signals

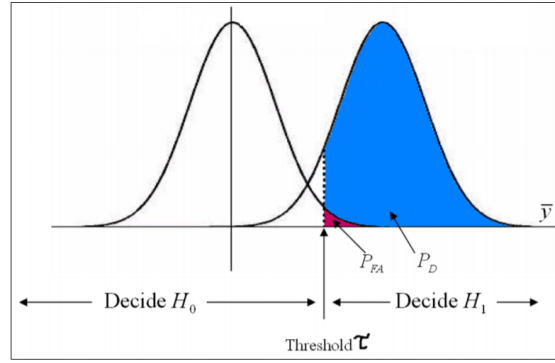


FIGURE 4.11: Neyman Pearson model, the null hypothesis and the alternative hypothesis are observed.

which provides a visual explanation of the proposed method, and is explained next.

To plot the pdf of a signal that responds to a normal distribution, it is necessary to apply

$$f(x) = \frac{1}{\sigma\sqrt{2\pi}} \exp \left\{ \frac{-1}{2} \left( \frac{x - \bar{x}(p)}{\sigma} \right)^2 \right\}; -\infty < x < \infty \quad (4.4)$$

where  $\sigma$  is the standard deviation and  $\bar{x}(p)$  is the mean of the distribution. By taking the samples of  $W(p)$  and  $X(p)$ , the equations that define both pdf curves, are  $f(x_W)$  and  $f(x_X)$  with  $\bar{W}(p)$  and  $\bar{X}(p)$  as the means,  $\sigma_W$  and  $\sigma_X$  as the standard deviations respectively, then the equations be:

$$f(x_W) = \frac{1}{\sigma_W\sqrt{2\pi}} \exp \left\{ \frac{-1}{2} \left( \frac{x - \bar{W}(p)}{\sigma_W} \right)^2 \right\} \quad (4.5)$$

$$f(x_X) = \frac{1}{\sigma_X\sqrt{2\pi}} \exp \left\{ \frac{-1}{2} \left( \frac{x - \bar{X}(p)}{\sigma_X} \right)^2 \right\} \quad (4.6)$$

now, considering that  $X(p)$  is a composite signal consisting of  $W(p) + S(p)$ , where  $S(p)$  is the energy of the PU and  $W(p)$  is the noise, it is very important to compare both pdf.

#### 4.4.2 Obtaining pdfs

##### RFE Device

Once the spectrum of interest is sensed, each RFE collects 112 samples with information given in  $dBm$ , the mean of the composite signal  $\bar{X}(p)$ , mean of the

noise  $\overline{W}(p)$ , standard deviation of the composite signal  $\sigma_X$ , and standard deviation of the noise  $\sigma_W$  are calculated and used to plot the pdfs as shows Figure 4.12(a).

### SA Device

Repeating the same procedure used for RFE device, now using the SA, 1005 samples are collected, and then after calculating the mean and the standard deviation, the pdfs are plotted as illustrated in Figure 4.12(b).

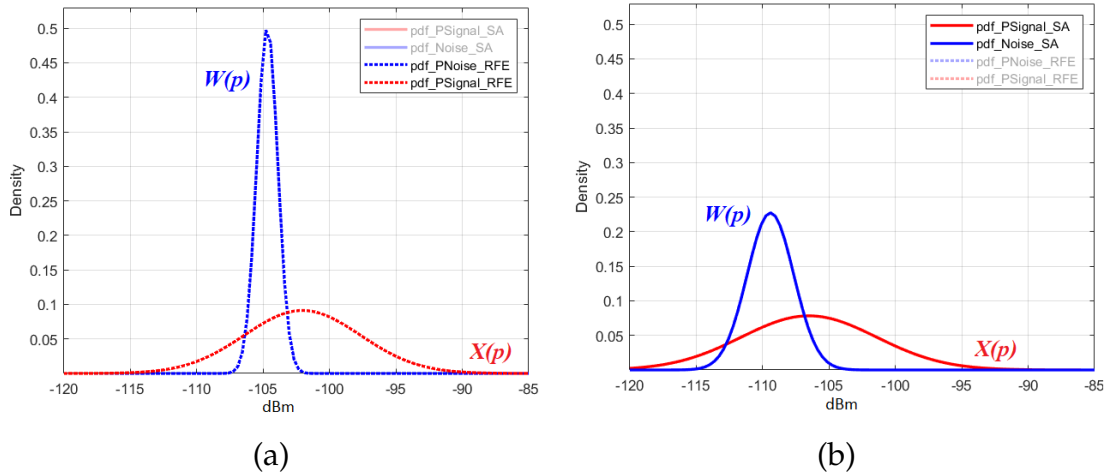


FIGURE 4.12: Pdf of  $W(p)$  in blue and  $X(p)$  in red, taken from the data collected with (a) RFE and (b) SA.

### 4.4.3 Performance Metrics

In order to visualize the performance metrics of spectrum sensing, i.e., probability of false alarm, probability of detection and probability of missed-detection, we need to consider the pdf curves and  $T$  together as shown in Fig. 4.13.

#### Probability of False Alarm: $P_{fa}$

$P_{fa}$  refers to the probability that a peak or peaks of the noise signal is detected above  $T$ , and is considered as a real signal of the PU when in reality no PU signal is present. In Figure 4.13,  $P_{fa}$  corresponds to the area bounded by  $T$  and  $W(p)$  colored with orange.



### Probability of Detection: $P_d$

$P_d$  is the probability that a real signal of the PU is detected above  $T$ , and is considered as a signal from PU. In Figure 4.13 it refers to the area bounded by  $T$  and  $X(p)$  coloured with yellow.

### Probability of Missed-Detection: $P_m$

$P_m$  is the probability that a real signal of the PU is not detected above  $T$ , and is considered as noise due to its low amplitude. In Figure 4.13 it is colored with light-blue.

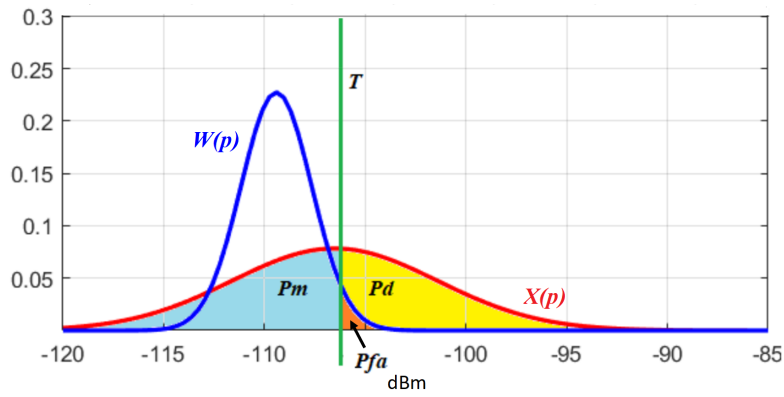


FIGURE 4.13: Graphical representation of the  $P_m$ ,  $P_{fa}$ , and  $P_d$ , generated by the  $T$  and the pdf curves for  $W(p)$  and  $X(p)$ .

#### 4.4.4 Calculation of Threshold $T$

In light of the previous discussion, it is evident that  $T$  is the most critical parameter for accurate sensing, and hence it must be meticulously calculated to permit the balance of  $P_{fa}$  and  $P_d$ . By obtaining  $M$  an adequate  $T$  can be calculated. Basically,  $M$  is the product of the standard deviation  $\sigma$  and the value of  $z$ .

It is possible to define a minimum limit  $M_{min}$  and a maximum limit  $M_{max}$  for  $M$ , as observed in Figure 4.14.

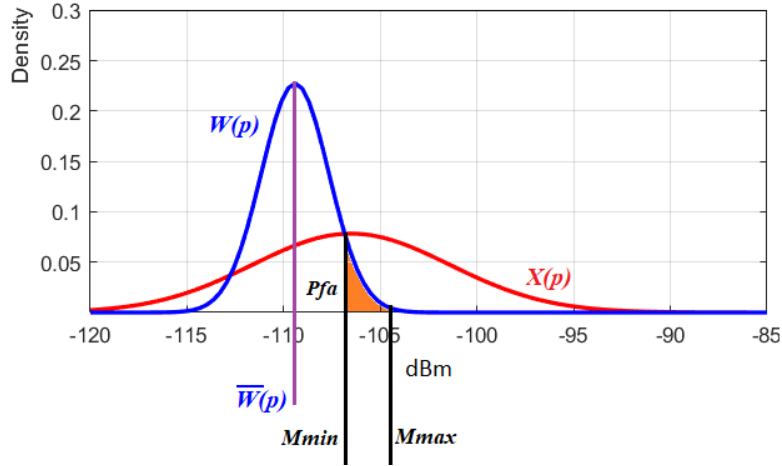


FIGURE 4.14: Minimum and maximum possible values for  $M$ .

In other words,  $M$  must remain between the maximum and minimum possible values.

$$M_{min} \leq M \leq M_{max} \quad (4.7)$$

where  $M_{min}$  is obtained calculating the intersection point of two plotted pdfs.

$$M_{min} = W(p) \cap X(p) \quad (4.8)$$

which is a complex operation considering Equations 4.5 and 4.6.

The value of  $M_{max}$  is calculated using

$$M_{max} = \sigma z \quad (4.9)$$

where  $\sigma$  is the standard deviation of the distribution and  $z$  is obtained from the  $F(z)$  function, which defines the area under the curve in terms of the standard deviation [49].

The possible intervals for  $M$  are illustrated in Figure 4.15 for data taken with RFE and SA respectively.

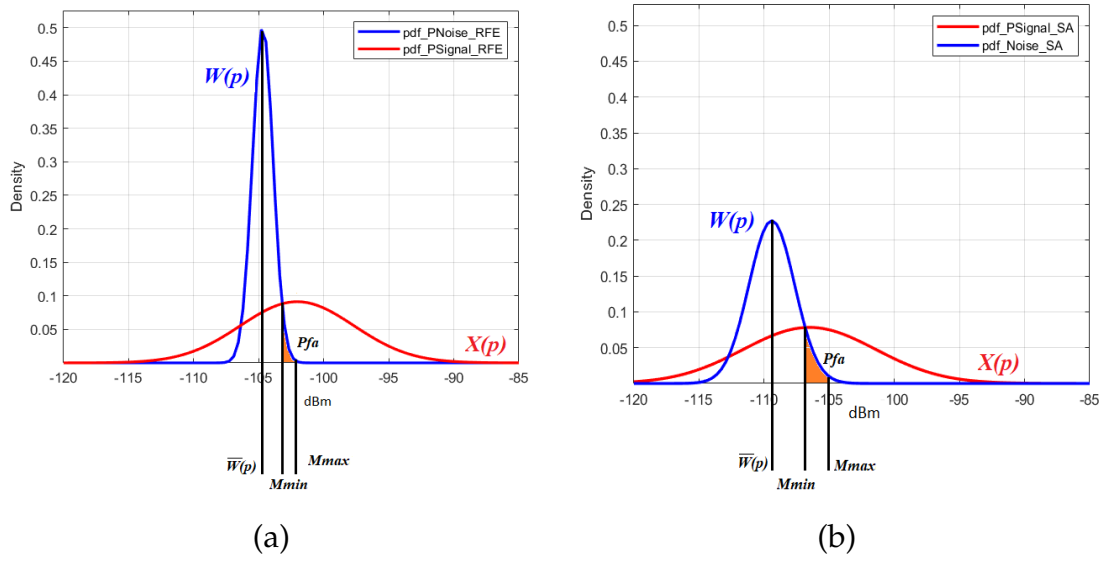


FIGURE 4.15: pdf of the  $W(p)$  and  $X(p)$  taken from the data read with (a) RFE and (b) SA, the  $M_{min}$  and  $M_{max}$  are identified.

### Threshold Minimum and Maximum

To calculate  $T$ , the standard deviation and the value of  $z$  must be considered. The expression for noise is given by

$$T = \bar{W}(p) + \sigma_W z_W \quad (4.10)$$

and for the composite signal consisting of signal and noise is obtained with

$$T = \bar{X}(p) + \sigma_X z_X \quad (4.11)$$

To obtain  $T_{min}$ , it is necessary to solve the equation system (4.5) and (4.6) and eliminate  $x$ . The result will be expressed in  $dBm$ .

To calculate  $T_{max}$ , a  $P_{fa}$  of 1% is considered according to [20]. Once  $T$  is calculated in terms of  $\bar{W}(p)$ , it is possible to define  $P_{fa}$ .

$$P_{fa} = F^{-1}(z_W) \quad (4.12)$$

With the statistical and probabilistic information of  $W(p)$  and  $X(p)$ , for a given  $T$ , which is common for both pdf, the expression for  $z_X$  is given by

$$\bar{W}(p) + \sigma_W z_W = \bar{X}(p) + \sigma_X z_X \quad (4.13)$$

$$z_X = \frac{\bar{W}(p) - \bar{X}(p) + \sigma_W z_W}{\sigma_X} \quad (4.14)$$

and  $P_d$ , related to  $X(p)$  is obtained with

$$P_d = F^{-1}(z_X) \quad (4.15)$$

Table 4.1 lists the values of  $F(z)$  which is the desired area under the pdf curve for a desired  $P_{fa}$ , and its corresponding value of  $z$ . The complete table can be observed in Appendix C.

TABLE 4.1: Estimated values for  $P_{fa}$ ,  $F(z)$ , and  $z$ .

Ord	$F(z)$	$P_{fa}$	$z$
1	90.0 %	10.0 %	1.29
2	90.5 %	9.5 %	1.31
3	91.0 %	9.0 %	1.34
4	91.5 %	8.5 %	1.37
5	92.0 %	8.0 %	1.41
6	92.5 %	7.5 %	1.44
7	93.0 %	7.0 %	1.48
8	93.5 %	6.5 %	1.51
9	94.0 %	6.0 %	1.56
10	94.5 %	5.5 %	1.60
11	95.0 %	5.0 %	1.65
12	95.5 %	4.5 %	1.70
13	96.0 %	4.0 %	1.75
14	96.5 %	3.5 %	1.81
15	97.0 %	3.0 %	1.88
16	97.5 %	2.5 %	1.96
17	98.0 %	2.0 %	2.06
18	98.5 %	1.5 %	2.17
19	99.0 %	1.0 %	2.33
20	99.5 %	0.5 %	2.58

The information provided by  $P_{fa}$  vs  $P_d$  permits to understand the relation between these two probabilities, that defines the optimal value for the proposed adaptive  $T$ , as is observed in Figure 4.16. For both devices, RFE and SA, the adaptive  $T$  proposed in this research are closer to the  $\bar{W}(p)$ . In this manner, it avoids missed-detections, and observes enough separation, reducing the  $P_{fa}$  to a value of 3%. The most important factor is that the proposed adaptive  $T$  will maintain the same behaviour even if the noise floor or the signal strength experience any variation.

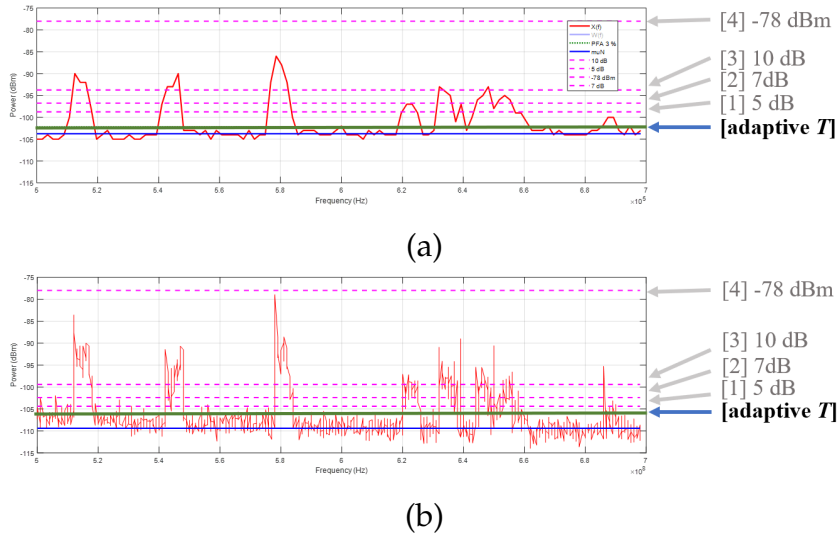


FIGURE 4.16: Comparison of the signal sensed with (a) RFE and (b) SA. In both panels the adaptive  $T$  is plotted, comparing with the  $T$  proposed by other related works.

### 4.4.5 Adaptive Threshold

To obtain the adaptive  $T$ , two signals, i.e., the noise  $W(f)$  and the composite signal  $X(f)$  are sensed in parallel in point P11, obtaining the data shown in Figure 4.17(a).

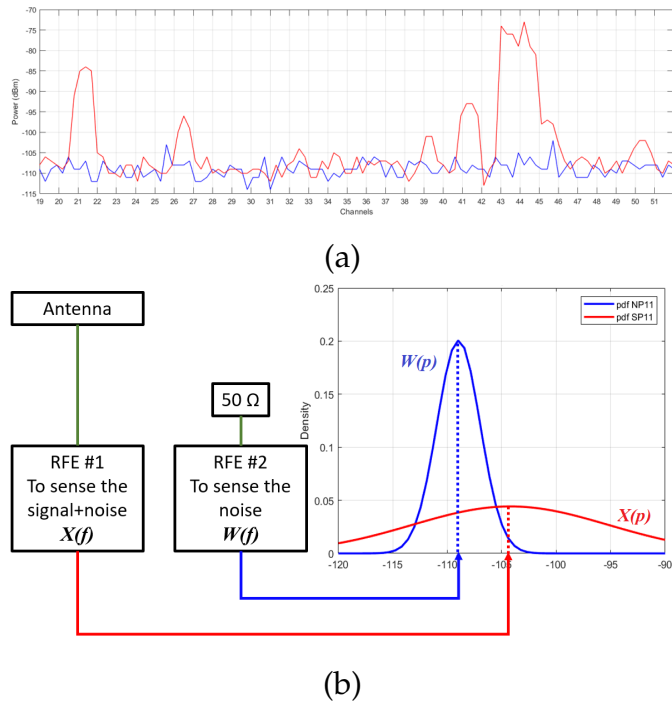


FIGURE 4.17: Composite signal and noise sensed in point P11, (a) Frequency vs power, (b) pdf of the sensed signals.

From the saved data, the statistical components like mean values and standard deviations are obtained and the pdfs are plotted, as shown in Figure 4.17(b).

If a  $T$  with a  $P_{fa}$  of 3% is considered, then  $z_W = 1.88$ , as shown Table 4.1 and Figure 4.18.

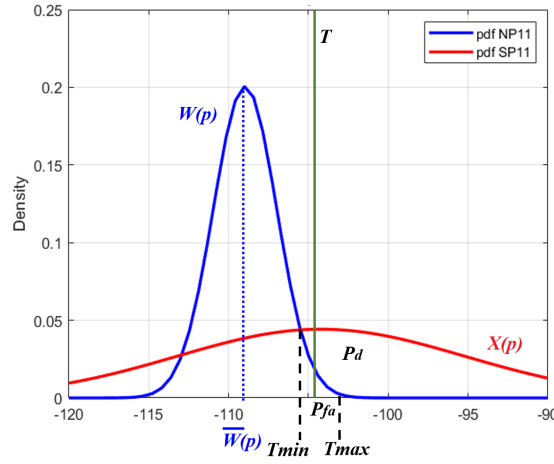


FIGURE 4.18: Visual representation of a  $T$  that observes a  $P_{fa}=3\%$ .

The selected  $T$  is common for both pdfs. By using Equations (4.10), (4.11) (4.13),(4.14), and (4.15), we calculate the value of  $P_d$ .

The relation between  $P_{fa}$  and  $P_d$  is observed in Figure 4.19(a), which is called the Receiver Operating Characteristics (ROC) curve [50]. On this plot, the axis represents the values for  $P_{fa}$  and  $P_d$  respectively, and both values have a full-scale form 0% to 100%. Note that  $P_{fa}$  for this  $T$  is located in the lower part of the axis, so the area of interest for this study is reduced to the light-blue coloured area in the plot. Here it is important to highlight that the ROC of the Neyman Pearson model is shown in Figure 4.19(b), and differs from the one shown in (a), because both pdf curves are partially overlapped.

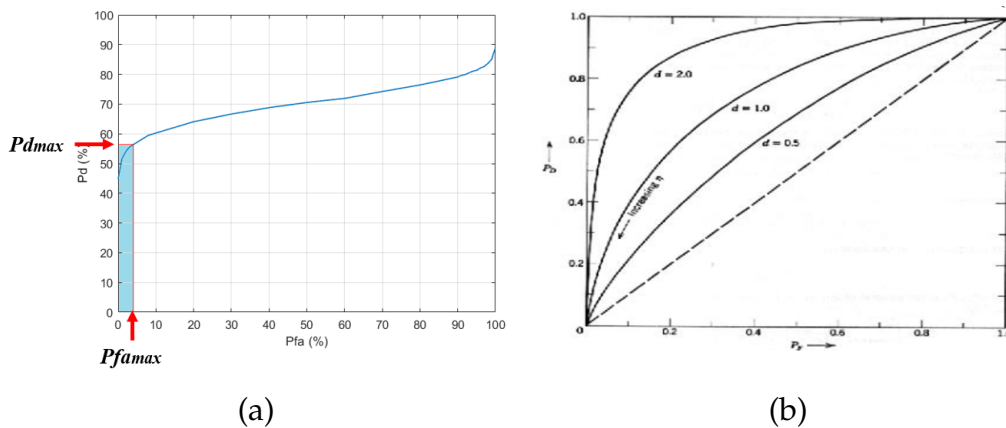


FIGURE 4.19: ROC: (a) for the proposed model with the area of interest coloured; (b) for Neyman Pearson model.

By zooming the area of interest, the maximum values for  $P_{fa}$  and the  $P_d$  are observed in Figure 4.20. The limits of our area of interest are  $P_{famax}$  and  $P_{dmax}$ , these values become the new maximum possible values, i.e., 99.99% for each one, the obtained values in this research will be recalculated based on the new maximum limits.

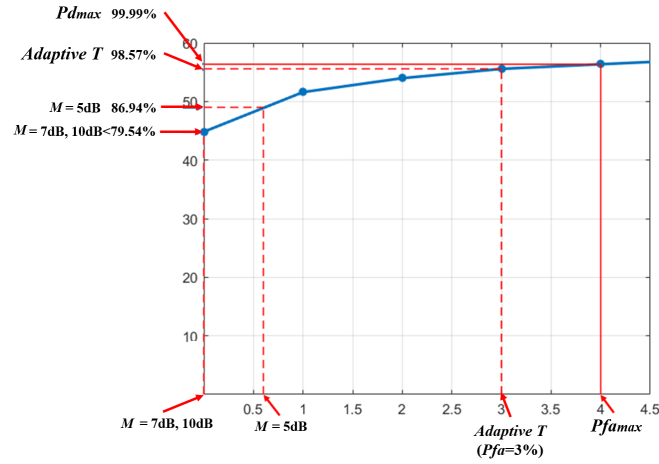


FIGURE 4.20: Detailed ROC curve for samples taken.

The value of  $P_{dmax}$  corresponds to 99.99%, the proposed adaptive  $T$  gives 98.57% of probability of detection whereas with  $M=5dB$  [41] it is 86.94%. Finally, for 7dB [42] and 10dB [43], the probability of detection stands at 79.54% or less from the new-scaled values, as is explained above.

## Chapter 5

# Proposed Model

In this chapter, the proposed model for sensing UHF TV spectrum to identify TVWS is proposed. In particular, the hardware configuration, and the stochastic considerations for collecting processing data is described in detail.

### 5.1 Hardware Configuration

Depending on the nature of the surrounding environment, two different spectrum sensing hardware configurations are proposed. They are :

- (i) Spectrum Sensing Station (SSS)
- (ii) Mobile Spectrum Sensing Station (M-SSS)

#### 5.1.1 Spectrum Sensing Station (SSS)

The SSS is assembled on a cart, and it can be used in two modes. In the first mode, which we refer to as the "Fixed" mode, the station is connected to the antenna installed on the roof of the CEI building, University of Windsor. It is used to collect outdoor information of the TV spectrum. On the other hand, the second mode is a portable version, where the SSS is connected to the internal antenna attached to the prototype and is used to sense the spectrum in indoor environments. It can be mentioned that, unlike the first mode, the second mode is a "Portable" version of the SSS.

As Figure 5.1 illustrates, the SSS uses RFE, SA and RTL-SDR devices connected in parallel to collect and measure a common signal received by the external or internal antenna. We use the same antenna model for both indoor and outdoor environments. The objective of using both SA and RFE is to analyze their comparative performance and to confirm the accuracy of measurement at a given time instant. And, as mentioned before, RTL-SDR works well only



within a narrow band, and for that reason, we use it primarily for pilot detection.

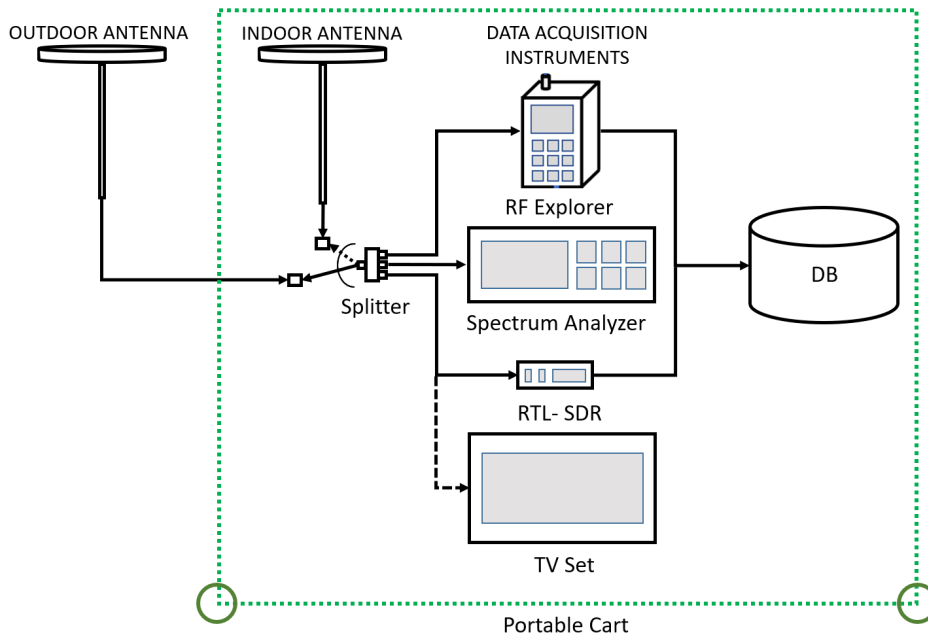


FIGURE 5.1: Proposed SSS for fixed outdoor and portable indoor sensing purposes.

The components of the SSS are shown in Figure 5.2. It shows the attached antenna, RFE module, SA, the PC that contains the DB, splitter, RTL-SDR, cables and connectors. This configuration provides enough portability inside buildings for collecting the data of interest. As seen from Figure 5.2, the SSS also has an attached TV set which is used to only verify the reception of a specific TV channel and is not used in the TVWS availability decision procedure.

### Energy considerations

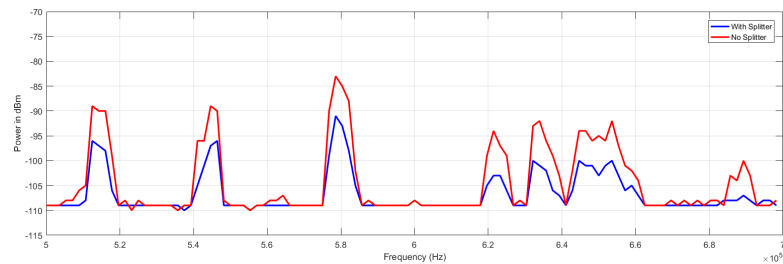
The SSS needs to be connected to a 120V AC, 60Hz source to operate. Thus while operated in the portable mode, there is a constraint on the portability and the continuity of spectrum sensing in indoor locations.



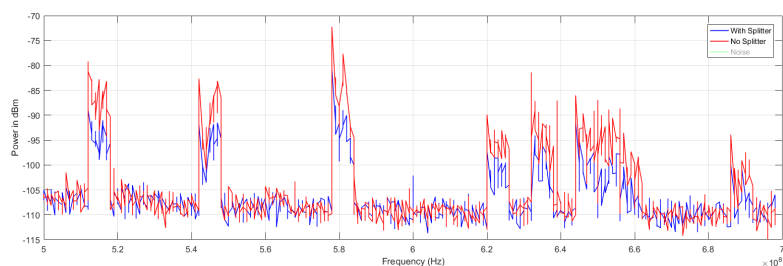
FIGURE 5.2: Portable SSS to sense the spectrum in indoor environments.

### Attenuation Consideration

In this configuration, it is necessary to consider that the presence of the splitter that divides the incoming signal into the three DAI devices, introduces an attenuation of 7dB in the peaks of the PU signals [51], as is observed in Figure 5.3 (a) for RFE and (b) for SA. However, this attenuation does not affect the results of the proposed adaptive  $T$  of sensing the PU signals.



(a)



(b)

FIGURE 5.3: Attenuation introduced by the splitter, the theoretical value is 7 dB, (a) for RFE and (b) for SA.

## Devices Connection and Communication

The DAI-PC connection and the associated software details are listed in Table 5.1. As seen from this Table, the RFE is connected using the USB port of the computer, and an open application named RF Explorer for Windows is being used. The SA is connected using the RJ45 port interface of the PC and is accessed through a web browser using an IP address. The RTL-SDR receptor uses a USB port, and an AIRSPY SDR application must be installed. Figure 5.4 represents the graphical user interface of the applications used to collect data.

TABLE 5.1: Communication from the three DAI to the PC to save data collected in the DB.

Device	Port	App	Address/ID
RFE	USB	RF Explorer for Windows	COM 3
SA	Ethernet 0	MDO4054B-3 Web-Enabled-User	192.168.3.2
RTL-SDR	USB	AIRSPY SDR Software	COM 4

Almost all the applications used to read data from the DAI devices are open source tools. An exception is the SA Tektronix MDO4054B-3 which was provided by the WiCIP lab of the University of Windsor.

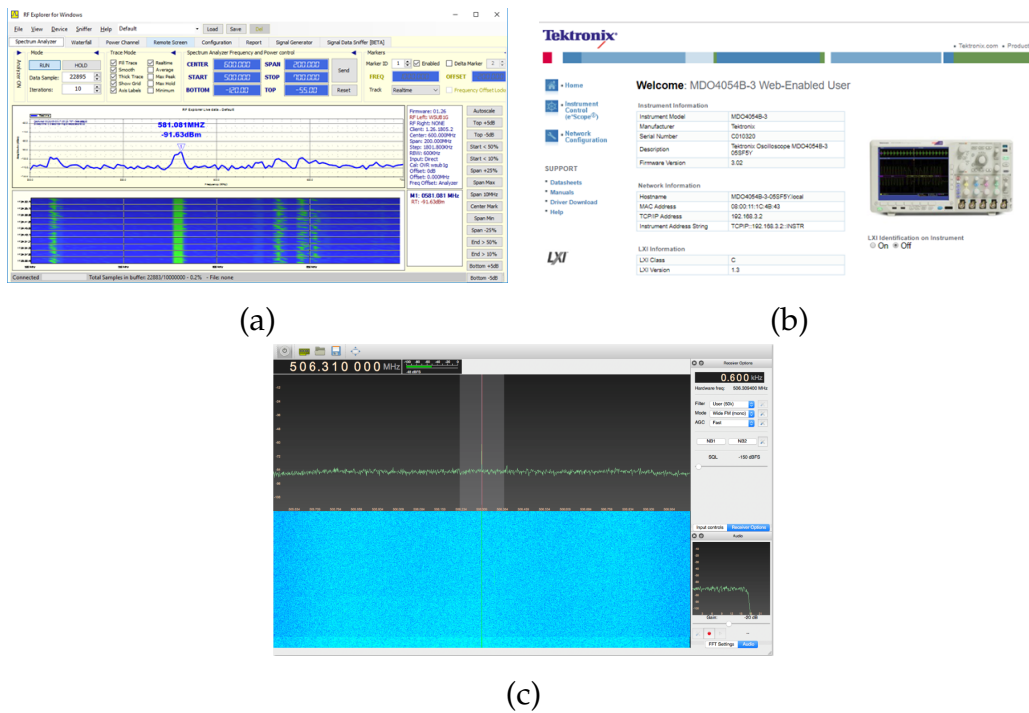


FIGURE 5.4: Applications used to collect data, (a) for RFE, (b) for SA, and (c) for RTL-SDR.

### 5.1.2 Mobile Spectrum Sensing Station (M-SSS)

In Chapter 3, an initial M-SSS has been proposed. Then, based on considerations mentioned in Chapter 4, modifications were made to the design. The earlier design is shown in Figure 5.5(a) whereas the final one is shown in Figure 5.5(b). The basic difference between them is the addition of an RFE device with a  $50\Omega$  matched impedance. This addition is made in order to simultaneously sense the noise level of the system  $W(f)$  along with the composite signal  $X(f)$ .

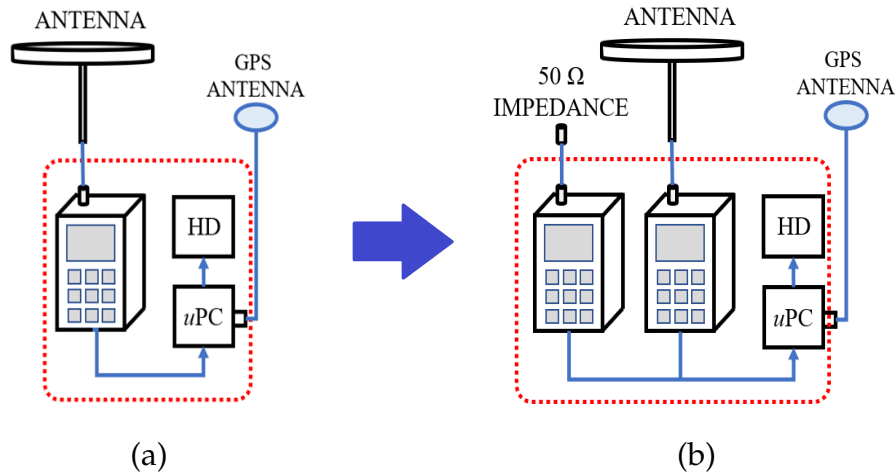


FIGURE 5.5: M-SSS to sense spectrum over a mobile platform to sense wide geographical areas, (a) original diagram, (b) proposed configuration.

Besides the spectrum sensing devices, the M-SSS has an Universal Serial Bus (USB) GPS receptor antenna for capturing the Geo-location information, i.e., Longitude and Latitude. The readings of both RFEs, the timestamp of the sample, i.e., hour, minute, seconds, and milliseconds and Geo-locations are saved in the DB. Table 5.2 details the device, port, app used, and address to allow this data transfer. Now, since M-SSS is a mobile system, components must be lightweight, low power consumption, easy to handle. Because of these constraints, SA could not be used here.

TABLE 5.2: Communication from the three DAI to the PC to save data collected in the DB.

Device	Port	App	Address/ID
RFE # 1	USB	RF Explorer for Windows	COM 3
RFE # 2	USB	RF Explorer for Windows	COM 4
GPS Antenna	USB	Cool Term V 1.5.0	COM 6

### Energy considerations

When the M-SSS is used to sense the UHF TV spectrum from a moving vehicle, the energy provision must be considered. In the proposed system, the only energy source available is the laptop computer battery. Though the RFE devices have their internal batteries, when connected to the laptop computer USB port, automatically starts to charge their internal batteries. Thus, the laptop battery becomes the only power source. The laptop can be charged from the vehicle battery to prolong the time of data collection.

### Spatial Separation of the Data Readings

Depending on the posted city road speed limits, vehicle speed changes and can be as high as 120Km/h. The RFE used takes readings every 0.340s and it means that the spatial distance among samples can vary. Table 5.3 lists the variation of spatial distance corresponding to the different possible travelling speeds of the vehicle.

TABLE 5.3: Distance between data readings and speed.

Speed (Km/h)	Speed (m/s)	Distance between readings (m)
120	33.33	11.33
100	27.77	9.44
80	22.22	7.55
60	16.66	5.66
40	11.11	3.77
20	5.55	1.88

According to this table, the maximum spatial separation of the samples is 11.33m which is the worst-case sample separation. This value is within acceptable range ensuring that all the sensed area is covered avoiding loss of information or coverage holes.

### Amount of Data Collected

The RFE device scans 198MHz bandwidth of the 500MHz to 698MHz UHF TV spectrum with a separation of 1.76MHz at a given time instance. It means there are  $198\text{MHz}/1.76\text{MHz} = 112$  samples reading per RFE at a given time instance. Along with two RFE devices, we are using one GPS device. Hence, a single reading constitutes of 112 Signal power in  $dBm$ , 112 Noise power in  $dBm$ , and 1 location-timestamp data samples. The RFE devices took readings every 0.340s

which implies that for a duration of 1 minute, we had  $(112+112+1)*(60/0.34) = 39705.88$  data samples. Figure 5.6 illustrates these concepts.

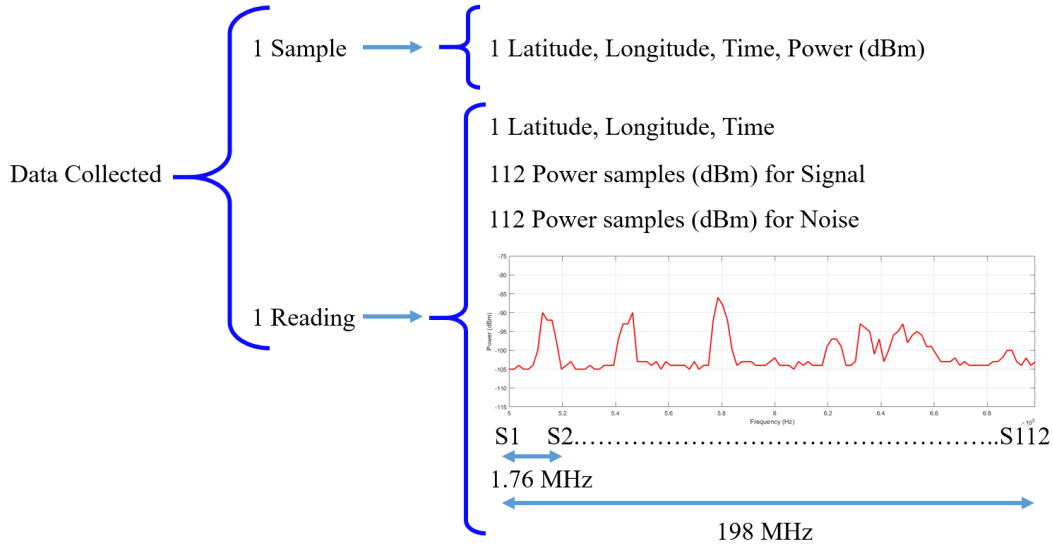


FIGURE 5.6: Data collection, 1 reading is composed by 112 samples for the composite signal, 112 samples for noise, separation between two samples is 1.76 MHz, all 112 samples covers 198 MHz which is the UHF TV bandwidth.

## 5.2 Data Processing

The ultimate goal of our proposed system is to make a decision about the presence or absence of a PU signal within a UHF TV Channel. For this, the collected data emerging from different sources need to be processed. In our proposed data processing models, depending on the mode of operation, the underlying data processing also differs.

### 5.2.1 Data Processing - SSS

As is observed in Figure 5.7, the proposed decision-making model for SSS consists of two inputs, five blocks, and one output. The composite signal  $X(f)$  is collected by the antenna and is fed to three DAI devices, i.e., an RFE, a SA, and an RTL-SDR. The RFE and SA are in the ED block, whereas the RTL-SDR is in the PD block.

In ED, the information is acquired by the RFE and the SA. These two devices have different characteristics, for instance, the RFE collects 112 samples, and SA in the same reading collects 1005 samples. Thus use of SA ensures higher accuracy of sensing and this is an advantageous point of SSS over M-SSS.

SC block takes the readings from ED and calculates the mean of the noise  $\bar{W}(f)$ , and the statistical characteristics of the sensed signal. With this information, it finds the adaptive threshold  $T$  and obtains the channels where the presence of energy is detected.

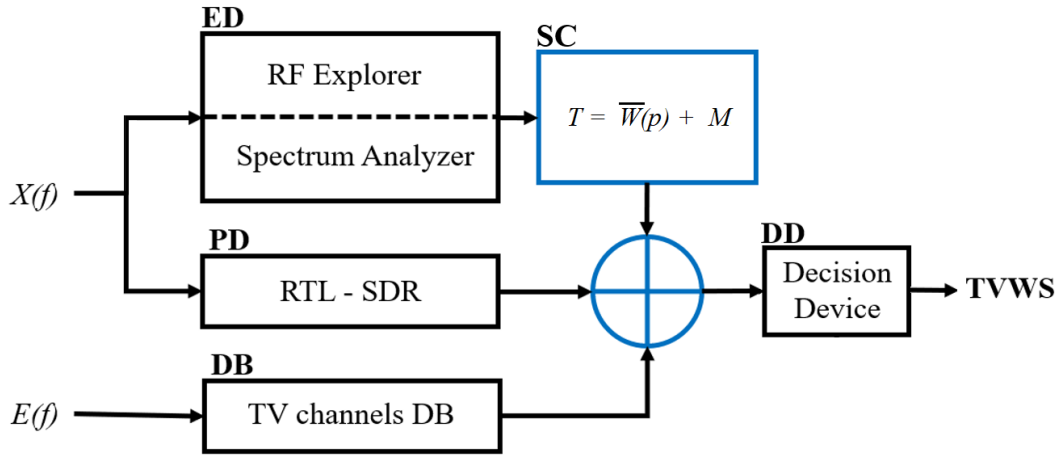


FIGURE 5.7: Proposed SSS for fixed and portable sensing purposes in outdoor and indoor environments.

PD block inspects a very narrow frequency band and is tuned to the frequency at which a TV broadcasting pilot tone is expected, i.e., 310KHz above the lower edge of each channel. And it identifies those channels where pilot tones are present. The DB block represents stored information about channel occupancy,  $E(f)$ , collected from an external source. Finally, the DD block uses the combined information provided by ED, SC, PD, and DB blocks to decide the presence or absence of TVWS in the sensed spectrum.

### 5.2.2 Data Processing - M-SSS

For M-SSS, the data is processed in a different manner than the fixed version. In this particular case, it is mandatory to collect samples of composite signal  $X(f)$  and noise signal  $W(f)$  in parallel at each instant of time  $t_i$ . This is due to the fact that because of the fast-changing of position of the MSSS, there can be significant changes in spectrum characteristics. Figure 5.8, illustrates the proposed decision making model for MSSS.

In contrast to Figure 5.7, we see in Figure 5.8 that the SA devices in the ED block have been replaced by an RFE device. The objective of this RFE device is to collect data about the noise of the system  $W(f)$ . To allow this, a  $50\Omega$  matched impedance is attached to this additional RFE. The second RFE collects the information of the composite signal  $X(f)$ .

Let us consider that, because the data are collected by a mobile station, a GPS antenna must have been attached to the M-SSS, this is to collect information related to the Latitude and Longitude of the sensed point.

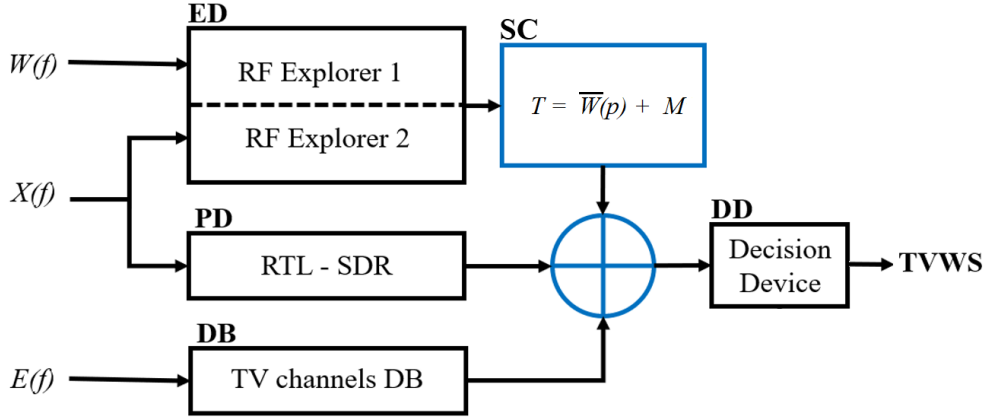


FIGURE 5.8: Proposed M-SSS to sense spectrum over a mobile platform to sense wide geographical areas.

Now, the ED block, simultaneously senses  $X(f)$  and  $W(f)$ . This feature permits to know at any time the level of noise of the system. In SC block, the data collected by RFE #1 and RFE #2 are analyzed, next their statistical characteristics are obtained, i.e.,  $\bar{W}(f)$ ,  $M$ , and adaptive  $T$ . After this, the energy of the channels is detected as is detailed in Chapter 4. The PD, DB and DD block work in the same way as their counterpart of the SSS data processing model. Finally, it might be noted that information obtained by PD and  $E(f)$  can be taken with a lower periodicity i.e., every 3 months or more because this information has a very low variation rate.

### 5.3 Stochastic Considerations

For decision making, the proposed model takes into account the statistical characteristics of noise  $W(f)$  and composite signal  $X(f)$ , both simultaneously sensed at the same location. These two signals present differences that are used to identify TVWS. In other words, the statistical characteristics of the noise signal  $W(f)$  which is Normally distributed, provides information as the mean of the noise  $\bar{W}(f)$ , its standard deviation  $\sigma$  and the  $P_{fa}$  necessary to calculate the adaptive  $T$ . With all this information, we can apply the ED technique to the composite signal  $X(f)$ .



The summarized procedure is visualized in Figure 5.9. The first RFE provides  $X(f)$ , the second RFE collects information from  $W(f)$ . From these signals, statistical information like  $\bar{W}(p)$ ,  $\sigma_W$ , and  $z_W$  for a  $P_{fa}$  equivalent to 3% are obtained. The same information is obtained from  $X(f)$ , i.e.,  $\bar{X}(p)$ ,  $\sigma_X$ , and  $z_X$ .

Considering the data from both signals, we obtain the adaptive  $T$ .

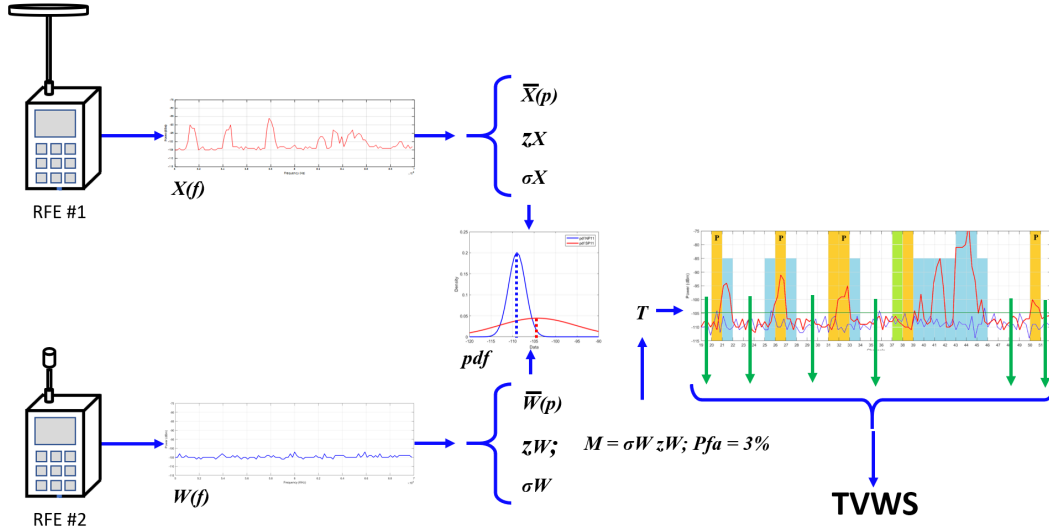


FIGURE 5.9: Proposed M-SSS to sense spectrum over a mobile platform to sense wide geographical areas.

It is necessary to assume  $X(p)$  as a Normally distributed signal, to reduce the complexity of the calculations to find the value for  $T$ .

### 5.3.1 Decision Procedure

The results obtained from ED, SC, PD and  $E(f)$  are processed together by DD to determine the presence of PU. Table 5.4 shows the possible scenario with corresponding decision outcomes.

- (i) If ED, PD, and DB output are negative, then the channel is marked as unused ( $H_0$ ).
- (ii) If ED is negative ( $X(f) < T$ ), but either PD or DB or both are positive, then the channel is marked as used ( $H_1^*$ ), which indicates that the channel is only occupied in urban area of the city, i.e., available in the rural area.
- (iii) If ED is positive then the channel is marked as used ( $H_1$ ), irrespective of PD and DB outputs.

This procedure is applicable to both the SSS and M-SSS prototypes.

TABLE 5.4: Decision Procedure, true table.

Group	ED	PD	DB	Decision
(i)	0	0	0	$H_0$
(ii)	0	0/1	1/0	$H_1^*$
(iii)	1	0/1	1/0	$H_1$

\* If the point is in the urban area of the city

### 5.3.2 Output Representation

The most attractive manner to show results is using an intuitive visual representation. Figure 5.10 shows such a representation. In this representation, 32 UHF TV channels can be observed and immediately determined if the channel is used or if it is considered as a TVWS.

Figure 5.10 shows a set of vertical bars where the number on the horizontal axis i.e. 19 to 51 represent the UHF TV channels number. The green horizontal line represents the calculated adaptive  $T$  in dBm. The red plot represents the detected energy (dBm) of the composite signal  $X(f)$  and the blue plot shows the noise level  $W(f)$  (dBm). The detected Pilot tones are marked by the letter "P" printed on the top of the channel bar. If the channel was found in DB, its corresponding vertical bar appears in yellow. Channel 37 is used for radio astronomy and it appears coloured with green. TVWS appears in white (absence of colours). Finally, if a channel does not have a detected pilot tone or is not mentioned in the DB, but energy is detected, it will appear painted in cyan.

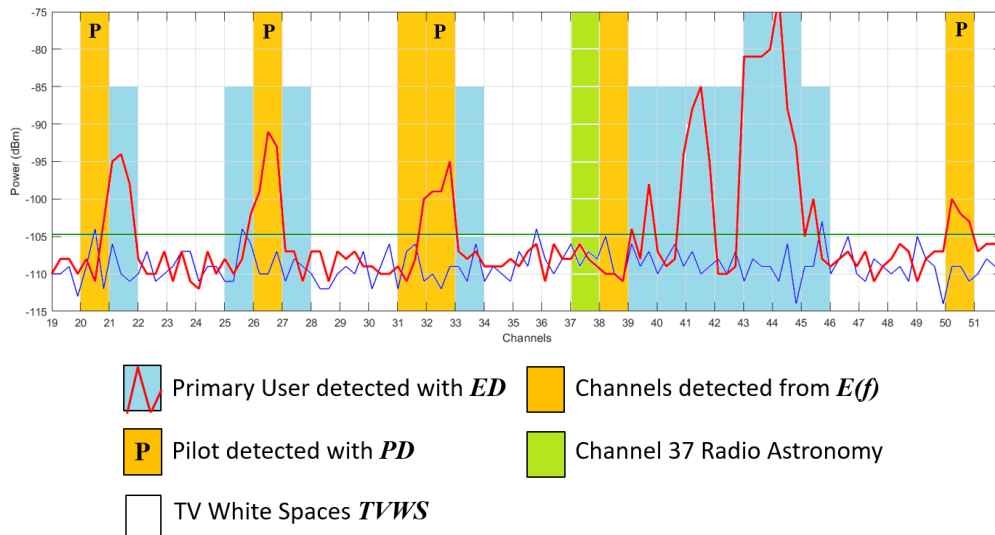


FIGURE 5.10: Proposed graphical representations of results.

## Chapter 6

# Results and Discussion

This Chapter shows and discusses the results obtained from scanning the UHF TV spectrum in the city of Windsor using the proposed sensing model. It also explains the different parametric considerations that are needed to accurately distinguish between occupied and idle channels.

### 6.1 Data Characteristics

Measurements using the M-SSS were taken in the city of Windsor, following the trajectories shown in Figure 6.1. For better understanding, we are showing the trajectories and locations of this Figure, which was also shown before in Figure 3.3. The M-SSS takes samples in a continuous manner. The relevant data collection setup parameters are listed in Table 6.1. As seen in this Table, 36,176 readings which represent 4,051,712 samples, since there are 112 samples per reading. The same process is used to sample noise data with another RFE device; in total, 8,103,424 samples were collected. The time interval between each reading is 0.340 seconds. The signal and noise data samples, along with the GPS information of Latitude and Longitude is saved in the DB of the prototype. The total distance traveled to collect the samples was 103.2km.

TABLE 6.1: Number of readings and samples collected with each RFE.

Trajectory	Distance in Km	Readings	Noise Samples	Signal Samples
T1	16.05	5,417	612,752	612,752
T2	32.45	10,419	1,166,928	1,166,928
T3	31.48	12,924	1,447,488	1,447,488
T4	23.22	7,362	824,544	824,544
<b>Total</b>	<b>103.20</b>	<b>36,176</b>	<b>4,051,712</b>	<b>4,051,712</b>

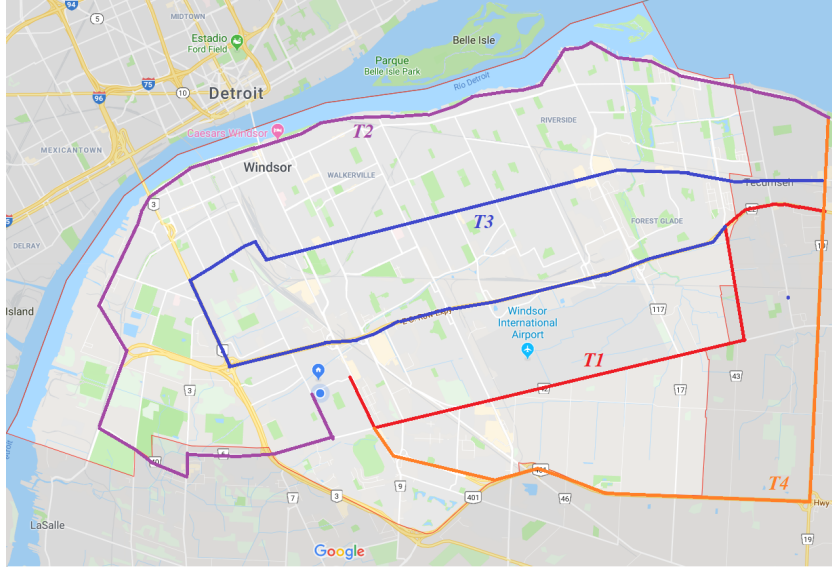


FIGURE 6.1: Four trajectories were defined to sense the UHF TV spectrum in the city of Windsor, T1 red, T2 purple, T3 blue, and T4 orange.

As mentioned in Chapter 4, the value of  $P_{fa}$  was selected as 3% for processing the collected data. The obtained results are shown and discussed in the following sections.

### Considerations

The M-SSS is mounted on a vehicle to collect the samples. The maximum speed limit ( $v$ ) in the city at the expressway is 120 km/h, considering that the RFE takes a sample every 0.340 seconds ( $t_s$ ), the maximum distance ( $d$ ) between two successive samples taken is given by

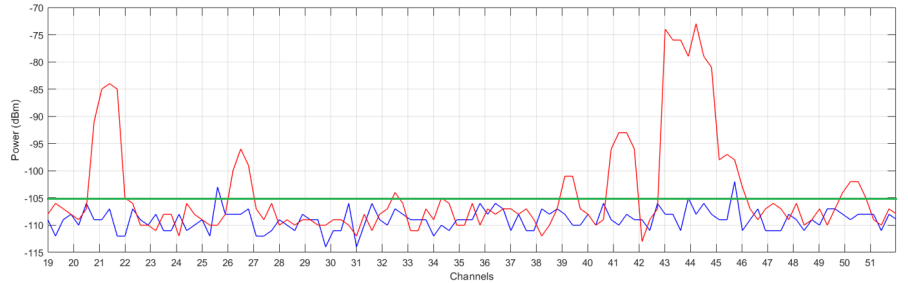
$$d = v * t_s \quad (6.1)$$

according to this,  $d$  is 11.33m. When the vehicle is travelling faster, this value can decrease according to the speed variations. This maximum distance of the samples taken is small enough to plot the spectrum with an accurate level that represents how the spectrum is being used in the sampled area.

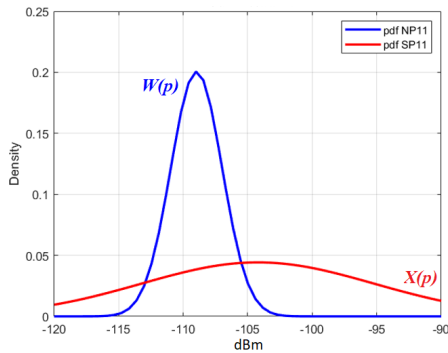
## 6.2 Samples Analysis

For a particular reading, Figure 6.2 illustrates (a) the plot of the spectrum vs power, (b) the  $pdf$  of the composed signal combined with the  $pdf$  of the noise, and (c) the ROC curve of the  $P_{fa}$  vs  $P_d$ . This information is used to identify the

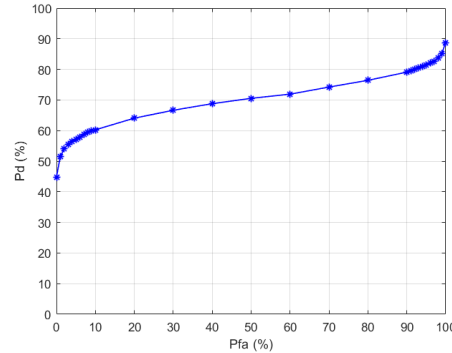
presence of PU in a sensed band, the level of the noise, and permits calculation of the adaptive  $T$  for each case. This adaptive  $T$  is also shown on Figure 6.2(a). In the horizontal axis are represented channels from 19 to 51, and the vertical axis has the absolute power of the signal measured in  $dBm$ .



(a)



(b)



(c)

FIGURE 6.2: P11 (a) Spectrum diagram, (b) pdf of the noise and composite signal, and (c) Receiver Operation Characteristics curve with the  $P_{fa}$  vs  $P_d$ .

Using the same concept of Figure 6.2, Figures 6.3, 6.4, and 6.5 show the spectrum diagram, pdfs of noise and composite signal, and Receiver Operation Characteristics (ROC) curve respectively for ten different locations.

In Figure 6.3(a), for channel 21 and channels 39 - 45, we observe that the signal energy is above  $T$ . We also observe that some noise peaks are also about  $T$ . This reading was taken in a location which is on the eastern end of the city. The subsequent readings are taken in a trajectory that approaches to the central part of the city. In Figure 6.3(b), it is observed that signal energy is detected in channels 31 and 32 in addition to the channels mentioned in Figure 6.3(a). From Figure 6.3(c), it appears that there are energy peaks in channel 50 along with channels 31 and 32 but the energy of channel 21 decreases to a level below  $T$ . In Figure 6.3(d) the energy of the detected channels maintains its values in relation to the previous figure. In Figure 6.3(e) there are well-defined peaks of energy in channels 20-21, 26, 31-32, 38 to 46, and 50. In Figure 6.3(f) the profile

is maintained, the general levels of energy decreases, but the same channels are detected. For Figures (g), (h), (i), and (j) the energy detected does not present any significant variation and it is the usual energy profile of the channels detected in the central area of the city. The channels detected are 20-21, 25-26, 31-32, 38 to 46, and 50.

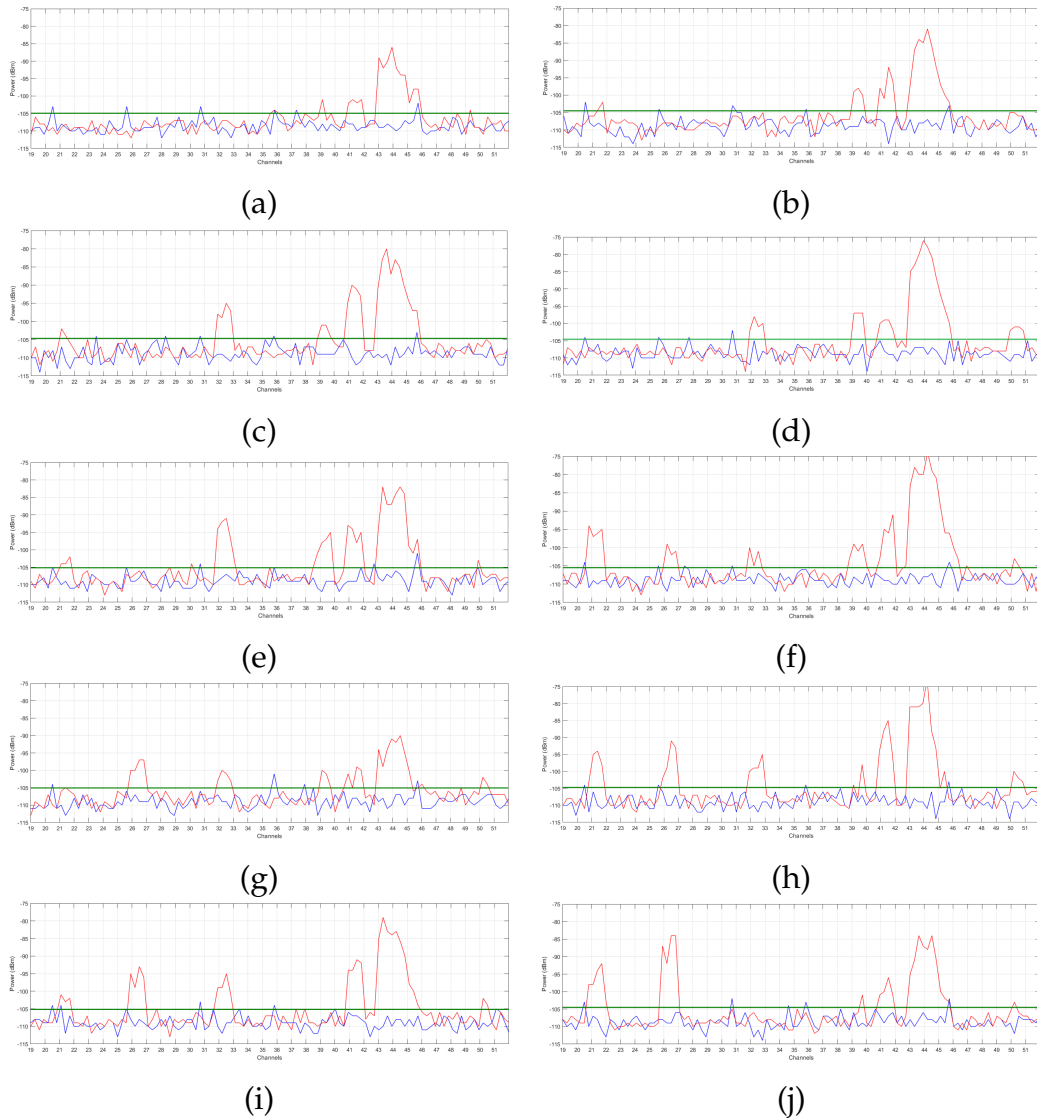


FIGURE 6.3: Sub-figures (a) to (j) spectrum vs power sensed in Points 1 - 10, there are variations on the energy detected due to the different location in which the samples were taken.

For the next block of plots in Figure 6.4, the pdf of the noise  $W(p)$ , and the composite signal  $X(p)$  are shown. Its relative amplitude and position vary depending on the presence of energy and noise detected. These small variations mark the difference that determined to set adaptive  $T$  for each case.

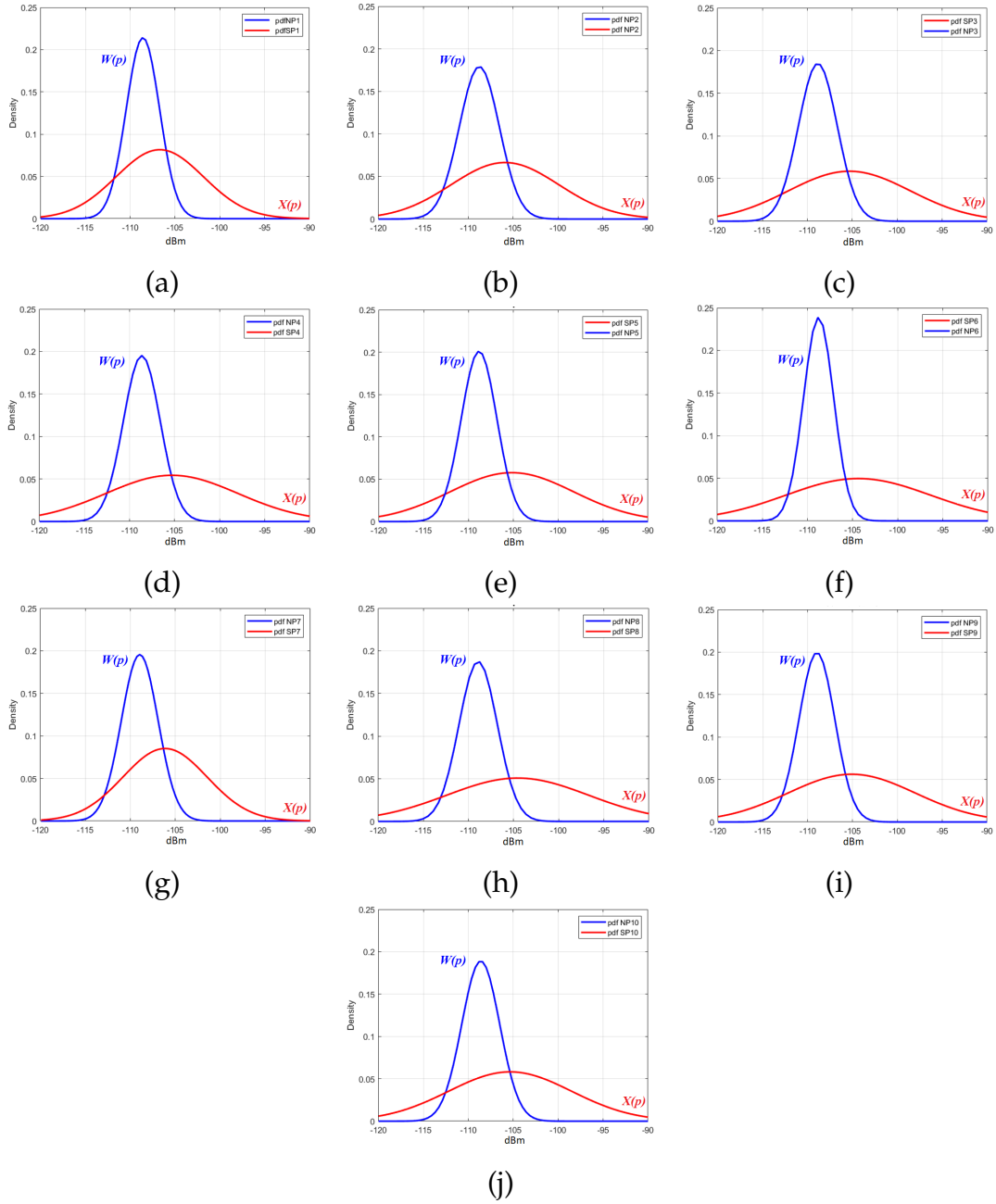


FIGURE 6.4: Sub-figures (a) to (j) pdf of the  $W(p)$  and  $X(p)$  sensed in Points 1 - 10.

In Figure 6.5, the ROC curves from each of the ten locations are plotted. These curves represent the relation between  $P_{fa}$  and  $P_d$  in each case. The different values respond to the variations previously registered in the sensed locations. These curves have enough information to reveal the behaviour of the spectrum.

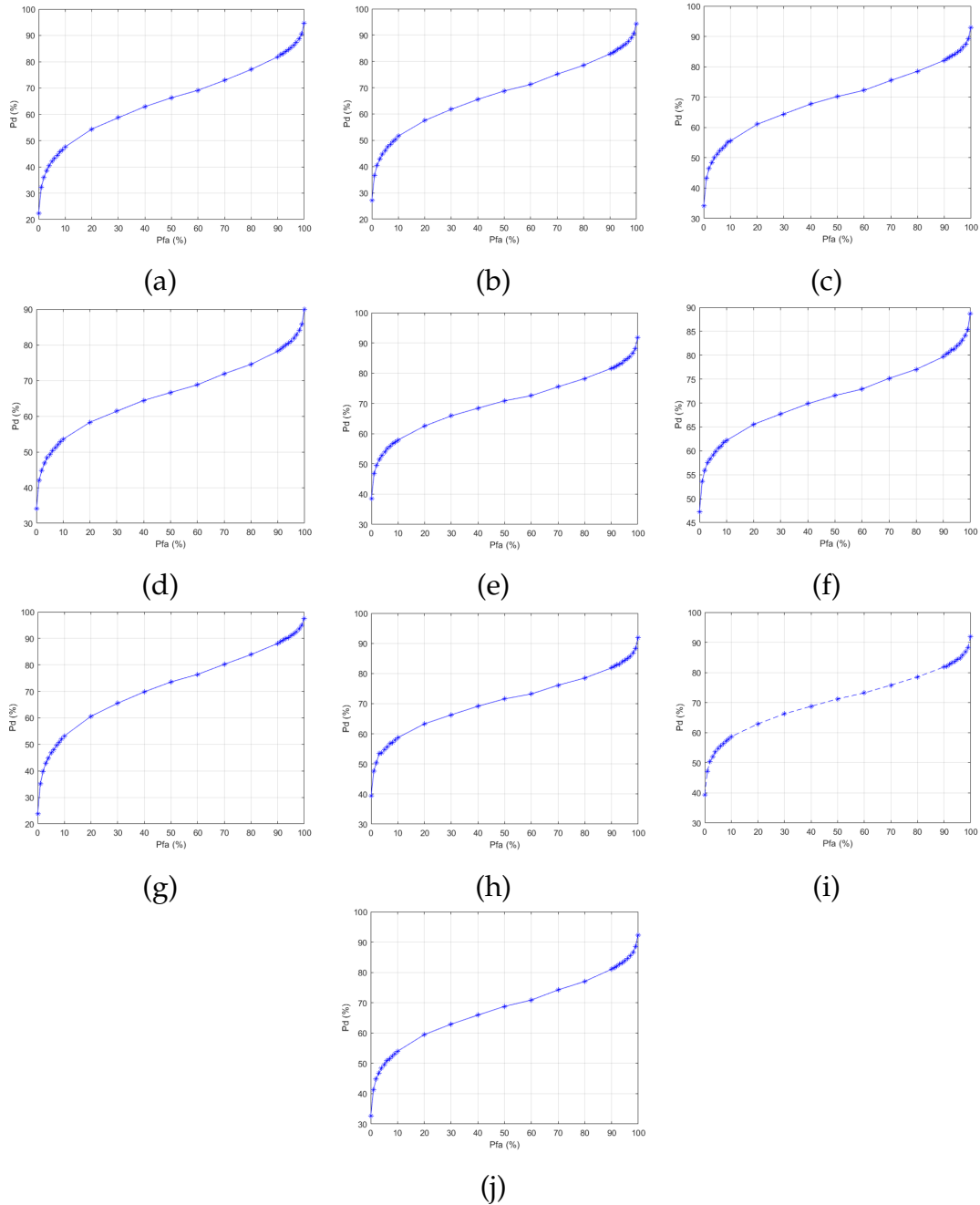


FIGURE 6.5: Sub-figures (a) to (j) ROC curves of the signal sensed in Points 1 to 10.

It is important to note that each reading provides valuable information to determine the state of the spectrum in that specific location at an instant of time  $t_i$ . To obtain a global view of the proposed method and its applicability, it is necessary to compare all the obtained curves together to find usable relationship, if any.

Figure 6.6(a) plots the ROC curves ( $P_{fa}$  vs  $P_d$ ) of the ten analyzed locations. It is quite clear that each location has its own characteristics which differ from



others.

Figure 6.6(b) depicts the same ROC curves shown in 6.6(a) but focuses on a  $P_{fa}$  a range of 0% to 4%. Additionally, the dotted vertical lines represent the adaptive  $T$  in red, the  $T$  obtained with a  $M = 5dBm$  in blue,  $M = 7dBm$  in green, and  $M = 10dBm$  in brown respectively. The Y-coordinate value of the intersection of a particular  $T$  and the ROC curve of a location represents  $P_d$ . For example in P3, for a  $P_{fa}$  of 3% corresponds a  $P_d$  of 48.4%.

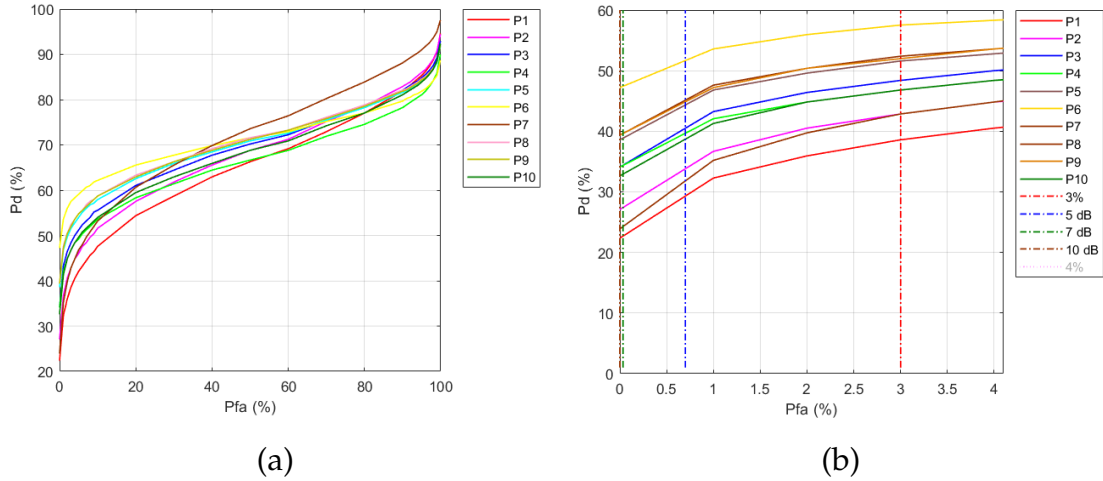


FIGURE 6.6: ROC curves obtained from P1 - P10, in (a) are present all the curves, and in (b) are shown the same plot but zooming in to observe the curves with a  $P_{fa}$  closer to the one defined by the adaptive  $T$  of 3%.

To visualize the accuracy of the model that proposes an adaptive  $T$ , the ROC curve of the  $P_{fa}$  vs  $P_d$  is obtained by calculating the average of 36,176 readings or 4,051,712 samples. By using Equations (4.4), (4.8), (4.14), and (4.15), the  $P_{famax}$  is obtained and corresponds to 4%. Figure 6.7 illustrates the average curve, the  $P_{famax}$ , the adaptive  $T$ , and the values for  $T$  using a margin  $M$  of 5, 7, and 10 dB. Considering that  $P_{famax}$  defines the  $P_{dmax}$  which becomes 99.999% of the signals that are possible to be detected.

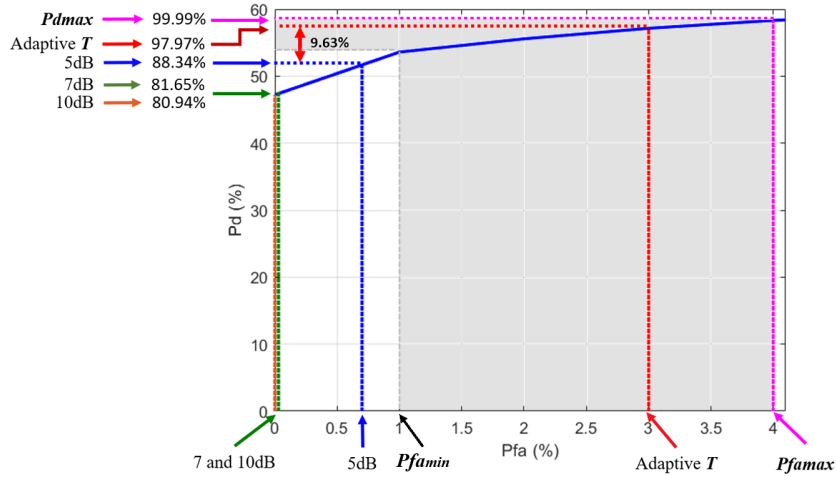


FIGURE 6.7: Dotted lines are the  $P_{famax}$ ,  $P_{fa}$  calculated with the adaptive  $T$ , and  $T$  obtained by using a  $M$  of 5, 7, and 10dB respectively. It is observed that the adaptive  $T$  proposed increases at least 9.63% of  $P_d$  than the values used by other authors.

## 6.3 Results Presentation

### Channels Occupancy

In this project, 33 UHF TV channels (Channel 19 to channel 51), each having a bandwidth of 6MHz were sensed. Channel 37 is assigned to radio astronomy and it is not used for TV broadcast, results are given for the remaining 32 TV channels. According to the information collected and applying the proposed model which considers  $ED$ ,  $PD$ , and  $DB$ , six channels were found to have enough energy above  $T$  and the PU presence was confirmed by visually observing TV channel captured by the attached TV set. These 6 channels are divided into 19 sub-channels where six of them are High Definition (HD), 12 are Standard Definition (SD), and one is used for audio only (910 KHz AM radio) as was detailed in Table 3.1 of Chapter 3. In Figure 6.8 are plotted the geographical points in which its occupation is represented.

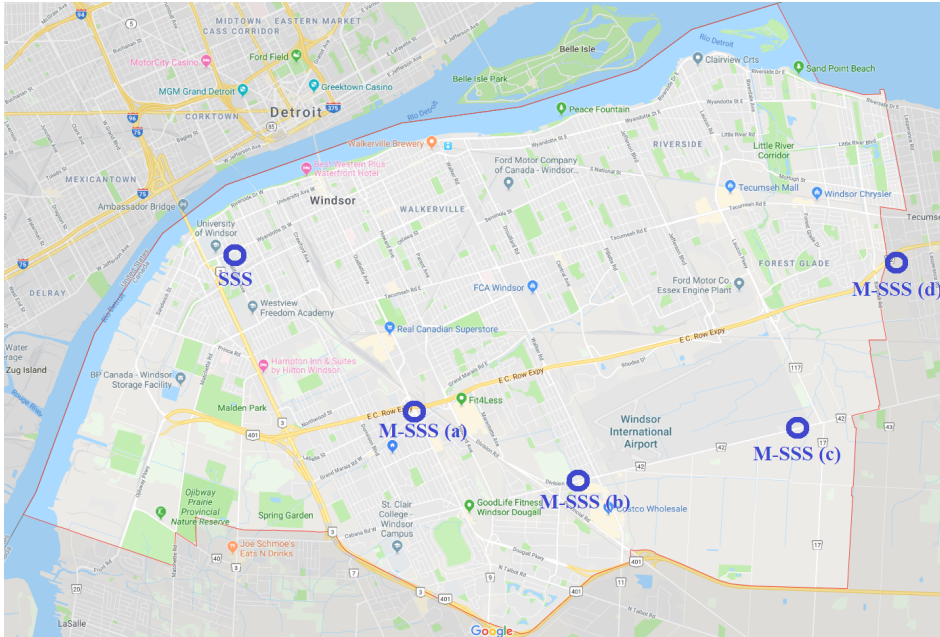


FIGURE 6.8: Location of the represented points

### Spectrum Sensing Station SSS

By using the SSS, we found the existence of PU in 23 channels while scanning the location around the University of Windsor, marked as (SSS) in Figure 6.8. So it shows 72% of TV spectrum used and 28% idle spectrum. The later can be considered as potentially TVWS allowing DSA as SU.

### Mobile Spectrum Sensing Station M-SSS

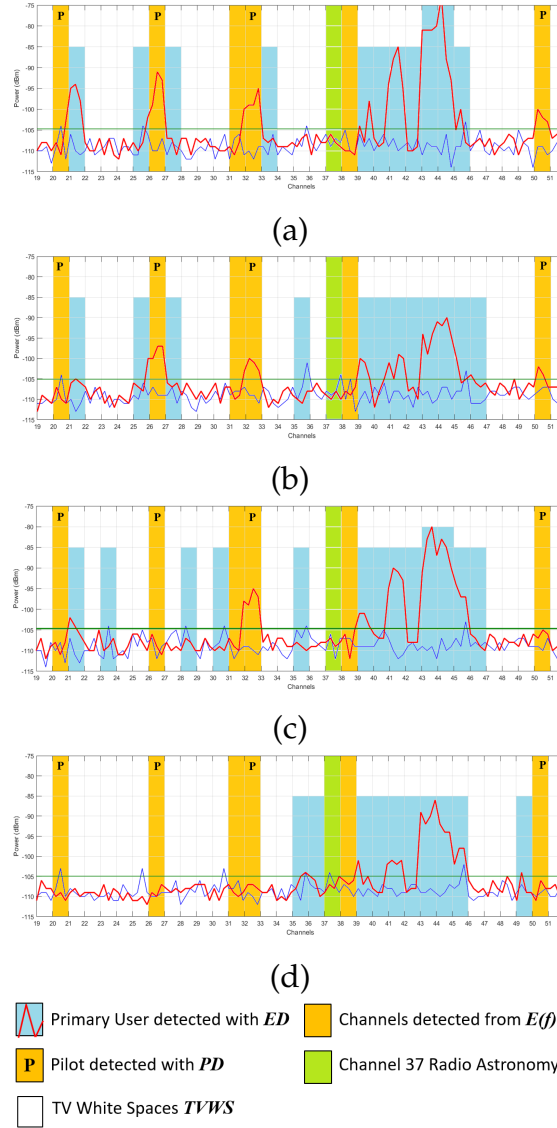
When the M-SSS is used to sense the UHF TV spectrum, the results can vary according to the geographical location of the sensed data, as is observed in Figure 6.9(a), in the central south (a) part of the city, we find six TV channels present in Windsor (yellow coloured), and 11 channels for which signal was detected by the DAI (in cyan), this is 53% of TV spectrum used, and 47% idle spectrum.

In Figure 6.9(b) that correspond to the south (b) part of the city, there are six TV channels (yellow coloured) and 12 channels for which signal was detected by the DAI (in cyan), this represents 57% of used spectrum and 43% of TVWS.

In Figure 6.9(c) which is the middle-east (c) part of the city, there are six TV channels (yellow coloured) and 13 channels for which signal was detected by the DAI (in cyan), this represents 60% of used spectrum and 40% of TVWS.

Finally, In Figure 6.9(d) which is the east (d) limit of the city, there are six TV channels (yellow coloured) and 10 channels for which signal was detected by the DAI (in cyan), this represents 50% of used spectrum and 50% of TVWS.

These results are given considering that the six channels mentioned in the  $E(f)$  are effectively occupied by PU, which is not necessarily the truth. It can produce that the percentage of TVWS increases for each case.



### Legend

FIGURE 6.9: Spectrum detected and analyzed with the proposed model. (a) central south part of the city, (b) southeast, (c) middle east, and (d) eastern limit of the city of Windsor. Note that as far of the center the sample is taken, less PU are detected.

## 6.4 Variability of the sensed Signals

The reason to take simultaneous samples of the noise  $W(f)$  and the composite signal  $X(f)$  at each time instant  $t_i$ , is due to the variations experienced in the

UHF TV spectrum by the above-mentioned signals. From Figure 6.10 we can observe the pdf of the average values for  $W(p)$  and  $X(p)$ . To obtain this pdf, from trajectory T2, a number of 1,166,928 samples for noise, and a similar number for the composite signal were collected. The mean values of the signals were obtained, and a Confidence Interval (CI) corresponding to 95% was calculated and plotted.

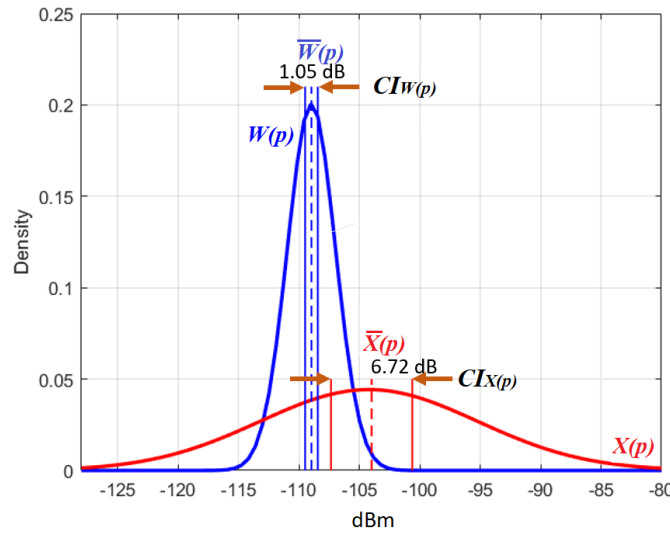


FIGURE 6.10: Plot of the Confidence Interval (CI) of average values for  $W(p)$  and  $X(p)$ , the variations are represented in dB.

Figure 6.10 also shows that the noise mean  $\bar{W}(p)$  has a value of -108.9725 and can have a variation of 1.05dB. The mean of the composite signal  $\bar{X}(p)$  has a value of -103.9889 with a CI of 6.72dB.

Around  $\bar{X}(p)$ , represented with a red dashed line, the mean of the composite signal values, could vary in 6.72 dB. Now, it means that sometimes the respective pdf of the noise and the composite signal can be closer or separated from each other. This variation is confirmed by the plots represented in Figure 6.4. In order to avoid any error produced by the variation mentioned above, it is recommended to obtain separate readings for signal and noise. This is more applicable when the M-SSS is used and the samples are taken in different geographical location every  $t_i$ .

## Chapter 7

# Conclusion and Future Work

### 7.1 Conclusions

In this thesis, a probabilistic model to identify the occupancy of the UHF TV spectrum has been proposed. The model is based on the probability of false alarm and the probability of detection of the sensed signals. For collecting information, two spectrum sensing station prototypes were designed and constructed. The first one was named as Spectrum Sensing Station (SSS) and the second one as Mobile Spectrum Sensing Station or M-SSS. The SSS was operated in two modes, a fixed mode that uses an external antenna to sense the outdoor TV spectrum, and a portable mode which is used for indoor spectrum sensing purposes. The mobile station M-SSS was designed for mounting on a vehicle, for sensing broad geographical areas. It uses lightweight components, consumes low power, and is easy to handle. Another mention-worthy feature of the M-SSS is that it uses a technique that senses the spectrum with two RFE devices connected in parallel for sensing composite signal and noise signal simultaneously for improved detection capability.

To reduce the risk of missed detection, in the proposed model, two sensing techniques, i.e., energy detection and pilot detection outputs are combined with primary users' information. This information is obtained from an external source, and it is based on the geographical location of the primary users. This technique attempts to reduce errors and increase detection probability by considering diverse information from different sources.

A mention-worthy aspect of this proposal is the probabilistic model that considers the probability of false alarm and the probability of detection; both used to calculate an adaptive threshold. This is obtained from the simultaneous reading of the noise and the composite signal samples, taken every instant of time  $t_i$ , which ensures the quality of the results compared to existing methods.

The probability of false alarm and the probability of detection values are

calculated assuming that the noise and the composite signal are normally distributed. While the noise signal truly follows a normal distribution, in order to reduce computational complexity related to probabilistic analysis and yet preserve efficiency, the composite signal is also assumed to be a normally distributed signal. We consider this assumption to be an acceptable one since the fundamental calculations involved in finding the probability of false alarm is based only on the noise signal, which as mentioned before, follows a Normal distribution as the Kolmogorov-Smirnov test has verified. The optimal probability of false alarm is used as an input in the receiver operating characteristic curve function, and the optimal probability of detection is obtained.

Two spectrum sensing stations have been designed and implemented to demonstrate the developed technique for TVWS spectrum sensing. The first one, consist of a high-precision, expensive spectrum analyzer which is used to sense the spectrum from a fixed location. Readings collected with the spectrum analyzer serve as a reference to compare the readings taken with the RF Explorer, a low-cost open hardware/software device used to sense the same spectrum in parallel. The RF Explorer was found to give a good performance. With these results, a second mobile spectrum sensing station was implemented where two RF Explorer devices were mounted on a vehicle and used to sense the spectrum across the city of Windsor, collecting more than 8 million samples.

Performance-wise, our model demonstrated 9.63% higher probability of detection ( $P_d$ ) compared to other methods found in literature. And, from our collected data, we observed that in the central area of the city, about 28% of the sensed spectrum are TVWS and as we move to the outer edges of the city, up-to 65% of the TV channels sensed were found to be TVWS. This observation clearly suggests that there lies a significant number of unused TV channels which can be used for different opportunistic services through the implementation of cognitive radio-enabled dynamic spectrum access. Finally, it can be concluded that the proposed mobile spectrum sensing station along with the proposed probabilistic model for sensing the UHF TV spectrum can be used in any other location.

## 7.2 Future Work

From the growing interest of spectrum sensing for cognitive radios, it is understood that research scopes in this field are immense. Extending our current research, our future research plans include but are not limited to the following: Exploring beyond TVWS, by designing and developing sensing prototypes

that are not restricted to TV bands and cover the bands under 3 GHz. Disaster management, by developing a proposal of telecommunications for disaster situations that uses the UHF TV bands as an alternative communications channel for connecting affected people and rescue teams. Pilot tests on TVWS, implementing a pilot to use a single 6MHz TV channel to transmit specific information, i.e., voice, data, and video to test digital spectrum access to this spectrum in both indoor and outdoor environments. TV Gray Space, by diffusing the use and sharing of TV bands in indoor environments, exploiting the bands known as TV Gray Spaces.



# Bibliography

- [1] Y.-C. Liang, K.-C. Chen, G. Y. Li, and P. Mahonen, "Cognitive radio networking and communications: An overview", *IEEE transactions on vehicular technology*, vol. 60, no. 7, pp. 3386–3407, 2011.
- [2] D. Datla, A. M. Wyglinski, and G. J. Minden, "A spectrum surveying framework for dynamic spectrum access networks", *IEEE Transactions on Vehicular Technology*, vol. 58, no. 8, pp. 4158–4168, 2009.
- [3] T. X. Brown, E. Pietrosemoli, M. Zennaro, A. Bagula, H. Mauwa, and S. M. Nleya, "A survey of tv white space measurements", in *International Conference on e-Infrastructure and e-Services for Developing Countries*, Springer, 2014, pp. 164–172.
- [4] S. J. Shellhammer *et al.*, "Spectrum sensing in ieee 802.22", *IAPR Wksp. Cognitive Info. Processing*, pp. 9–10, 2008.
- [5] F. Akhtar, M. H. Rehmani, and M. Reisslein, "White space: Definitional perspectives and their role in exploiting spectrum opportunities", *Telecommunications Policy*, vol. 40, no. 4, pp. 319–331, 2016.
- [6] M. J. Marcus, "Where does the radio spectrum end?", *IEEE Wireless Communications*, vol. 20, no. 3, pp. 6–7, 2013.
- [7] J. Mitola, G. Q. Maguire, *et al.*, "Cognitive radio: Making software radios more personal", *IEEE personal communications*, vol. 6, no. 4, pp. 13–18, 1999.
- [8] H. Yoshino, "Itu-r standardization activities on cognitive radio", *IEICE transactions on communications*, vol. 95, no. 4, pp. 1036–1043, 2012.
- [9] International Telecommunications Union, ITU, *Frequency bands allocated to terrestrial broadcasting services*, Accessed 26-09-2019 at <https://www.itu.int/en/ITU-R/terrestrial/broadcast/Pages/Bands.aspx>, 2019.
- [10] D. Corral-De-Witt, A. Younan, A. Fatima, J. Matamoros, F. A. Awın, K. Tepe, and E. Abdel-Raheem, "Sensing tv spectrum using software defined radio hardware", in *Electrical and Computer Engineering (CCECE), 2017 IEEE 30th Canadian Conference on*, IEEE, 2017, pp. 1–4.

- [11] I. F. Akyildiz, W.-Y. Lee, M. C. Vuran, and S. Mohanty, "Next generation/dynamic spectrum access/cognitive radio wireless networks: A survey", *Computer networks*, vol. 50, no. 13, pp. 2127–2159, 2006.
- [12] E. Fcc, *Docket no 03-222 notice of proposed rule making and order*, 2003.
- [13] S. Haykin *et al.*, "Cognitive radio: Brain-empowered wireless communications", *IEEE journal on selected areas in communications*, vol. 23, no. 2, pp. 201–220, 2005.
- [14] X. Jing and D. Raychaudhuri, "Spectrum co-existence of ieee 802.11 b and 802.16 a networks using the csc etiquette protocol", in *First IEEE International Symposium on New Frontiers in Dynamic Spectrum Access Networks, 2005. DySPAN 2005.*, IEEE, 2005, pp. 243–250.
- [15] C. Cordeiro, K. Challapali, D. Birru, S. Shankar, *et al.*, "Ieee 802.22: An introduction to the first wireless standard based on cognitive radios", *Journal of communications*, vol. 1, no. 1, pp. 38–47, 2006.
- [16] L. A. Rusch, "Indoor wireless communications: Capacity and coexistence on the unlicensed bands", *Intel Technology Journal Q*, vol. 3, p. 2001, 2001.
- [17] IEEE, *Ieee 802.22 working group on wireless regional area networks*, Accessed 31-03-2019 at <http://www.ieee802.org/22/>, 2019.
- [18] Y. Zeng and Y.-C. Liang, "Eigenvalue-based spectrum sensing algorithms for cognitive radio", *IEEE transactions on communications*, vol. 57, no. 6, pp. 1784–1793, 2009.
- [19] E Pietrosevoli and M Zennaro, "Tv white spaces—a pragmatic approach", in *Proceedings of the Sixth International Conference on Information and Communication Technologies and Development*, 2013.
- [20] Y. Chen and H.-S. Oh, "A survey of measurement-based spectrum occupancy modeling for cognitive radios", *IEEE Communications Surveys & Tutorials*, vol. 18, no. 1, pp. 848–859, 2016.
- [21] M. R. Manesh, S. Subramaniam, H. Reyes, and N. Kaabouch, "Real-time spectrum occupancy monitoring using a probabilistic model", *Computer Networks*, vol. 124, pp. 87–96, 2017.
- [22] D. Corral-De-Witt, E. V. Carrera, J. A. Matamoros-Vargas, S. Muñoz-Romero, J. L. Rojo-Álvarez, and K. Tepe, "From e-911 to ng-911: Overview and challenges in ecuador", *IEEE Access*, vol. 6, pp. 42 578–42 591, 2018.

- [23] D. Câmara, "Cavalry to the rescue: Drones fleet to help rescuers operations over disasters scenarios", in *Antenna Measurements & Applications (CAMA), 2014 IEEE Conference on*, IEEE, 2014, pp. 1–4.
- [24] P. Bupe, R. Haddad, and F. Rios-Gutierrez, "Relief and emergency communication network based on an autonomous decentralized uav clustering network", in *SoutheastCon 2015*, IEEE, 2015, pp. 1–8.
- [25] S. Ghafoor, P. D. Sutton, C. J. Sreenan, and K. N. Brown, "Cognitive radio for disaster response networks: Survey, potential, and challenges", *IEEE Wireless Communications*, vol. 21, no. 5, pp. 70–80, 2014.
- [26] W. Zuo, C. Guo, J. Liu, X. Peng, and M. Yang, "A police and insurance joint management system based on high precision bds/gps positioning", *Sensors*, vol. 18, no. 1, p. 169, 2018.
- [27] L. Doyle, *Essentials of cognitive radio*. Cambridge University Press, 2009.
- [28] Y. Zeng and Y.-C. Liang, "Spectrum-sensing algorithms for cognitive radio based on statistical covariances", *IEEE transactions on Vehicular Technology*, vol. 58, no. 4, pp. 1804–1815, 2009.
- [29] T. Yucek and H. Arslan, "A survey of spectrum sensing algorithms for cognitive radio applications", *IEEE communications surveys & tutorials*, vol. 11, no. 1, pp. 116–130, 2009.
- [30] W. A. Gardner, "Exploitation of spectral redundancy in cyclostationary signals", *IEEE Signal processing magazine*, vol. 8, no. 2, pp. 14–36, 1991.
- [31] H. Reyes, S. Subramaniam, N. Kaabouch, and W. C. Hu, "A spectrum sensing technique based on autocorrelation and euclidean distance and its comparison with energy detection for cognitive radio networks", *Computers & Electrical Engineering*, vol. 52, pp. 319–327, 2016.
- [32] M. López-Benítez and F. Casadevall, "Improved energy detection spectrum sensing for cognitive radio", *IET communications*, vol. 6, no. 8, pp. 785–796, 2012.
- [33] H. Urkowitz, "Energy detection of unknown deterministic signals", *Proceedings of the IEEE*, vol. 55, no. 4, pp. 523–531, 1967.
- [34] A. Ahmed, Y.-F. Hu, and J. M. Noras, "Enhanced energy detection based spectrum sensing in cognitive radio networks using random matrix theory", in *Communication Systems, Networks & Digital Signal Processing (CSNDSP), 2014 9th International Symposium on*, IEEE, 2014, pp. 384–389.

- [35] RF Explorer, *Rf explorer spectrum analyzer*, Accessed 29-03-2019 at <http://j3.rf-explorer.com/40-rfe/article/48-introducing-rf-explorer>, 2018.
- [36] A. E. Leu, K. Steadman, M. McHenry, and J. Bates, "Ultra sensitive tv detector measurements", in *First IEEE International Symposium on New Frontiers in Dynamic Spectrum Access Networks, 2005. DySPAN 2005.*, IEEE, 2005, pp. 30–36.
- [37] Tektronix, *Mdo 4000 series manual*, Accessed 29-03-2019 at <https://www.tek.com/oscilloscopes/mdo4000-manual/mdo4000-series-0>, 2018.
- [38] NooElec, *Software defined radio*, Accessed 12-04-2018 at <http://www.nooelec.com/store/nesdr-smart-sdr.html>, 2018.
- [39] GQRX, *Gqrx sdr*, Accessed 12-04-2018 at <http://gqrx.dk/download>, 2018.
- [40] D. Lekomtcev and R. Maršálek, "Comparison of 802.11 af and 802.22 standards—physical layer and cognitive functionality", *Elektro Revue*, vol. 3, no. 2, pp. 12–18, 2012.
- [41] T. Harrold, R. Cepeda, and M. Beach, "Long-term measurements of spectrum occupancy characteristics", in *2011 IEEE International Symposium on Dynamic Spectrum Access Networks (DySPAN)*, IEEE, 2011, pp. 83–89.
- [42] V. Valenta, R. Maršálek, G. Baudoin, M. Villegas, M. Suarez, and F. Robert, "Survey on spectrum utilization in europe: Measurements, analyses and observations", in *2010 Proceedings of the fifth international conference on cognitive radio oriented wireless networks and communications*, IEEE, 2010, pp. 1–5.
- [43] International Telecommunications Union ITU, *Handbook spectrum monitoring, chapter 3*, Accessed 31-03-2019 at <https://extranet.itu.int/brdocsearch/R-HDB/R-HDB-23/R-HDB-23-2002/R-HDB-23-2002-OAS-PDF-E.pdf>, 2019.
- [44] K. A. Qaraqe, H. Celebi, A. Gorcin, A. El-Saigh, H. Arslan, and M.-s. Alouini, "Empirical results for wideband multidimensional spectrum usage", in *2009 IEEE 20th International Symposium on Personal, Indoor and Mobile Radio Communications*, IEEE, 2009, pp. 1262–1266.
- [45] J. M. Chambers, *Graphical methods for data analysis: 0*. Chapman and Hall/CRC, 2017.
- [46] F. J. Massey Jr, "The kolmogorov-smirnov test for goodness of fit", *Journal of the American statistical Association*, vol. 46, no. 253, pp. 68–78, 1951.

- [47] J. Neyman and E. S. Pearson, "Ix. on the problem of the most efficient tests of statistical hypotheses", *Philosophical Transactions of the Royal Society of London. Series A, Containing Papers of a Mathematical or Physical Character*, vol. 231, no. 694-706, pp. 289–337, 1933.
- [48] S. G. Hofmann, "Fisher's fallacy and nhst's flawed logic.", 2002.
- [49] Z Table, *Z score table*, Accessed 18-04-2019 <http://www.z-table.com/>, 2019.
- [50] C. D. Brown and H. T. Davis, "Receiver operating characteristics curves and related decision measures: A tutorial", *Chemometrics and Intelligent Laboratory Systems*, vol. 80, no. 1, pp. 24–38, 2006.
- [51] ANTOP, *Antop rf splitter at-706 3-way*, Accessed 28-06-2019 at <https://antopusa.com/product/accessories-splitter-at-706/>, 2019.

# Appendix A

## Copyright permission (Article for CCECE-2017)

Dear Co-authors,

I hope you are doing well. I am emailing in regards to having your permission to refer our publication in my Ph.D. thesis.

**Article:**  
Sensing TV Spectrum Using Software Defined Radio Hardware.

**Conference:**  
2017 IEEE 30th Canadian Conference on Electrical and Computer Engineering (CCECE) (pp. 1-4). IEEE.

According to graduate studies regulations, though the thesis includes the statement of declaration of co-authorship and previous publication; your permission should be appended in the thesis.

Best regards

[Danilo Corral De Witt](#)

Corral-De-Witt, D., Younan, A., Fatima, A., Matamoros, J., Awin, F. A., Tepe, K., & Abdel-Raheem, E.

 **Aaron Younan**

Hi Danilo,

Sure, go for it. Best of luck!


Thanks  
Aaron

 **Arooj Fatima**

Hi Danilo,

Please go ahead! All the best.

Regards,  
Arooj Fatima


 **José Antonio Matamoros Vargas**

Hello Danilo,

You have my approval.

Congratulations!


Jose Matamoros

 **Farooq Awin**

Good morning Danilo


I have no problem with that you add it to your thesis.

Best regards

 **Kemal Tepe**

you have permission to include these in your thesis.

Kemal Tepe

 **Esam Abdel-Raheem**

Dear Danilo

You can go ahead and use the published paper. You have my permission.

best regards

**Esam Abdel-Raheem PhD, PEng**  
Professor

# Appendix A

## Copyright permission (Article for MWSCAS-2018)

Dear Co-authors,

I hope you are doing well. I am emailing in regards to having your permission to refer our publication in my Ph.D. thesis.

**Article:**  
Multiplatform Spectrum Sensing Prototype.

**Conference:**  
2018 IEEE 61st International Midwest Symposium on Circuits and Systems (MWSCAS) (pp. 198-201). IEEE.

According to graduate studies regulations, though the thesis includes the statement of declaration of co-authorship and previous publication; your permission should be appended in the thesis.

Best regards

[Danilo Corral De Witt](#)


Corral-De-Witt, D., Younan, A., Ariful, D., Zhang, L., & Tepe, K.

 **Aaron Younan**


Hi Danilo,

Sure. Is there a way to blanket this permission to all articles/work that we collaborated on? I have no problem with you using anything that you might need; papers, code, data, whatever you like.

Thanks  
Aaron Younan

 **Dewan Arif**

Yes, I approve.

 **Lining Zhang**

Dear Danilo,

This is the confirmation that I grant the copyright permission of the article "Multiplatform Spectrum Sensing Prototype" published by Danilo Corral De Witt.

Best regards,  
Lining Zhang

 **Kemal Tepe**

You have my permission.

# Appendix A

## Copyright permission (Article for ISSPIT-2018)

Dear Co-authors,

I hope you are doing well. I am emailing in regards to having your permission to refer our publication in my Ph.D. thesis.

**Article:**

Narrowband Data Transmission in TV White Space: An Experimental Performance Analysis.

**Conference:**

2018 IEEE International Symposium on Signal Processing and Information Technology (ISSPIT) (pp. 252-257). IEEE.

According to graduate studies regulations, though the thesis includes the statement of declaration of co-authorship and previous publication; your permission should be appended in the thesis.

Best regards

**Danilo Corral De Witt**

Co-authors: Hassan, D. M. A., Corral-De-Witt, D., Ahmed, S., & Tepe, K.2



**Dewan Arif**

Yes, go ahead.



**Sabbir Ahmed**

Hi Danilo,

As a co-author, I give you my permission to refer to our publication in your Ph.D. thesis.

Wishing you all the best.

Regards

Sabbir



**Kemal Tepe**

You have my permission.



# Appendix A

## Copyright permission (Article submitted to MDPI 2019)

**Dear Co-authors,**

I hope you are doing well. I am emailing in regards to having your permission to refer our publication in my Ph.D. thesis.

**Article:**

An Accurate Probabilistic Model for TVWS Identification


**Journal:**

MDPI Applied Sciences


**Status:**

Submitted September 2019

Co-authors: Corral-De-Witt, D., Ahmed, S., Awin, F., Rojo-Álvarez, J., and Tepe, K.

 **Sabbir Ahmed**

Hi Danilo,  
You have my permission.  
Regards  
Sabbir


 **Faroq Awin**

Yes, of course you can.

 **José Luis Rojo Álvarez**

Dear Danilo and All,

Of course I also agree.

 **Kemal Tepe**

I give permission

Kemal

# Appendix B

## Mathematical Notation

Ord	Variable	Units and/or Observations
1	$F$	Frquency / MHz, KHz, Hz
2	$P$	Power of the signal / dBm
3	$M$	Margin / dB
4	$T$	Threshold / dBm
5	$R$	Matched impedance / $\Omega$ (Ohm)
6	$W(f)$	Noise in the frequency domain
7	$X(f)$	Composite signal in the frequency domain
8	$\overline{W}(f)$	Mean of the noise in the frequency domain
9	$\overline{X}(f)$	Mean of the composite signal in the frequency domain
10	$W(p)$	Normal curve of the noise
11	$Xo(p)$	Multi modal curve of the composite signal
12	$X(p)$	Normal curve of the composite signal
13	$\overline{W}(p)$	Mean value of the normal curve of the noise
14	$\overline{X}(p)$	Mean value of the normal curve of the composite signal
15	$Pfa$	False alarm probability / Percentage
16	$Pd$	Detction probability / Percentage
17	$z$	Area under the normal curve to the left of $z$ / Percentage
18	$F(z)$	$z$ function
19	$f(xW)$	Pdf of the noise
20	$f(xX)$	Pdf of the composite signal

# Appendix C

## Standard Normal Probabilities

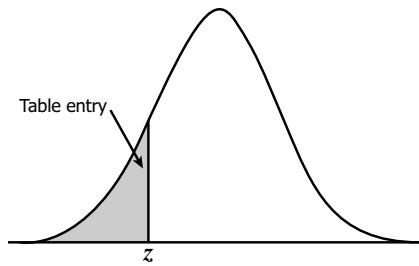


Table entry for  $z$  is the area under the standard normal curve to the left of  $z$ .

$z$	.00	.01	.02	.03	.04	.05	.06	.07	.08	.09
-3.4	.0003	.0003	.0003	.0003	.0003	.0003	.0003	.0003	.0003	.0002
-3.3	.0005	.0005	.0005	.0004	.0004	.0004	.0004	.0004	.0004	.0003
-3.2	.0007	.0007	.0006	.0006	.0006	.0006	.0006	.0005	.0005	.0005
-3.1	.0010	.0009	.0009	.0009	.0008	.0008	.0008	.0008	.0007	.0007
-3.0	.0013	.0013	.0013	.0012	.0012	.0011	.0011	.0011	.0010	.0010
-2.9	.0019	.0018	.0018	.0017	.0016	.0016	.0015	.0015	.0014	.0014
-2.8	.0026	.0025	.0024	.0023	.0023	.0022	.0021	.0021	.0020	.0019
-2.7	.0035	.0034	.0033	.0032	.0031	.0030	.0029	.0028	.0027	.0026
-2.6	.0047	.0045	.0044	.0043	.0041	.0040	.0039	.0038	.0037	.0036
-2.5	.0062	.0060	.0059	.0057	.0055	.0054	.0052	.0051	.0049	.0048
-2.4	.0082	.0080	.0078	.0075	.0073	.0071	.0069	.0068	.0066	.0064
-2.3	.0107	.0104	.0102	.0099	.0096	.0094	.0091	.0089	.0087	.0084
-2.2	.0139	.0136	.0132	.0129	.0125	.0122	.0119	.0116	.0113	.0110
-2.1	.0179	.0174	.0170	.0166	.0162	.0158	.0154	.0150	.0146	.0143
-2.0	.0228	.0222	.0217	.0212	.0207	.0202	.0197	.0192	.0188	.0183
-1.9	.0287	.0281	.0274	.0268	.0262	.0256	.0250	.0244	.0239	.0233
-1.8	.0359	.0351	.0344	.0336	.0329	.0322	.0314	.0307	.0301	.0294
-1.7	.0446	.0436	.0427	.0418	.0409	.0401	.0392	.0384	.0375	.0367
-1.6	.0548	.0537	.0526	.0516	.0505	.0495	.0485	.0475	.0465	.0455
-1.5	.0668	.0655	.0643	.0630	.0618	.0606	.0594	.0582	.0571	.0559
-1.4	.0808	.0793	.0778	.0764	.0749	.0735	.0721	.0708	.0694	.0681
-1.3	.0968	.0951	.0934	.0918	.0901	.0885	.0869	.0853	.0838	.0823
-1.2	.1151	.1131	.1112	.1093	.1075	.1056	.1038	.1020	.1003	.0985
-1.1	.1357	.1335	.1314	.1292	.1271	.1251	.1230	.1210	.1190	.1170
-1.0	.1587	.1562	.1539	.1515	.1492	.1469	.1446	.1423	.1401	.1379
-0.9	.1841	.1814	.1788	.1762	.1736	.1711	.1685	.1660	.1635	.1611
-0.8	.2119	.2090	.2061	.2033	.2005	.1977	.1949	.1922	.1894	.1867
-0.7	.2420	.2389	.2358	.2327	.2296	.2266	.2236	.2206	.2177	.2148
-0.6	.2743	.2709	.2676	.2643	.2611	.2578	.2546	.2514	.2483	.2451
-0.5	.3085	.3050	.3015	.2981	.2946	.2912	.2877	.2843	.2810	.2776
-0.4	.3446	.3409	.3372	.3336	.3300	.3264	.3228	.3192	.3156	.3121
-0.3	.3821	.3783	.3745	.3707	.3669	.3632	.3594	.3557	.3520	.3483
-0.2	.4207	.4168	.4129	.4090	.4052	.4013	.3974	.3936	.3897	.3859
-0.1	.4602	.4562	.4522	.4483	.4443	.4404	.4364	.4325	.4286	.4247
-0.0	.5000	.4960	.4920	.4880	.4840	.4801	.4761	.4721	.4681	.4641



# Vita Auctoris

**NAME:** Danilo R. Corral De Witt

**PLACE OF BIRTH:** Quito, Ecuador

**YEAR OF BIRTH:** 1968

**EDUCATION:**

Escuela Militar Eloy Alfaro, Second Lieutenant of the Army, Ecuador, 1992

Universidad de las Fuerzas Armadas ESPE, Electronic and Telecommunications Engineer, Ecuador, 2003

Universidad de las Fuerzas Armadas ESPE, Certificate of Higher Education Management, Ecuador, 2007

Universidad Rey Juan Carlos, M.Sc. Telecommunications Networks for Developing Countries, Spain, 2010

Instituto Tecnológico de Monterrey, International Diploma in Teaching Skills, Mexico, 2014

Universidad Rey Juan Carlos, Ph.D. Information and Communications Technologies, Spain, 2019

University of Windsor, Ph.D. Electrical Engineering, Canada, 2019